



THE HONG KONG
POLYTECHNIC UNIVERSITY

香港理工大學

Pao Yue-kong Library
包玉剛圖書館

Copyright Undertaking

This thesis is protected by copyright, with all rights reserved.

By reading and using the thesis, the reader understands and agrees to the following terms:

1. The reader will abide by the rules and legal ordinances governing copyright regarding the use of the thesis.
2. The reader will use the thesis for the purpose of research or private study only and not for distribution or further reproduction or any other purpose.
3. The reader agrees to indemnify and hold the University harmless from and against any loss, damage, cost, liability or expenses arising from copyright infringement or unauthorized usage.

If you have reasons to believe that any materials in this thesis are deemed not suitable to be distributed in this form, or a copyright owner having difficulty with the material being included in our database, please contact lbsys@polyu.edu.hk providing details. The Library will look into your claim and consider taking remedial action upon receipt of the written requests.

Power Distribution and Efficiency
Analysis of Quasi-Resonant Converters
Using Regulated Unified Model

by

Che Tat CHOI

A thesis submitted in partial fulfillment of the requirements
for the degree of Master of Philosophy

in

Department of Electronic and Information Engineering

The Hong Kong Polytechnic University

Hong Kong

Supervisor: Dr. Chi Kwong LI

November 2001



Pao Yue-kong Library
PolyU · Hong Kong

CERTIFICATE OF ORIGINALITY

I hereby declare that this thesis is my own work and that, to the best of my knowledge and belief, it reproduces no material previously published or written, nor material that has been accepted for the award of any other degree or diploma, except where due acknowledgement has been made in the text.

(Signed)

Che Tat Choi _____ (Name of student)

Abstract

This thesis analyzes the power distribution of the unified model in quasi-resonant converters. The major contribution is that the internal equivalent resistance of each component is taken into consideration for analysis so that the current and voltage waveforms can be found accurately. The switching waveforms of this near-practical model will be derived. However, an equation, which represents the resonant stage, cannot be written in explicit form. In order to achieve zero voltage or zero current switching condition, the equations must be solved numerically. By using the averaging techniques, the regulated large signal model can be predicted under different supply voltage and load current. In other words, the variation of switching frequency, which is a controller parameter, can be determined while output voltage is kept constant. Another contribution is to determine the switching frequency in order to regulate the output voltage under varying the supply voltage or load current. The results are very useful for predicting the performance of the quasi-resonant converters by using large signal models. The power distribution in the ideal frequency-modulated zero-voltage switching quasi-resonant switch (FM ZVS QRSW) is obtained. The internal resistance of each component of the unified quasi-resonant switch model (QRSW) is taken into consideration. The power dissipation is analyzed

so that the efficiency of the QRSW can be estimated. Moreover, the conduction loss of each component can be found and the maximum theoretical efficiency can be predicted by using the large signal model. In order to achieve high efficiency, finding the critical components in power dissipation is shown.

The large signal models of Buck, Boost, Buck-Boost, Cuk, Sepic and Zeta QRC are analyzed in this thesis. The output load is assumed to be resistive only. The loading current can be varied according to the analysis. The regulated model means that the output load voltage will keep constant under regulation even though the operating conditions or loading current are changed at any time. The system is assumed to be in steady state. Only the active power is considered in the power distribution analysis because the active power dissipation is the major component and there is no power transformer in the models. Only the equivalent resistances of the components will be considered. The parasitic inductance in the capacitors and parasitic capacitance in the inductors will be neglected. The transient value, transient analysis and stability are not in the scope of analysis.

The state-space averaging techniques are used to derive the system equations in each switching stage. There are two state variables: $V_{Cr}(t)$ and $I_{Cr}(t)$ in the system equations. Because the large signal model is derived, only the steady state value or averaging value is used. A mean value is used to represent a varying value over a time period or a switching cycle. The transient value, transient analysis and stability are not considered when calculating the state variables. The MATLAB simulation tools [6] are used to implement the derived system equations by using numerical methods to find the numerical switching frequency in order to regulate the output voltage even though the operating conditions say output current and supply voltage are changed. Having determined the system parameters, the switching frequency,

current in each voltage node and voltage across each current branch can be found.

The results are represented by numerical values. In order to present the numerical results easily, 2-D and 3-D diagrams are used to describe the trend and shape of the findings. The power distribution and power loss in each circuit component can be predicted under different operating conditions because the current passing through the voltage nodes and the voltage across the current branches are calculated by using the derived system equations. They are presented in 3-D diagrams, so view angle of the diagrams can be rotated in the simulation tools. Moreover, by comparing the input and output power, the efficiency of the regulated large signal model can be represented in a 3-D diagram. The independent variables are supply voltage and load current respectively.

Acknowledgments

First of all, I would like to express my deep gratitude towards my supervisor Dr. Chi Kwong Li for his great support, invaluable comments and guidance. During my MPhil study, Dr. Li gave me much encouragement so that I could submit more than seven conference papers [31]-[37]. One was accepted and presented in IEEE 7th Workshop on Computers in Power Electronics (COMPEL2000) in USA [34]. Another paper was also accepted and presented in 39th IEEE Conference on Decision and Control (CDC2000) in Australia [31].

Moreover, I would like to thank Prof. Yim Shu Lee, Dr. Peter K. S. Tam, Dr. Frank H. F. Leung and Dr. Shek Wai Ng for giving me invaluable comment and advice. On the other hand, the laboratory technician Dr. Kwok Fai Wan gave me a lot of technical support as well.

Contents

Abstract	i
Acknowledgments.....	iv
List of Figures.....	viii
List of Tables.....	xii
Chapter 1 Introduction.....	1
Chapter 2 Overview of Ideal Model of PWMSW and QRSW.....	4
Chapter 3 Power Distribution Analysis of Ideal ZVS QRSW	20
3.1 QR Buck Converter.....	23
3.2 QR Boost Converter	23
3.3 QR Buck-Boost Converter	24
3.4 QR Cuk Converter.....	24
3.5 QR Sepic Converter.....	25
3.6 QR Zeta Converter	26

Chapter 4 Modeling of Practical FM ZVS QR Buck Converter	33
4.1 Capacitor Charging Stage [T ₀ , T ₁]	35
4.2 Resonant Stage [T ₁ , T ₂]	36
4.3 Inductor Discharging Stage [T ₂ , T ₃].....	39
4.3.1 First Inductor Discharging Stage [T ₂ , T _a].....	40
4.3.2 Second Inductor Discharging Stage [T _a , T ₃]	41
4.4 Free-Wheeling Stage [T ₃ , T _s]	43
Chapter 5 Modeling of Practical FM ZVS QR Boost Converter.....	44
5.1 Capacitor Charging Stage [T ₀ , T ₁]	44
5.2 Resonant Stage [T ₁ , T ₂].....	46
5.3 Inductor Discharging Stage [T ₂ , T ₃].....	48
5.3.1 First Inductor Discharging Stage [T ₂ , T _a].....	49
5.3.2 Second Inductor Discharging Stage [T _a , T ₃]	51
5.4 Free-Wheeling Stage [T ₃ , T _s]	52
Chapter 6 Modeling of FM ZVS Converters Using Unified Model.....	54
6.1 Capacitor Charging Stage [T ₀ , T ₁]	55
6.2 Resonant Stage [T ₁ , T ₂].....	57
6.3 Inductor Discharging Stage [T ₂ , T ₃].....	60
6.3.1 First Inductor Discharging Stage [T ₂ , T _a].....	61
6.3.2 Second Inductor Discharging Stage [T _a , T ₃]	62
6.4 Free-Wheeling Stage [T ₃ , T _s]	64
Chapter 7 Power Distribution and Efficiency Analysis.....	66
7.1 Non-regulated Operating Mode.....	67

7.2	Regulated Operating Mode	74
Chapter 8	Conclusion.....	84
Glossary	87
Appendix A: MATLAB Scripts		94
A.1	Regulated Buck QRC.....	94
A.2	Regulated Boost QRC.....	97
A.3	Regulated Buck-Boost QRC.....	99
A.4	Regulated Cuk QRC	102
A.5	Regulated Sepic QRC	105
A.6	Regulated Zeta QRC	108
A.7	Regulated Lossy Buck QRC	111
A.8	Regulated Lossy Boost QRC	119
A.9	Regulated Lossy Buck-Boost QRC	129
A.10	Regulated Lossy Cuk QRC	140
References	152

List of Figures

Fig. 2.1.	Unified Model of PWM Converters.....	5
Fig. 2.2.	Conventional PWM Converters. Left: Basic Circuits. Right: Operation Models. (a) Buck, (b) Boost, (c) Buck-Boost, (d) Cuk, (e) Sepic and (f) Zeta.....	6
Fig. 2.3.	General Operation Model of Conventional PWM Converters.....	8
Fig. 2.4.	Operational Ideal Model of FM ZVS QR Switch.	10
Fig. 2.5.	Switching waveforms of FM ZVS QRSW.....	12
Fig. 2.6.	Maximum Transfer Function $g_{\max}(\alpha)$ at $f_{\max}(\alpha)$	16
Fig. 2.7	Transfer Function $g(\alpha)$ at a fixed switching frequency $f_s = 260\text{kHz}$	17
Fig. 2.8.	Half-wave Type of FM ZVS QR Converters in Operation Model: (a) Buck, (b) Boost, (c) Buck-Boost, (d) Cuk, (e) Sepic and (f) Zeta.....	18
Fig. 2.9.	General Operation Model of Half-wave Type of FM ZVS QR Converters:....	19
Fig. 3.1.	Power Distribution of Half-wave Type of FM ZVS QR Buck Converters.....	27
Fig. 3.2.	Power Distribution of Half-wave Type of FM ZVS QR Boost Converters.....	28
Fig. 3.3.	Power Distribution of Half-wave Type of FM ZVS QR Buck-Boost Converters.	29
Fig. 3.4.	Power Distribution of Half-wave Type of FM ZVS QR Cuk Converters.....	30
Fig. 3.5.	Power Distribution of Half-wave Type of FM ZVS QR Sepic Converters.	31
Fig. 3.6.	Power Distribution of Half-wave Type of FM ZVS QR Zeta Converters.	32
Fig. 4.1.	Practical Model of FM ZVS QR Switch.	34

Fig. 4.2. Capacitor Charging Stage [T_0, T_1] of FM ZVS QR Buck Converter.....	36
Fig. 4.3. Resonant Stage [T_1, T_2] of FM ZVS QR Buck Converter.	37
Fig. 4.4. Inductor Discharging Stage [T_2, T_a] of FM ZVS QR Buck Converter.	41
Fig. 4.5. Inductor Discharging Stage [T_a, T_3] of FM ZVS QR Buck Converter.	42
Fig. 4.6. Free-Wheeling Stage [T_3, T_s] of FM ZVS QR Buck Converter.	43
Fig. 5.1. Capacitor Charging Stage [T_0, T_1] of FM ZVS QR Boost Converter.....	45
Fig. 5.2. Resonant Stage [T_1, T_2] of FM ZVS QR Boost Converter.	47
Fig. 5.3. Inductor Discharging Stage [T_2, T_a] of FM ZVS QR Boost Converter.	50
Fig. 5.4. Inductor Discharging Stage [T_a, T_3] of FM ZVS QR Boost Converter.	51
Fig. 5.5. Free-Wheeling Stage [T_3, T_s] of FM ZVS QR Boost Converter.....	53
Fig. 6.1. Unified Practical Model of FM ZVS QR Converter.	55
Fig. 6.2. Capacitor Charging Stage [T_0, T_1] of FM ZVS QR Unified Model.....	56
Fig. 6.3. Resonant Stage [T_1, T_2] of FM ZVS QR Unified Model.	57
Fig. 6.4. First Inductor Discharging Stage [T_2, T_a] of FM ZVS QR Unified Model.....	61
Fig. 6.5. Second Inductor Discharging Stage [T_a, T_3] of FM ZVS QR Unified Model.	
.....	64
Fig. 6.6. Free-Wheeling Stage [T_3, T_s] of FM ZVS QR Unified Model.	65
Fig. 7.1. Power Distribution of Half-wave Type of FM ZVS QR Buck Converter.	68
Fig. 7.2. Power Distribution of Half-wave Type of FM ZVS QR Boost Converter.	69
Fig. 7.3. Power Loss of Each Component in FM ZVS QR Buck Converter.....	70
Fig. 7.4. Power Loss of Each Component in FM ZVS QR Boost Converter.....	71
Fig. 7.5. Efficiency of Half-wave Type of FM ZVS QR Buck Converter.	72
Fig. 7.6. Efficiency of Half-wave Type of FM ZVS QR Boost Converter.	73

Fig. 7.7. QR Regulated Buck Converter (a) Switching Frequency f_s , (b) Regulated Load Voltage V_{i3} , (c) Supply Current I_{12} , (d) Supply Power P_{v12} and Load Power P_{i3}	76
Fig. 7.8. QR Regulated Boost Converter (a) Switching Frequency f_s , (b) Regulated Load Voltage V_{12} , (c) Supply Current I_{3a} , (d) Supply Power P_{i3a} and Load Power P_{v12}	77
Fig. 7.9. QR Regulated Buck-Boost Converter (a) Switching Frequency f_s , (b) Regulated Load Voltage V_{12b} & Intermediate Voltage Branch V_{i3c} , (c) Supply Current I_{12a} & Intermediate Current Branch I_{3c} , (d) Supply Power P_{i3a} and Load Power P_{v12}	78
Fig. 7.10. QR Regulated Cuk Converter (a) Switching Frequency f_s , (b) Regulated Load Voltage V_{i3b} & Intermediate Voltage Branch V_{12} , (c) Supply Current I_{3a} & Intermediate Current Branch I_{v12} , (d) Supply Power P_{i3a} and Load Power P_{i3b}	79
Fig. 7.11. QR Regulated Sepic Converter (a) Switching Frequency f_s , (b) Regulated Load Voltage V_{12b} & Intermediate Voltage Branch V_{12a} , V_{i3c} (c) Supply Current I_{3a} & Intermediate Current Branch I_{v12a} , I_{3c} (d) Supply Power P_{i3a} and Load Power P_{v12b}	80
Fig. 7.12. QR Regulated Zeta Converter (a) Switching Frequency f_s , (b) Regulated Load Voltage V_{i3b} & Intermediate Voltage Branch V_{12b} , V_{i3c} (c) Supply Current I_{v12a} & Intermediate Current Branch I_{v12b} , I_{3c} (d) Supply Power P_{v12a} and Load Power P_{i3b}	81
Fig. 7.13. Power Loss of Each Component in FM ZVS QR Buck Converter.....	82
Fig. 7.14. Efficiency of Half-wave Type FM ZVS QR Buck Converter.....	83

List of Tables

Table 2-1. Power Attributes of PWM Converters	9
Table 3-1. Power Attributes of FM ZVS QR Converters.....	22

Chapter 1 Introduction

The switching mode power supply industry is looking for solutions that can develop small size, low weight, low switching losses and high efficiency power supply. The concept of quasi-resonant power conversion and zero-voltage switching (ZVS) were introduced by F. C. Lee and his collaborators in [1] and [2] respectively. The power loss and efficiency of quasi-resonant converters (QRCs) were analyzed in [3]. However, the modeling, synthesis and analysis of QRCs were generalized and unified in [4]. Article [5] mentioned that decreasing the "active" power losses in transistor is also highly desirable, so the additional investigations are needed to optimize the overall converter efficiency. Working out an efficient power supply is a complex problem and it is necessary to investigate the deep understanding of physical effects in all converter elements.

The power loss and efficiency analysis has not been studied by using these new models. Therefore, the major contribution of this paper introduces a new approach to analyze the power loss of each component in the quasi-resonant converters by using the unified approach. The advantage of using unified model is to summarize the analysis into one for different topologies such as Buck, Boost, Buck-Boost, Cuk,

Sepic and Zeta. The derived equations are applicable for all above topologies.

From the system control point of view, the small signal model [16]-[17] is used to analyze the stability, the transient response, the frequency response, the phase margin, the frequency margin, the poles and zeros. Adding pole(s) and/or zero(s) in the feedback path can optimize the performance of a controlled system to adapt the sudden change of operating conditions. However, the parameters in a small signal model may be different and varied under different operating points. For example, the supply voltage or the load current may be varied according to the environmental conditions such as temperature, humidity or loading conditions. The system can be non-linear because the components: diodes and switches are non-linear. A large signal model used in this thesis can help determine the DC operating points. The analysis of a large signal model is essential if the parameters in a small signal model are dependent on the operating points in the large signal model. Therefore, the large signal modeling techniques in this thesis can be used to identify the operating points of the quasi-resonant converters.

In this paper, Chapter 2 will review the ideal model of pulse-width modulated switch (PWMSW) and quasi-resonant switch (QRSW). Obviously, the PWMSW can be unified in a basic circuit: a switch and a diode. It simplifies the analysis of PWM converters because the topology consists of a current branch and a voltage loop. The operation model of Buck, Boost, Buck-Boost, Cuk, Sepic and Zeta Converter can be generalized into one general operation model. Adding a capacitor in parallel with the switch and an inductor in series with the diode to the PWMSW can form the QRSW. One example of the half-wave frequency-modulated zero-voltage switching quasi-resonant switch (FM ZVS QRSW) will be mentioned. Analogously, other types of QRCS can be derived from the basic model of QRSW. In Chapter 3, the power

distribution in the ideal half-wave FM ZVS QR Converters will be analyzed. However, it is assumed that they are not operating in the regulation mode because the frequency is fixed. The purpose of this analysis is mainly to verify the power attributes derived in Chapter 2. The major contributions for this thesis are mentioned starting from Chapter 4. They are divided into different chapters. Chapter 4 and Chapter 5 will derive the switching waveforms of the near-practical model of Buck and Boost Converter respectively. Chapter 6 will summarize the techniques used in Chapter 4 and Chapter 5. It shows the capability of using unified model to simplify the analysis. Finally, in Chapter 7, the power efficiency of this lossy model will be considered. All the terms are defined and listed in the Glossary. The simulation algorithms are listed in the Appendix A.1 – A.10.

Chapter 2 Overview of Ideal Model of PWMSW and QRSW

The unified ideal model of the pulse-width modulated (PWM) converters shown in Fig. 2.1 that has been analyzed in [4]. It consists of a main switch, a diode, a voltage branch and a current node. The main switch can be a MOSFET, a BJT or other type of transistors. The diode provides a unidirectional current path when the main switch is turned off. Basically, the constant current branch I_3 is generated by an inductor that has a DC component of current flow. The large signal model is considered, so only the DC component of the signal is taken into consideration. In order to simplify the large signal analysis, a constant current branch I_3 can replace the switching current in the inductor if it is in continuous conduction mode. The current node at point 3 should obey the Kirchhoff's current law (KCL). On the other hand, the voltage branch V_{12} may be a voltage source or a capacitor voltage. The voltage between node 1 and 2 should obey the Kirchhoff's voltage law (KVL) as well. The generalization concept is discussed in this chapter. The equivalent

operation models of Buck, Boost, Buck-Boost, Cuk, Sepic and Zeta Converter are shown in Fig. 2.2(a)-(f). All converters are assumed to be operating in continuous conduction mode (CCM), where the filter inductor is assumed to be a constant current source and the filter capacitor is assumed to be a constant voltage source.

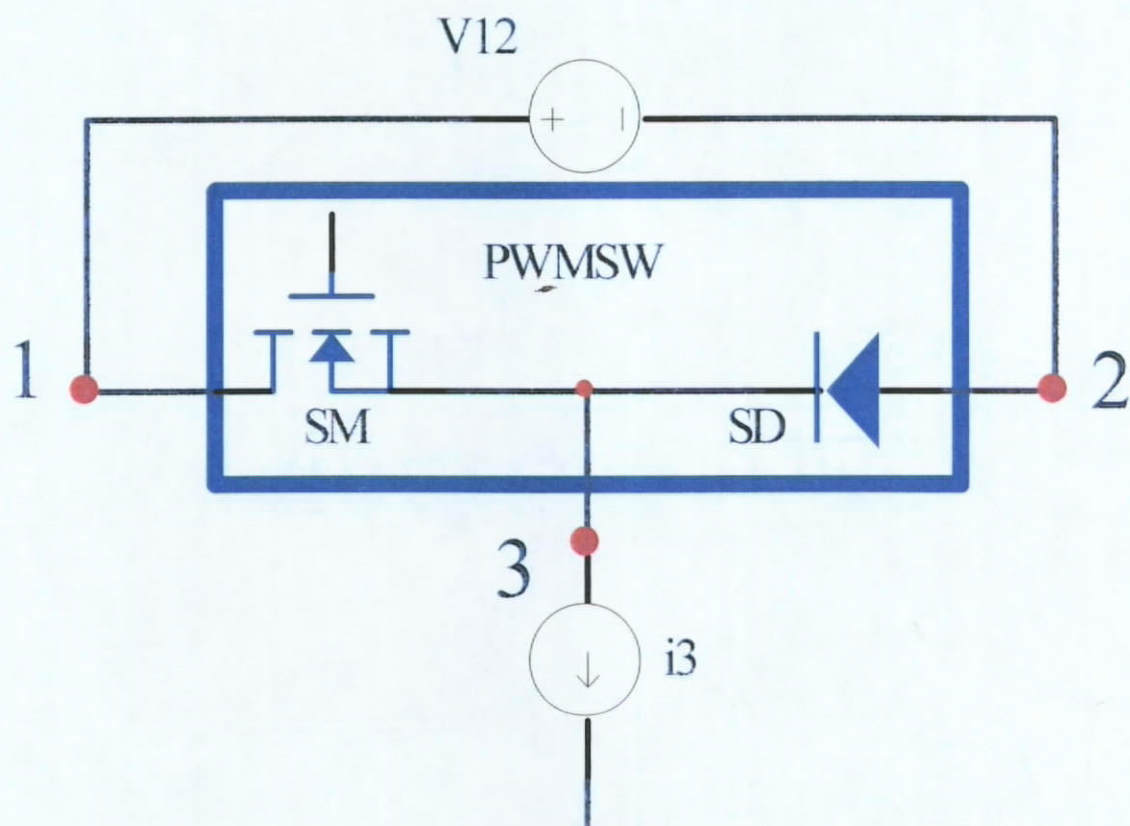


Fig. 2.1. Unified Model of PWM Converters.

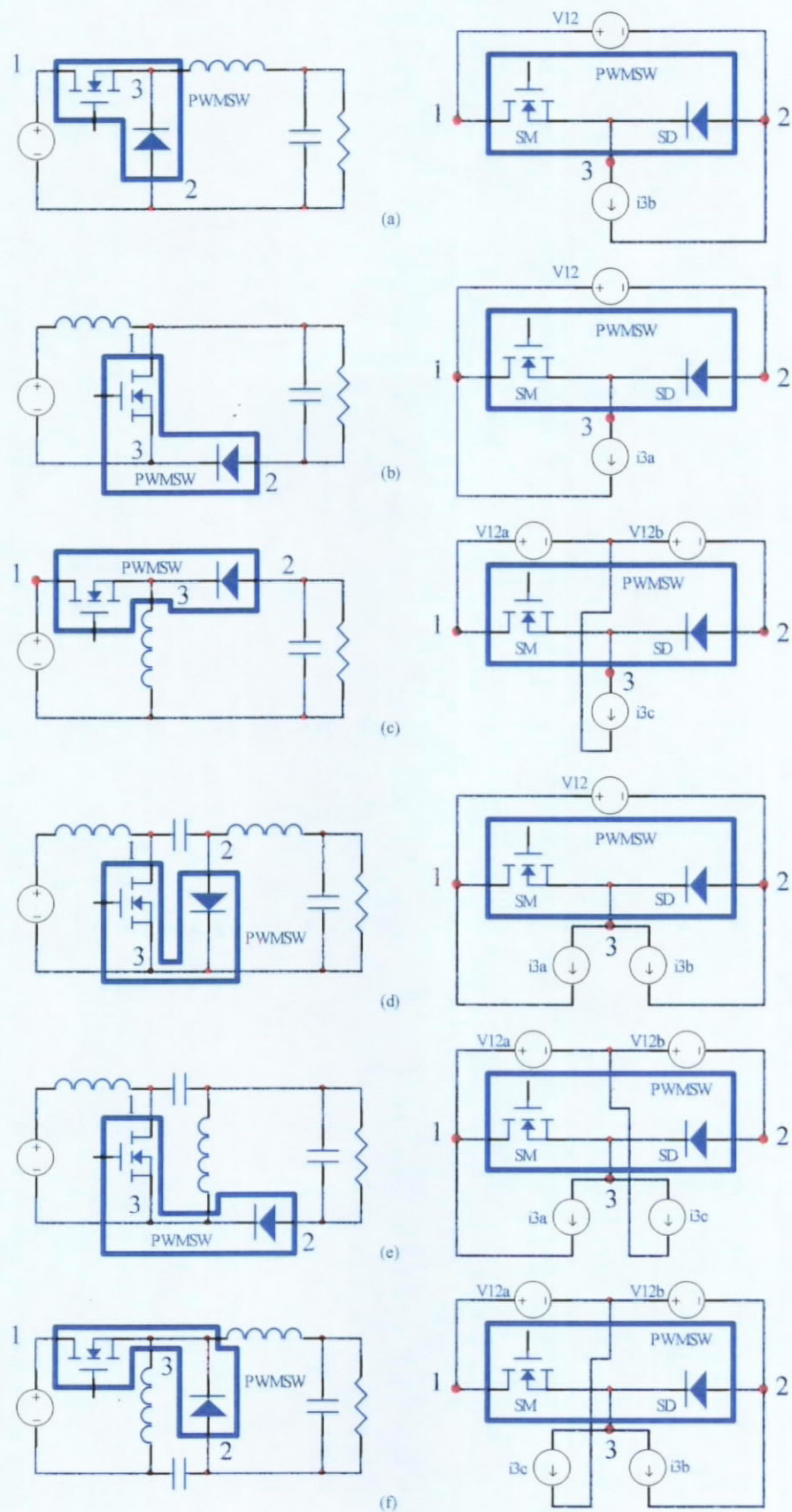


Fig. 2.2. Conventional PWM Converters. Left: Basic Circuits. Right: Operation Models. (a) Buck, (b) Boost, (c) Buck-Boost, (d) Cuk, (e) Sepic and (f) Zeta.

From Fig. 2.2, we know that a different topology of interconnection of v_{12} and i_3 will result in a different type of converter. In case Fig. 2.2(c), the voltage node v_{12a} and v_{12b} can be considered as the split of the original voltage node v_{12} in case Fig. 2.2(a) and (b). Moreover, in case Fig. 2.2(d), the current branch i_{3a} and i_{3b} can be considered as the split of the original current branch i_3 in case Fig. 2.2(a) or (b). Similarly, all the operation models in Fig. 2.2 can be generalized into the unified operation model shown in Fig. 2.3. Having compared the basic circuits with the operation model, the current branch i_3 in Fig. 2.2 can be split into a load current, a source current and an intermediate current branch. Moreover, the voltage node V_{12} can also be split into a load voltage, a source voltage and an intermediate voltage node.

The following analysis is derived by the author. The transformation from the PWM converters to the unified model shown in Fig. 2.2 and Fig. 2.3 has some conditions. For example, in Fig. 2.2(a) – Buck converter, the voltage source V_{12} is transformed from a power source and is supplying the power to the circuit. The power dissipation in the node V_{12} should be negative which means that the component is delivering the energy. On the other hand, the current branch I_{3b} is transformed from an inductor and a load with a paralleled capacitor. The direct current will flow through the inductor but there is alternating voltage on it. The alternating voltage will make the inductor current up and down but it is assumed that the current will be in a steady state which is defined as I_{3b} by using the averaging technique. Moreover, the net potential difference voltage should be zero because there should be no power dissipation in an ideal inductor. Therefore, the net voltage drop is on the load and the capacitor. The net current flowing into the capacitor should be zero because there should be no power dissipation in a capacitor as well. In

other words, only the load will dissipate the power. In the unified model shown in Fig. 2.2(a), the power dissipation in the current branch I_{3b} should be positive which means that the component is dissipating the energy. The positive power dissipation is defined as a current flowing into a device from the terminal of larger potential voltage to the other terminal of smaller potential voltage.

The power attributes in each current branch and voltage node for different converters are summarized in Table 2-1.

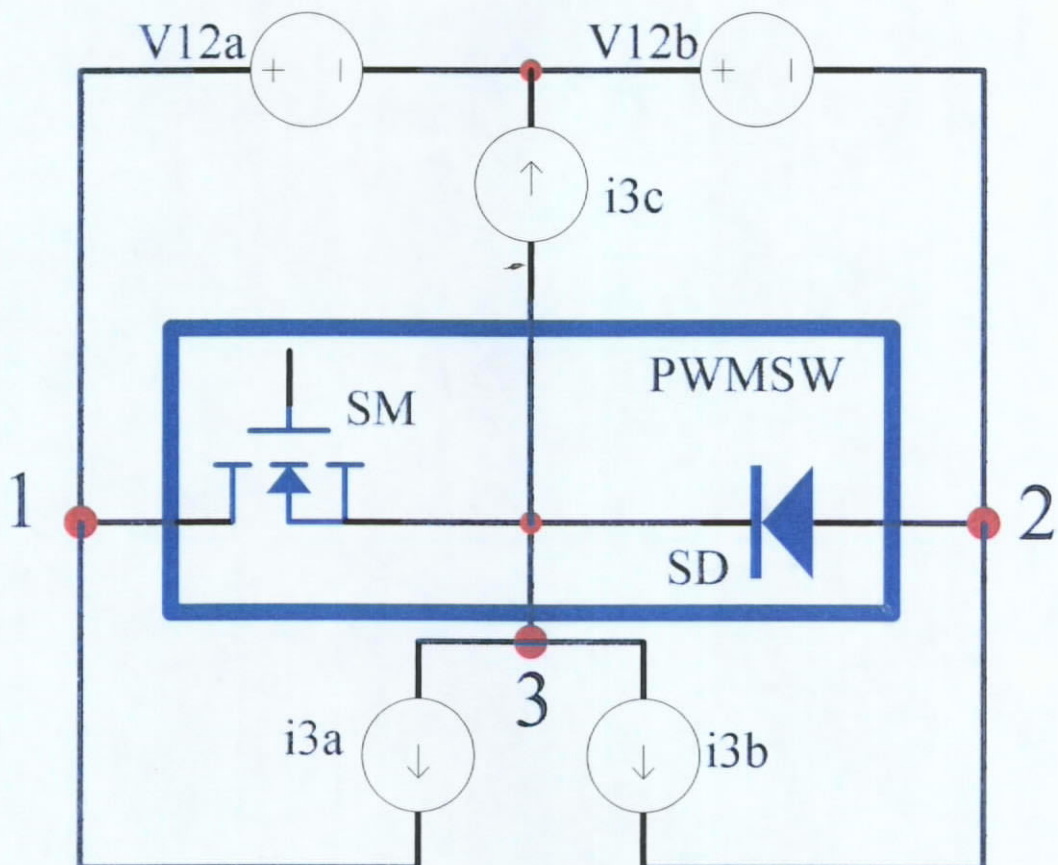


Fig. 2.3. General Operation Model of Conventional PWM Converters.

Table 2-1. Power Attributes of PWM Converters

PWM Converters	Voltage Node / Current Branch	Power Attributes	Power Dissipation
Buck	V_{12}	Voltage Source	Negative
	I_{3b}	Current Load	Positive
Boost	V_{12}	Voltage Load	Positive
	I_{3a}	Current Source	Negative
Buck-Boost	V_{12a}	Voltage Source	Negative
	V_{12b}	Voltage Load	Positive
	I_{3c}	Intermediate Current Branch	Zero
Cuk	V_{12}	Intermediate Voltage Node	Zero
	I_{3a}	Current Source	Negative
	I_{3b}	Current Load	Positive
Sepic	V_{12a}	Intermediate Voltage Node	Zero
	V_{12b}	Voltage Load	Positive
	I_{3a}	Current Source	Negative
	I_{3c}	Intermediate Current Branch	Zero
Zeta	V_{12a}	Voltage Source	Negative
	V_{12b}	Intermediate Voltage Node	Zero
	I_{3c}	Intermediate Current Branch	Zero
	I_{3b}	Current Load	Positive

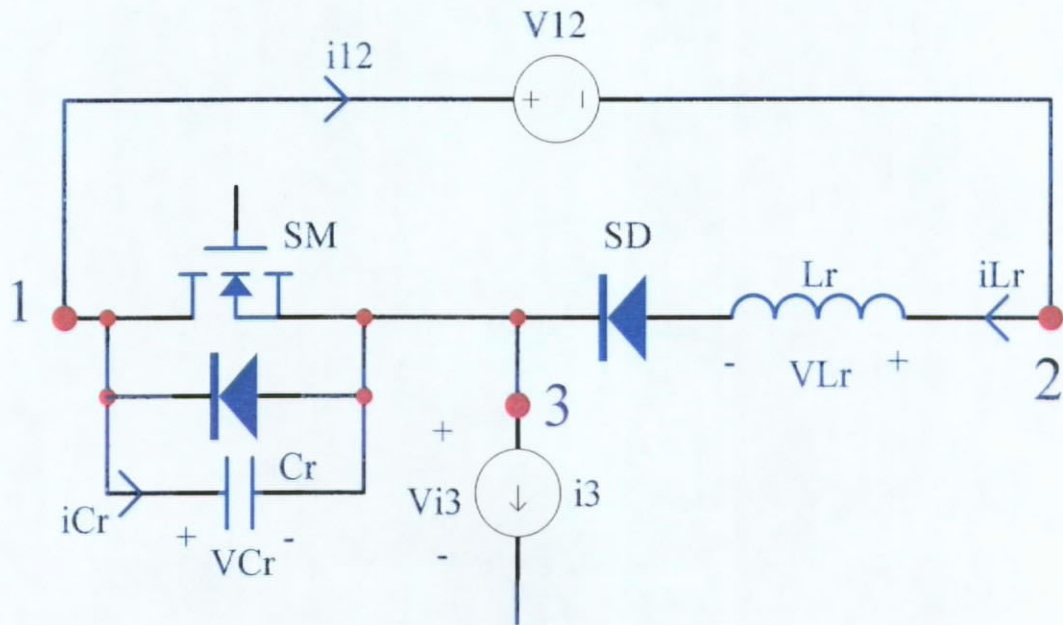


Fig. 2.4. Operational Ideal Model of FM ZVS QR Switch.

An LC resonant network can be added in PWMSW shown in Fig. 2.1 to form the quasi-resonant switch. One example of the QR switches is shown in Fig. 2.4. It is a half-wave FM ZVS QR switch. Actually, the switch SM becomes a current bi-directional switch by adding a capacitor in parallel in order to create the condition of resonant in capacitor voltage. The capacitor voltage will pass through zero point so that the condition of zero voltage switching (ZVS) can be generated. Fig. 2.8 shows the half-wave type of FM ZVS QR converters of (a) Buck, (b) Boost, (c) Buck-Boost, (d) Cuk, (e) Sepic and (f) Zeta. Analogously, all the operation models in Fig. 2.8 can be generalized in the model as shown in Fig. 2.9.

Article [4] derived the switching waveforms of this ideal half-wave FM QRSW shown in Fig. 2.5:

$$i_{Lr}(t) = \begin{cases} 0, & 0 < t < T_1 \\ i_2 \cdot (1 - \cos(w_r \cdot (t - T_1))), & T_1 < t < T_2 \\ i_3 \cdot (1 + \sqrt{1 - \alpha^2} - \alpha w_r (t - T_2)), & T_2 < t < T_3 \\ 0, & T_3 < t < T_s \end{cases} \quad (2.1)$$

and

$$v_{Cr}(t) = \begin{cases} \frac{V_{12} \cdot w_r}{\alpha} \cdot t, & 0 < t < T_1 \\ \frac{V_{12}}{\alpha} \cdot \sin(w_r \cdot (t - T_1)) + V_{12}, & T_1 < t < T_2 \\ 0, & T_2 < t < T_s \end{cases} \quad (2.2)$$

where

$$\begin{aligned} \alpha &= \frac{V_{12}}{Z_r \cdot i_3}, \quad w_r = \frac{1}{\sqrt{L_r C_r}}, \quad Z_r = \sqrt{\frac{L_r}{C_r}}, \quad T_1 = \frac{\alpha}{w_r}, \\ T_2 &= \frac{(\pi + \arcsin \alpha)}{w_r} + T_1 \text{ and } T_3 = \frac{1 + \sqrt{1 - \alpha^2}}{\alpha w_r} + T_2. \end{aligned} \quad (2.3)$$

The operation of the QR switch is that the on and off status of switch S_M and S_D is in sequence. Both switch S_M and S_D are off between T_0 and T_1 . The switch S_D will turn on after V_{Cr} is equal to V_{12} . When the V_{Cr} reaches at zero value at T_2 , the switch S_M will turn on that is called zero-voltage turn-on. The i_{Lr} will drop continuously until T_3 . The diode S_D will be off after T_3 but the switch S_M will remain on until next switching cycle T_s . Both capacitor and inductor provide the quasi-resonant characteristics in order to generate the zero-switching conditions. That's why QR regulators have low switching loss [2], [23].

From equation (2.1) and (2.3), the range of the parameter α can be found. The parameter α is a ratio between V_{12} and $Z_r \cdot i_3$ in equation (2.3).and it is inside a square root in equation (2.1). The parameter α should not be equal to zero because it is bounded by the T_1 and T_3 in equation (2.3) that T_1 should be larger than zero in equation (2.1). Moreover, it should not be a negative value and should be smaller than or equal to one. Therefore, α is bounded by

$$0 < \alpha \leq 1 . \quad (2.4)$$

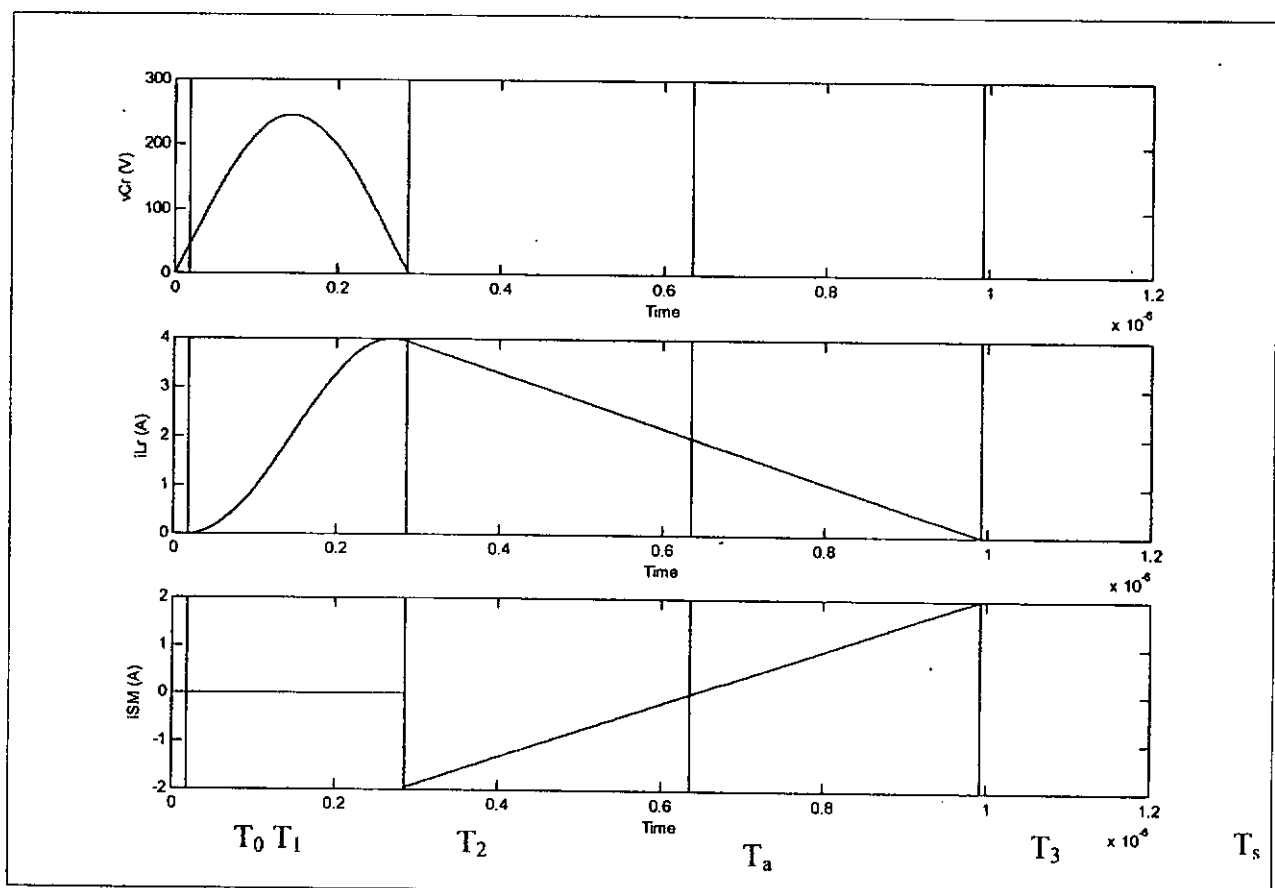


Fig. 2.5. Switching waveforms of FM ZVS QRSW.

By averaging $i_{Lr}(t)$ and $v_{Cr}(t)$ within a complete cycle T_s done in [4],

$$V_{Cr} = g(\alpha) \cdot v_{12} \text{ and } I_{Lr} = g(\alpha) \cdot i_3 , \quad (2.5)$$

where

$$g(\alpha) = \frac{f_s}{w_r} \left(\pi + \arcsin \alpha + \frac{\alpha}{2} + \frac{1 + \sqrt{1 - \alpha^2}}{\alpha} \right) . \quad (2.6)$$

From equation (2.5), the node voltage V_{12} is a variable to affect the capacitor voltage V_{Cr} . Moreover, the branch current i_3 is also another variable to affect the inductor current I_{Lr} . Actually, the function $g(\alpha)$ acts as a transfer function in equation (2.5). Furthermore, one complete switching cycle must be finished at T_3 where the inductor current $i_{Lr}(t)$ is zero. The next switching cycle must start after T_3 and depends on the variable $T_s (= 1/f_s)$. Therefore, the maximum switching frequency of f_s is bounded by

$$f_s \leq \frac{1}{T_3}$$

$$f_s \leq \frac{w_r}{\left(\alpha + \pi + \arcsin \alpha + \frac{1 + \sqrt{1 - \alpha^2}}{\alpha} \right)} . \quad (2.7)$$

Therefore, the maximum transfer function of $g(\alpha)$ can be found by substituting the upper bound of f_s in equation (2.7) for f_s in equation (2.6). The $g_{max}(\alpha)$ in equation (2.8) is defined as a maximum transfer function that the parameter α is the only independent variable. Therefore, the range of $g_{max}(\alpha)$ can be found by using numerical method for substituting the range of α mentioned in equation (2.4). The result is shown in Fig. 2.6 which depicts the upper bound of the transfer function $g(\alpha)$ that is $g_{max}(\alpha)$.

$$g_{\max}(\alpha) = \frac{f_{\max}(\alpha)}{w_r} \left(\frac{\alpha}{2} + \pi + \arcsin \alpha + \frac{1 + \sqrt{1 - \alpha^2}}{\alpha} \right), \quad (2.8)$$

where

$$f_{\max}(\alpha) = \frac{w_r}{\left(\alpha + \pi + \arcsin \alpha + \frac{1 + \sqrt{1 - \alpha^2}}{\alpha} \right)}.$$

Therefore,

$$g_{\max}(\alpha) = \frac{\left(\frac{\alpha}{2} + \pi + \arcsin \alpha + \frac{1 + \sqrt{1 - \alpha^2}}{\alpha} \right)}{\left(\alpha + \pi + \arcsin \alpha + \frac{1 + \sqrt{1 - \alpha^2}}{\alpha} \right)}. \quad (2.9)$$

The analysis of transfer function $g(\alpha)$ is another contribution of this thesis. In Fig. 2.6, the function $g_{\max}(\alpha)$ is nearly linear when the parameter α is larger than 0.3 under the condition of maximum switching frequency $f_{\max}(\alpha)$.

In Fig. 2.7, the function $g(\alpha)$ is highly nonlinear and there is large variation when a non-maximum fixed switching frequency is used. Contrarily, in Fig. 2.6, the function $g_{\max}(\alpha)$ is more linear and the slope is smaller when the maximum switching frequency is maintained for different value of α .

From the design point of view, using the fixed switching frequency is easy to design a quasi-resonant converter but it is difficult to stabilize the converter under varying operating conditions. However, although using the variable switching frequency to regulate this converter is optimal, it is not easy to design a controller under varying operating conditions because the transfer function $g(\alpha)$ is highly nonlinear.

From Fig. 2.6 and Fig. 2.7, the transfer function $g(\alpha)$ is a dependent variable and α is an independent variable because V_{12} or I_3 can be a varying parameter in different topologies. The solution is to find an appropriate value of switching frequency f_s so that the load voltage is kept constant under regulation.

For example, $V_{12} = V_{12a} + V_{12b}$ is a voltage source and I_{3b} is a current load in the Buck topology shown in Fig. 2.8(a). It should be assumed that the current I_{3b} is regulated parameter which is constant because the load condition is unchanged and the load voltage is assumed to be regulated. On the other hand, the supply voltage source V_{12} can be a varying parameter. Therefore, the switching frequency f_s should be found so that inductor voltage V_{Lr} is kept constant under regulation which implies that the voltage V_{13b} on current load I_{3b} is constant as well.

On the other hand, $V_{12} = V_{12a} + V_{12b}$ is a voltage load and I_{3a} is a current source in the Boost topology shown in Fig. 2.8(b). It should be assumed that the voltage V_{12} is regulated parameter which is constant because the load condition is unchanged and the load voltage is assumed to be regulated. On the other hand, the supply current source I_{3a} can be a varying parameter. Therefore, the switching frequency f_s should be found so that inductor current i_{Lr} is kept constant under regulation which implies that the current i_{12a} and i_{12b} on voltage load $V_{12a} + V_{12b}$ are constant as well.

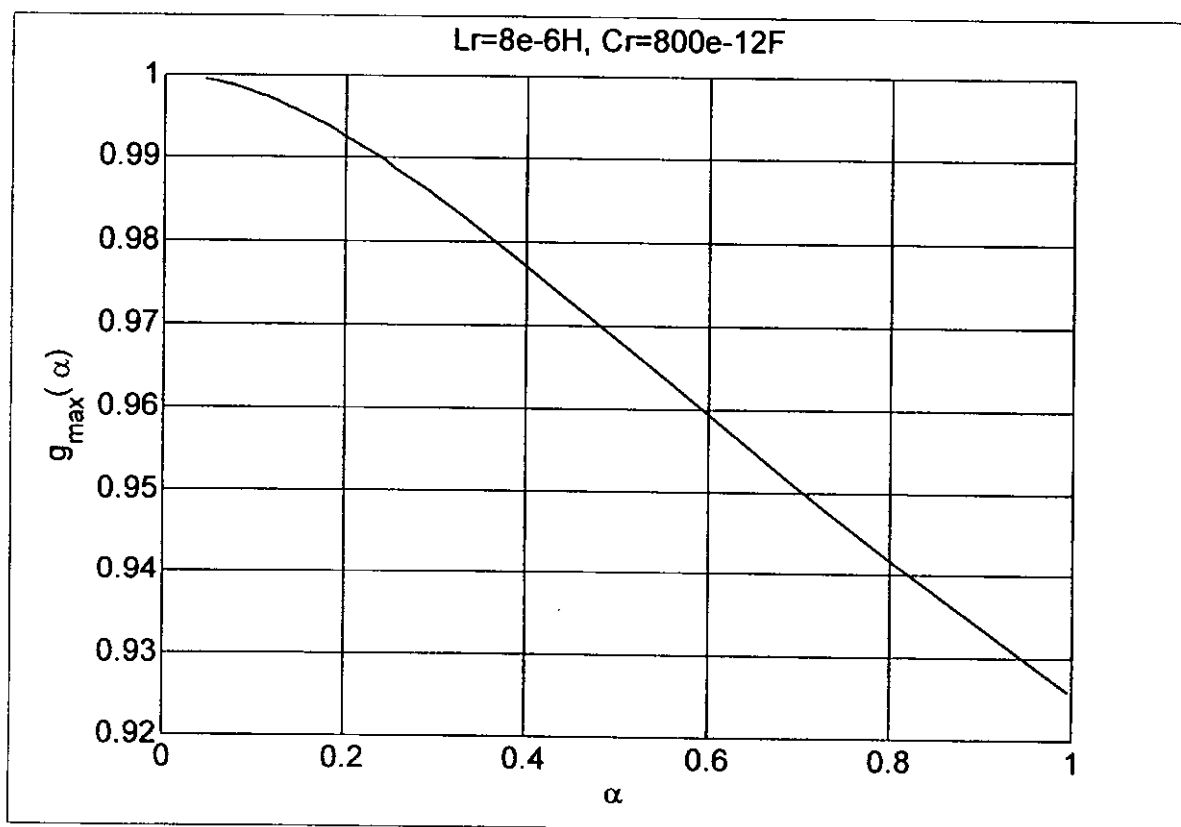


Fig. 2.6. Maximum Transfer Function $g_{\max}(\alpha)$ at $f_{\max}(\alpha)$.

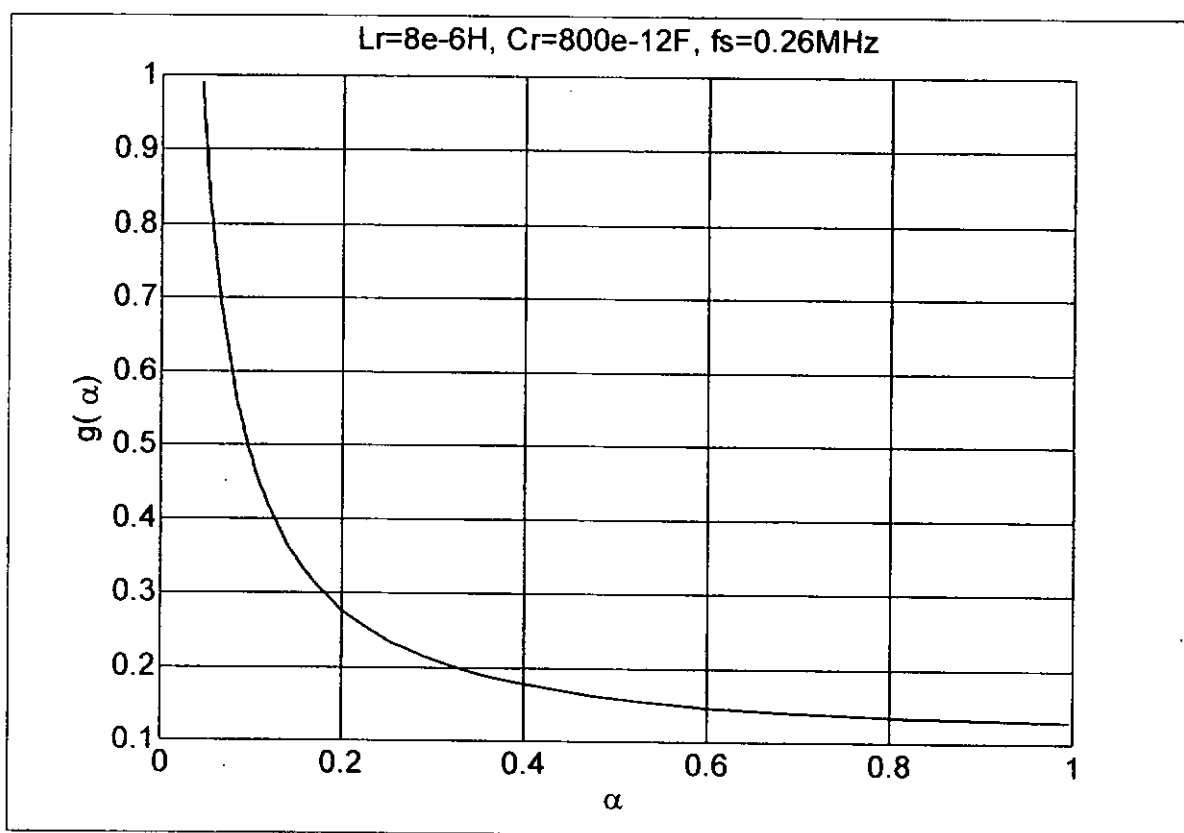


Fig. 2.7 Transfer Function $g(\alpha)$ at a fixed switching frequency $f_s = 260 \text{ kHz}$.

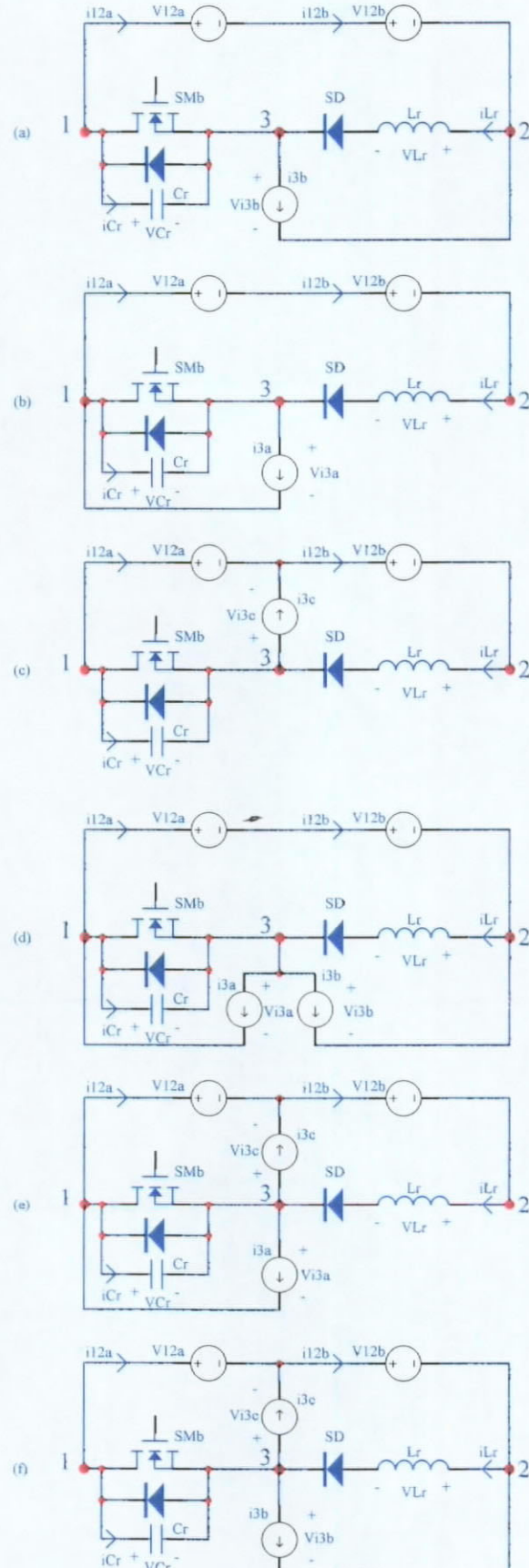


Fig. 2.8. Half-wave Type of FM ZVS QR Converters in Operation Model: (a) Buck, (b) Boost, (c) Buck-Boost, (d) Cuk, (e) Sepic and (f) Zeta.

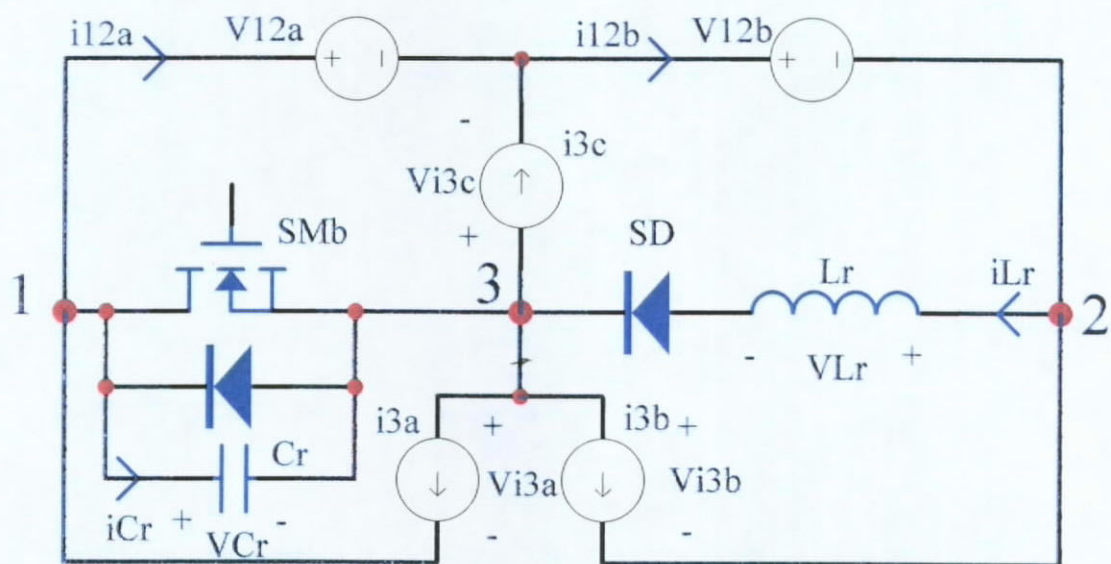


Fig. 2.9. General Operation Model of Half-wave Type of FM ZVS QR Converters.

Chapter 3 Power Distribution Analysis of Ideal ZVS QRSW

In Fig. 2.8, the constant voltage devices (voltage nodes) and constant current devices (current branches) can be considered as any power sources or power sinks. This chapter will try to analyze the impact and condition of the zero-voltage switching quasi-resonant switches. The theoretical active power distribution in the voltage nodes and current branches of each converter is plotted in Fig. 3.1 - Fig. 3.6. The positive value means that it is a power sink and the negative value means that it is a power source. They are summarized in Table 3-1.

In order to compare the simulation results with the experimental results in the TABLE II of [2] for Boost QRC, the following specifications are chosen because they used to compare with actual experimental results:

$$V_{12}=28.7, 37.6 \text{ and } 44.8V,$$

$$L_r=8\mu H,$$

$$C_r=800pF,$$

Fixed Switching Frequency $f_s=1\text{MHz}$.

The output load voltage is chosen to be 28.7V, 37.6V and 44.8V respectively because they are the experimental results under switching frequency at near 1MHz in [2]. The simulation result in Fig. 3.2 is comparable with the experimental results listed in TABLE II of [2]. From Table 3-1, it is interesting to note that the power attributes of the voltage nodes or current branches will change when the current i_3 increases. Moreover, in Buck-Boost and Cuk Converter, there is a zero cross point. It means that the active power in that voltage node or current branch is zero. On the other hand, in Sepic and Zeta Converter, there are two zero cross points. For example, the special operating point of Sepic is

$$\begin{aligned}\frac{V_{12a}}{V_{12a} + V_{12b}} &= \frac{i_{3c}}{i_{3a} + i_{3c}} \\ \frac{V_{12a}}{V_{12}} &= \frac{i_{3c}}{i_3}\end{aligned}\quad (3.1)$$

It is believed that the power loss at V_{12a} and i_{3c} is minimized at this operating point. If the constant voltage source V_{12a} and the constant current source i_{3c} are replaced by a capacitor and an inductor respectively, this operating condition must be achieved. It is because the ideal capacitor and the ideal inductor do not dissipate any active power. The only active power is considered because the large signal model is used to analyze the power distribution at the DC operating points in the complete switching cycle. Therefore, any instantaneous power components are neglected.

Starting from here to all the following sections, all the analysis was developed and observed by the author. They are the contributions to the new analysis in this thesis.

In the following sections, the conditions are analyzed in each topology by using Table 2-1, Fig. 2.2 and Fig. 2.8 so that all unknowns can be found by solving the system equations. Generally, the current in the voltage nodes and the voltage on the

current branches are unknowns. The load is assumed to be resistive due to simplifying the analysis and system equations.

Table 3-1. Power Attributes of FM ZVS QR Converters.

Converters	Power Equations (W)	Power Attributes	Zero Crossing Point	Voltage Node / Current Branch	Characteristic
Buck	$PV12a+V12b=(V12a+V12b) \times i3b \times (g(\alpha)-1)$	source		V12	Voltage Source
	$Pi3b=(V12a+V12b) \times i3b \times (1-g(\alpha))$	sink		i3b	Current Load
Boost	$PV12a+V12b=(V12a+V12b) \times i3a \times g(\alpha)$	sink		V12	Voltage Load
	$Pi3a=(V12a+V12b) \times i3a \times g(\alpha)$	source		i3a	Current Source
Buck-Boost	$PV12a=V12a \times i3c \times (g(\alpha)-1)$	source		V12a	Voltage Source
	$PV12b=V12b \times i3c \times g(\alpha)$	sink		V12b	Voltage Load
	$Pi3c=i3c \times (V12a-g(\alpha) \times (V12a+V12b))$	sink \Rightarrow source	$g(\alpha)=V12a / (V12a+V12b)$	i3c	Intermediate Current Branch
Cuk	$PV12a+V12b=(V12a+V12b) \times (g(\alpha) \times (i3a+i3b)-i3b)$	source \Rightarrow sink	$g(\alpha)=i3b / (i3a+i3b)$	V12	Intermediate Voltage Node
	$Pi3a=(V12a+V12b) \times i3a \times g(\alpha)$	source		i3a	Current Source
	$Pi3b=(V12a+V12b) \times i3b \times (1-g(\alpha))$	sink		i3b	Current Load
Sepic	$PV12a=V12a \times (g(\alpha) \times (i3a+i3c)-i3c)$	source \Rightarrow sink	$g(\alpha)=i3c / (i3a+i3c)$	V12a	Intermediate Voltage Node
	$PV12b=V12b \times (i3a+i3c) \times g(\alpha)$	sink		V12b	Voltage Load
	$Pi3a=(V12a+V12b) \times i3a \times g(\alpha)$	source		i3a	Current Source
	$Pi3c=i3c \times (V12a-g(\alpha)(V12a+V12b))$	sink \Rightarrow source	$g(\alpha)=V12a / (V12a+V12b)$	i3c	Intermediate Current Branch
Zeta	$PV12a=V12a \times (i3c+i3b) \times (g(\alpha)-1)$	source		V12a	Voltage Source
	$PV12b=V12b \times (g(\alpha) \times (i3c+i3b)-i3b)$	source \Rightarrow sink	$g(\alpha)=i3b / (i3c+i3b)$	V12b	Intermediate Voltage Node
	$Pi3c=i3c \times (V12a-g(\alpha) \times (V12a+V12b))$	sink \Rightarrow source	$g(\alpha)=V12a / (V12a+V12b)$	i3c	Intermediate Current Branch
	$Pi3b=i3b \times (V12a+V12b) \times (1-g(\alpha))$	sink		i3b	Current Load

3.1 QR Buck Converter

There are two unknowns in QR Buck Converter: the current i_{12} in the voltage source V_{12} and the voltage V_{i3b} on the current load I_{3b} . The transfer function will be a second order system because one capacitor and one inductor are in the circuit. Two system equations will be derived in order to solve the two unknowns. The i_{12} is dependent on i_{Lr} , and the V_{i3b} is also dependent on V_{Cr} , which are solved in equations (2.1) and (2.2) respectively. If the output voltage V_{i3b} is under regulation, the switching frequency f_s is chosen so that the output voltage V_{i3b} is kept constant. The active power P_{V12} on the voltage source V_{12} is negative under the definition of current flow direction because it delivers the power to the circuit. The active power P_{i3b} on the current load I_{3b} is positive because it dissipates the power from the circuit.

3.2 QR Boost Converter

There are two unknowns in QR Boost Converter: the current i_{12} in the voltage load V_{12} and the voltage V_{i3a} on the current source I_{3a} . The transfer function will be a second order system because one capacitor and one inductor are in the circuit. Two system equations will be derived in order to solve the two unknowns. The i_{12} is dependent on i_{Lr} , and the V_{i3a} is also dependent on V_{Cr} , which are solved in equations (2.1) and (2.2) respectively. If the output voltage V_{12} is under regulation, the switching frequency f_s is chosen so that the output current i_{12} is kept constant. The active power P_{i3a} on the current source I_{3a} is negative under the definition of current flow direction because it delivers the power to the circuit. The active power P_{V12} on the voltage load V_{12} is positive because it dissipates the power from the circuit.

3.3 QR Buck-Boost Converter

There are three unknowns in QR Buck-Boost Converter: the current i_{12a} in the voltage source V_{12a} , the current i_{12b} in the voltage load V_{12b} and the voltage V_{i3c} on the intermediate current branch I_{3c} . The transfer function will be a second order system because one capacitor and one inductor are in the circuit. Two system equations will be derived but three unknowns cannot be solved by using two system equations only. One more condition is needed. The intermediate current branch I_{3c} is transformed from an intermediate inductor shown in Fig. 2.2(c). The active power on I_{3c} should be near or equal to zero because the current and voltage are out of phase 90° in the intermediate inductor. Therefore, one more condition is the transfer function $g(\alpha) = V_{12a} / (V_{12a} + V_{12b})$ shown in Table 3-1 because the active power P_{i3c} on current branch I_{3c} is zero. Two KVL equations and one KCL equation can be derived. The i_{12b} is dependent on i_{Lr} , and the V_{i3c} is also dependent on V_{Cr} , which are solved in equations (2.1) and (2.2) respectively. If the output voltage V_{12b} is under regulation, the switching frequency f_s is chosen so that the output current i_{12b} is kept constant. The active power P_{V12a} on the voltage source V_{12a} is negative under the definition of current flow direction because it delivers the power to the circuit. The active power P_{V12b} on the voltage load V_{12b} is positive because it dissipates the power from the circuit.

3.4 QR Cuk Converter

There are three unknowns in QR Cuk Converter: the current i_{12} in the intermediate voltage node V_{12} , the voltage V_{i3a} on the current source I_{3a} and the voltage V_{i3b} on the current load I_{3b} . The transfer function will be a second order system because one capacitor and one inductor are in the circuit. Two system

equations will be derived but three unknowns cannot be solved by using two system equations only. One more condition is needed. The intermediate voltage node V_{12} is transformed from an intermediate capacitor shown in Fig. 2.2(d). The active power on V_{12} should be near or equal to zero because the current and voltage are out of phase 90° in the intermediate capacitor. Therefore, one more condition is the transfer function $g(\alpha) = I_{3b} / (I_{3a} + I_{3b})$ shown in Table 3-1 because the active power P_{V12} on intermediate voltage node V_{12} is zero. Two KVL equations and one KCL equation can be derived. The i_{12} is dependent on i_{Lr} , and the V_{i3a} and V_{i3b} are also dependent on V_{Cr} , which are solved in equations (2.1) and (2.2) respectively. If the output voltage V_{i3b} is under regulation, the switching frequency f_s is chosen so that the output voltage V_{i3b} and V_{Lr} are kept constant. The active power P_{i3a} on the current source I_{3a} is negative under the definition of current flow direction because it delivers the power to the circuit. The active power P_{i3b} on the current load I_{3b} is positive because it dissipates the power from the circuit.

3.5 QR Sepic Converter

There are four unknowns in QR Sepic Converter: the current I_{12a} in the intermediate voltage node V_{12a} , the current I_{12b} in the voltage load V_{12b} , the voltage V_{i3a} on the current source I_{3a} and the voltage V_{i3c} on the intermediate current branch I_{3c} . The transfer function will be a second order system because one capacitor and one inductor are in the circuit. Two system equations will be derived but four unknowns cannot be solved by using two system equations only. Two more conditions are needed. The intermediate voltage node V_{12a} is transformed from an intermediate capacitor and the intermediate current branch I_{3c} is transformed from an intermediate inductor shown in Fig. 2.2(e). The active power on V_{12a} and I_{3c} should

be near or equal to zero because the current and voltage are out of phase 90° in the intermediate capacitor and inductor. Therefore, two more conditions are the transfer function $g(\alpha) = I_{3c} / (I_{3a} + I_{3c})$ and $g(\alpha) = V_{12a} / (V_{12a} + V_{12b})$ shown in Table 3-1 because the active power P_{V12a} on intermediate voltage node V_{12a} and the active power P_{i3c} on intermediate current branch I_{3c} are zero. Two KVL equations and two KCL equations can be derived. The i_{12a} and i_{12b} are dependent on i_{Lr} , and the V_{i3a} and V_{i3c} are also dependent on V_{Cr} , which are solved in equations (2.1) and (2.2) respectively. If the output voltage V_{12b} is under regulation, the switching frequency f_s is chosen so that the output current I_{12b} is kept constant. The active power P_{i3a} on the current source I_{3a} is negative under the definition of current flow direction because it delivers the power to the circuit. The active power P_{V12b} on the voltage load V_{12b} is positive because it dissipates the power from the circuit.

3.6 QR Zeta Converter

There are four unknowns in QR Zeta Converter: the current I_{12a} in the voltage source V_{12a} , the current I_{12b} in the intermediate voltage node V_{12b} , the voltage V_{i3b} on the current load I_{3b} and the voltage V_{i3c} on the intermediate current branch I_{3c} . The transfer function will be a second order system because one capacitor and one inductor are in the circuit. Two system equations will be derived but four unknowns cannot be solved by using two system equations only. Two more conditions are needed. The intermediate voltage node V_{12b} is transformed from an intermediate capacitor and the intermediate current branch I_{3c} is transformed from an intermediate inductor shown in Fig. 2.2(f). The active power on V_{12b} and I_{3c} should be near or equal to zero because the current and voltage are out of phase 90° in the intermediate capacitor and inductor. Therefore, two more conditions are the transfer function

$g(\alpha) = I_{3b} / (I_{3b} + I_{3c})$ and $g(\alpha) = V_{12a} / (V_{12a} + V_{12b})$ shown in Table 3-1 because the active power P_{V12b} on intermediate voltage node V_{12b} and the active power P_{i3c} on intermediate current branch I_{3c} are zero. Two KVL equations and two KCL equations can be derived. The i_{12a} and i_{12b} are dependent on i_{Lr} , and the V_{i3b} and V_{i3c} are also dependent on V_{Cr} , which are solved in equations (2.1) and (2.2) respectively. If the output voltage V_{i3b} is under regulation, the switching frequency f_s is chosen so that the output voltage V_{i3b} and V_{Lr} are kept constant. The active power P_{V12a} on the voltage source V_{12a} is negative under the definition of current flow direction because it delivers the power to the circuit. The active power P_{i3b} on the current load I_{3b} is positive because it dissipates the power from the circuit.

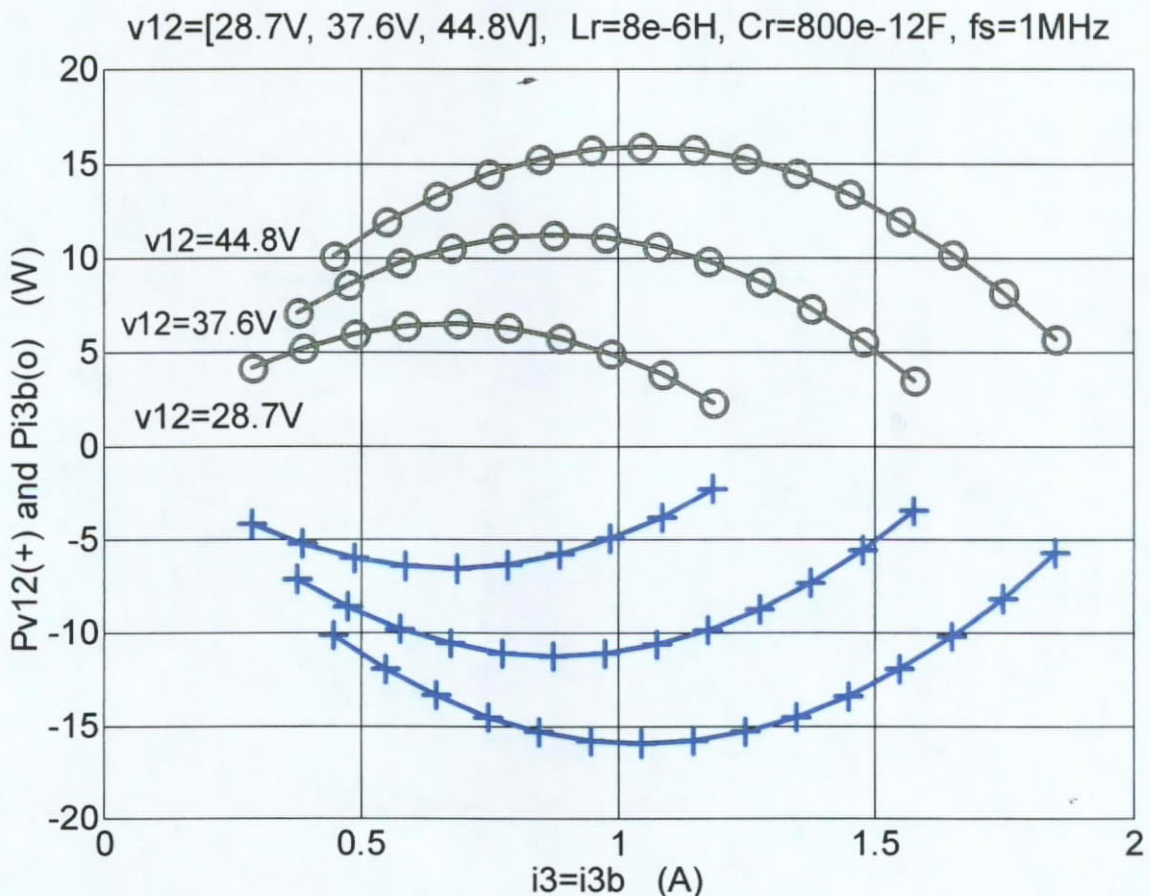


Fig. 3.1. Power Distribution of Half-wave Type of FM ZVS QR Buck Converters.

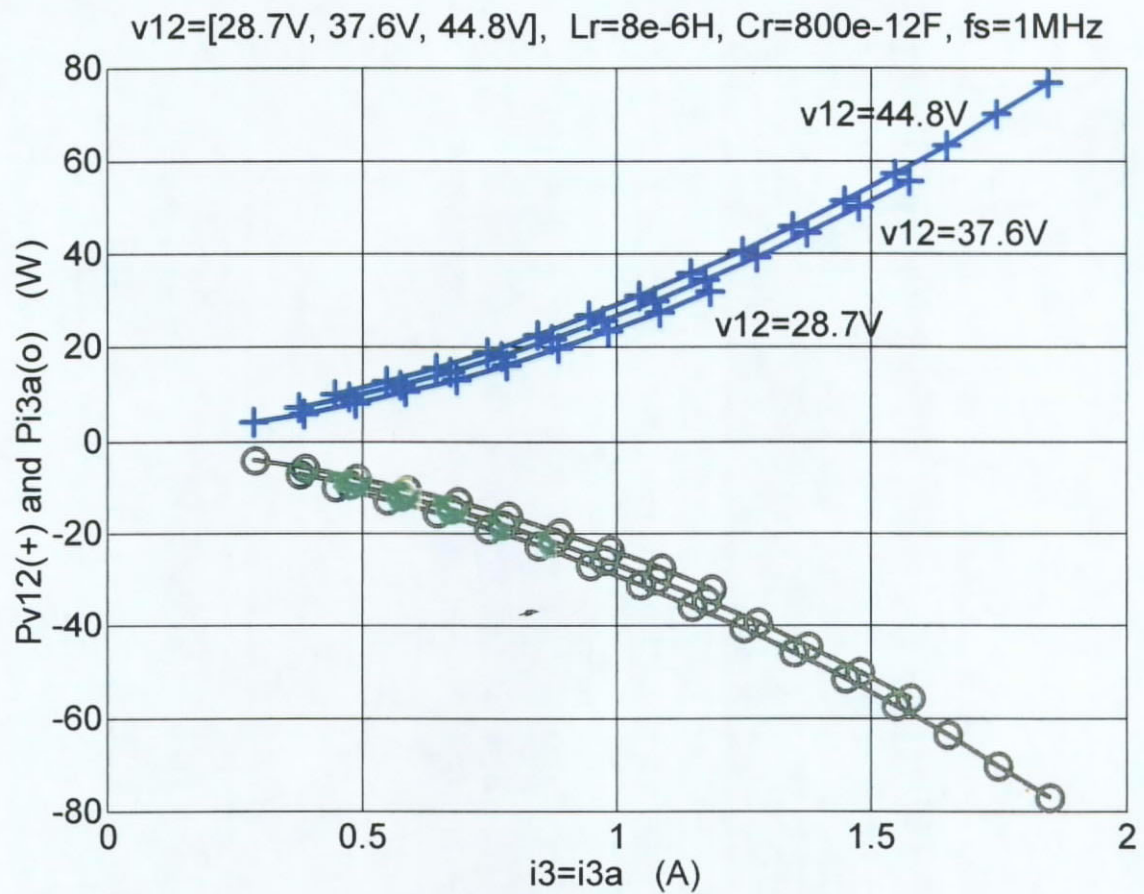


Fig. 3.2. Power Distribution of Half-wave Type of FM ZVS QR Boost Converters.

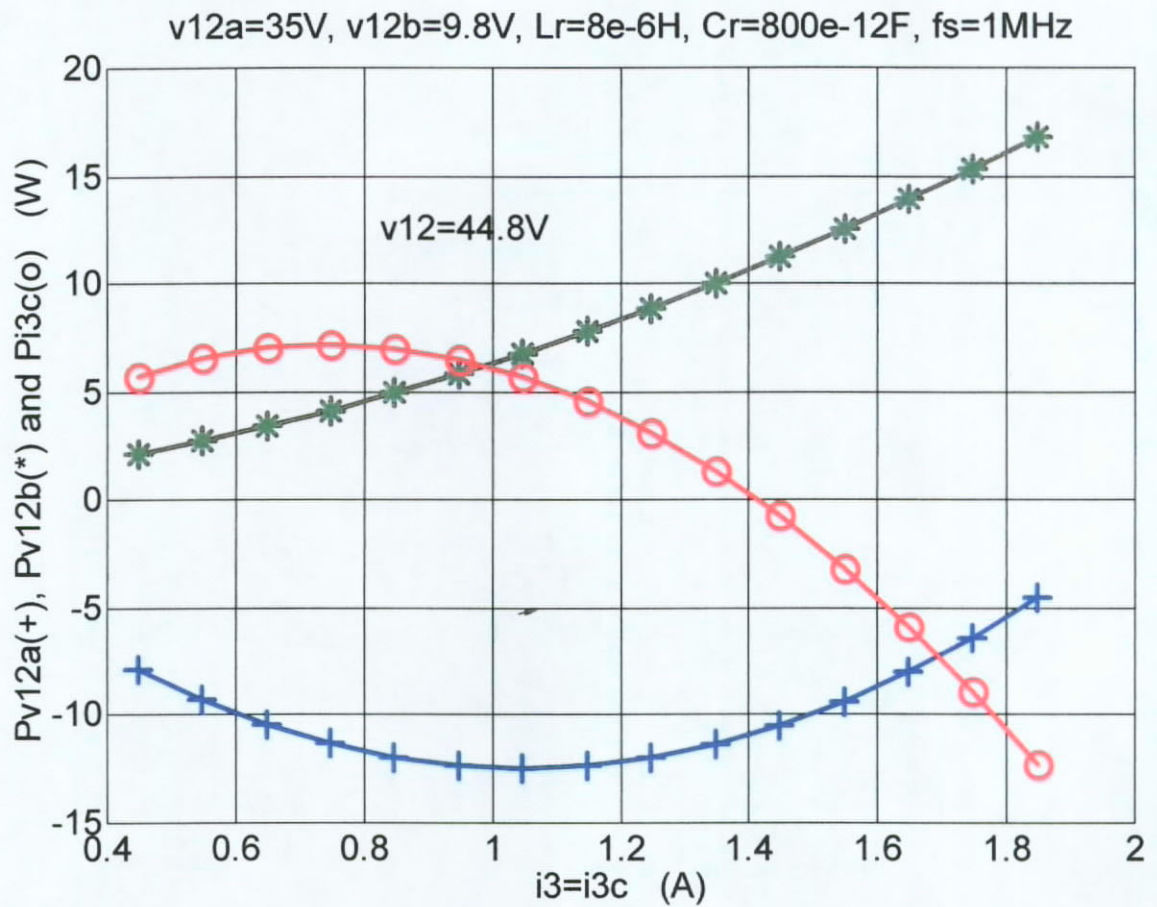


Fig. 3.3. Power Distribution of Half-wave Type of FM ZVS QR Buck-Boost Converters.

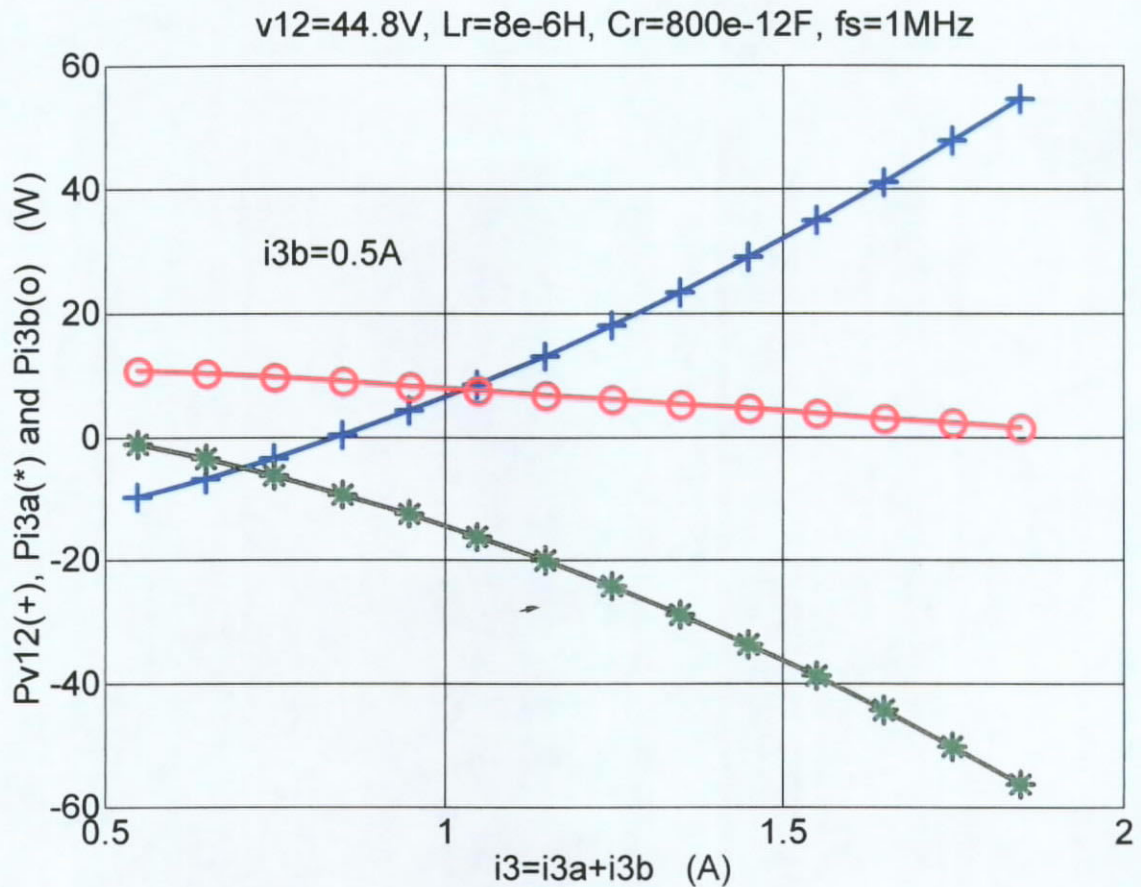


Fig. 3.4. Power Distribution of Half-wave Type of FM ZVS QR Cuk Converters.

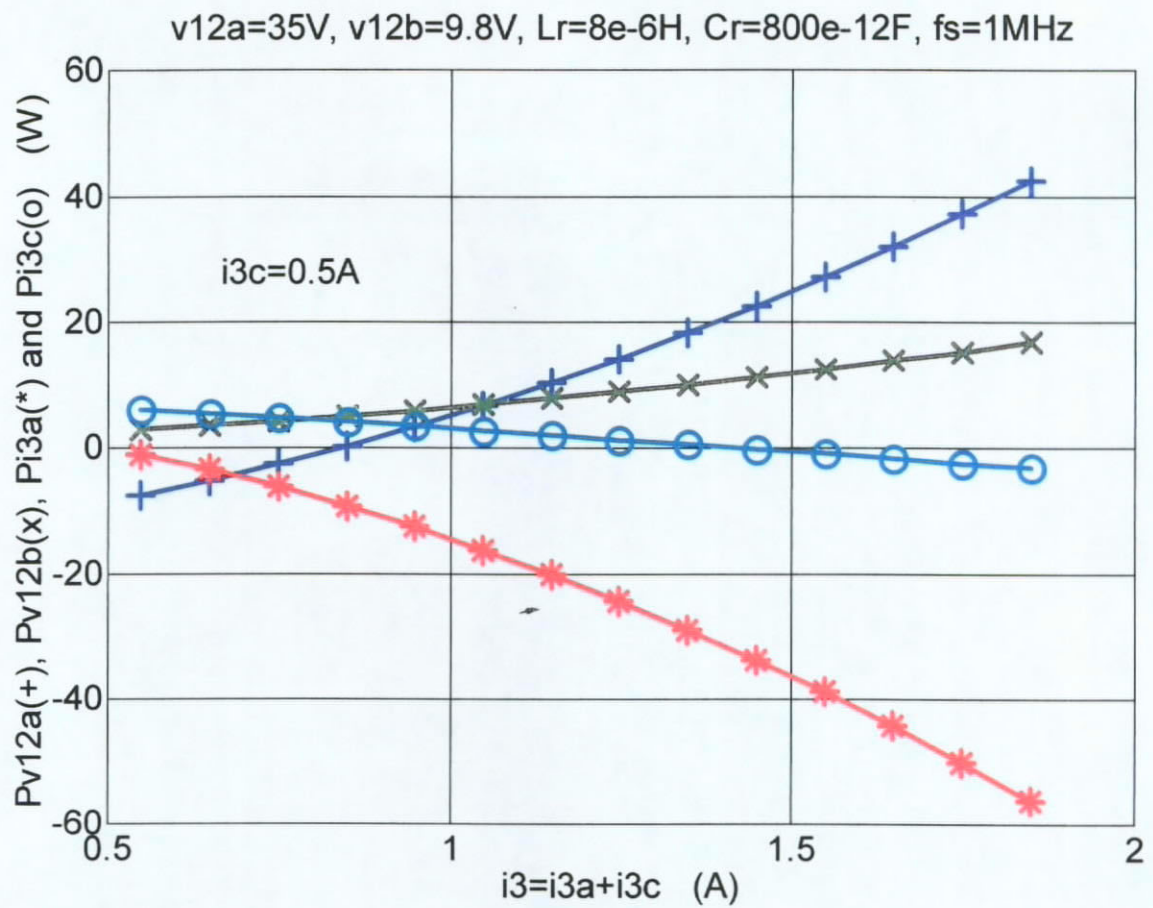


Fig. 3.5. Power Distribution of Half-wave Type of FM ZVS QR Sepic Converters.

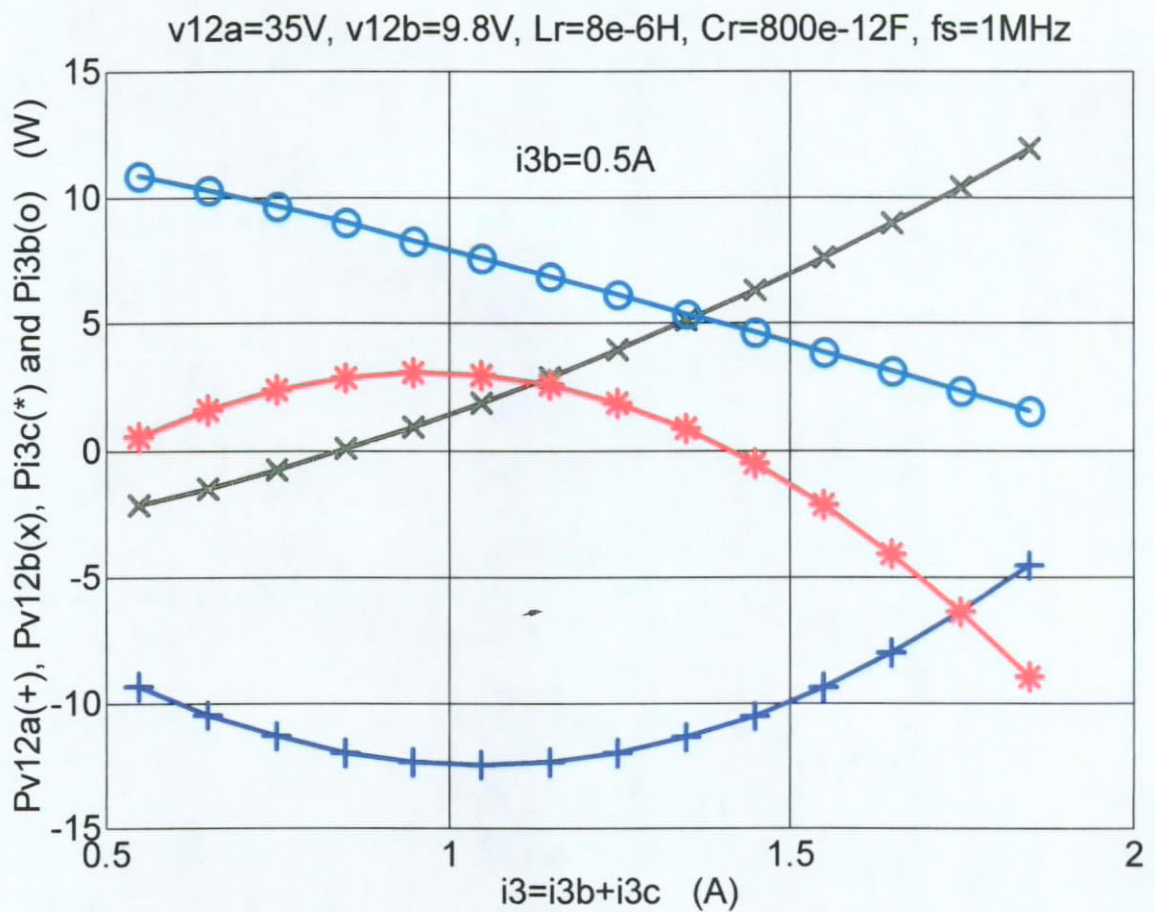


Fig. 3.6. Power Distribution of Half-wave Type of FM ZVS QR Zeta Converters.

Chapter 4 Modeling of Practical FM

ZVS QR Buck Converter

Starting from this chapter to all the following chapters, all the equations were developed and derived by the author. They are the major contributions to the new analysis in this thesis.

In order to analyze the efficiency of the converters, we have to consider the internal resistance of each component. After inserting the lossy components in the ideal model, a new near-practical model can be formed as shown in Fig. 4.1. The resistor R_{i3} is added to the current branch i_3 because the inductor current is originally replaced by i_3 . This component R_{i3} can be used to represent the equivalent resistance of the inductor. The components are defined as:

R_{12} is the internal equivalent resistance of V_{12} ,

R_{Cr} is the internal equivalent resistance of C_r ,

R_{Lr} is the internal equivalent resistance of L_r ,

R_{i3} is the internal equivalent resistance of i_3 ,

R_{SD} is the internal equivalent resistance of S_D ,

R_{SMa} is the internal equivalent resistance of S_{Ma} ,

R_{SMb} is the internal equivalent resistance of S_{Mb} ,

V_{FSD} is the forward bias voltage of S_D ,

V_{FSMa} is the forward bias voltage of S_{Ma} ,

V_{FSMb} is the forward bias voltage of S_{Mb} .

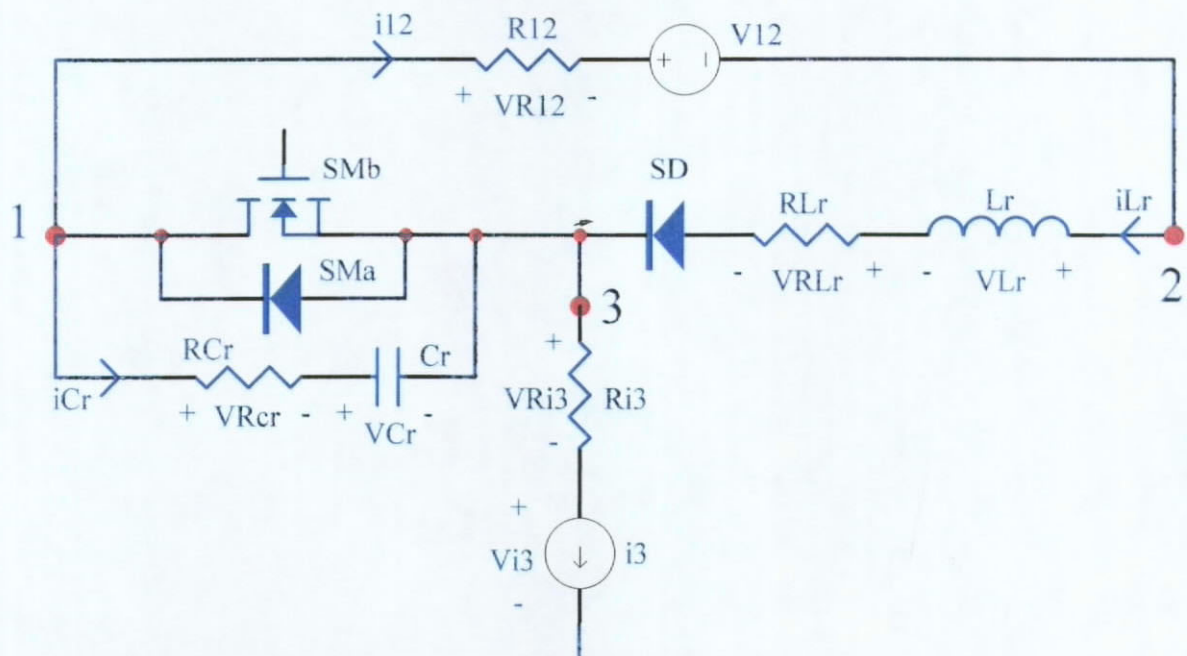


Fig. 4.1. Practical Model of FM ZVS QR Switch.

After the components are added, the switching waveforms are different from the ideal model. Therefore, we have to consider each converter again. The system equations are derived as follows:

4.1 Capacitor Charging Stage [T₀, T₁]

The diode S_D and the transistor S_M turn off at T₀, current i_{Cr}(t) flows through the capacitor C_r with internal resistance R_{Cr}. Because the current i₃ is assumed to be constant, the capacitor voltage V_{Cr}(t) rises linearly. Fig. 4.2 shows the equivalent circuit of FM ZVS QRSW in capacitor charging stage [T₀, T₁].

Initial conditions:

$$\begin{cases} i_{Lr}(0) = 0 , \\ v_{Cr}(0) = 0 . \end{cases} \quad (4.1)$$

State equations:

$$\begin{bmatrix} \frac{di_{Lr}(t)}{dt} \\ \frac{dv_{Cr}(t)}{dt} \end{bmatrix} = \begin{bmatrix} \frac{v_{Lr}(t)}{L_r} \\ \frac{i_{Cr}(t)}{C_r} \end{bmatrix} = \begin{bmatrix} 0 \\ \frac{i_3}{C_r} \end{bmatrix}. \quad (4.2)$$

The switching waveforms in capacitor charging stage are:

$$\begin{cases} v_{Cr}(t) = \frac{i_3}{C_r} \cdot t = \frac{V_{12} \cdot w_r}{\alpha} \cdot t , \\ i_{Cr}(t) = C_r \cdot \frac{dv_{Cr}(t)}{dt} = i_3 , \\ i_{Lr}(t) = 0 , \\ v_{Lr}(t) = L_r \cdot \frac{di_{Lr}(t)}{dt} = 0 , \end{cases} \quad (4.3)$$

where

$$\alpha = \frac{V_{12}}{Z_r \cdot i_3} . \quad (4.4)$$

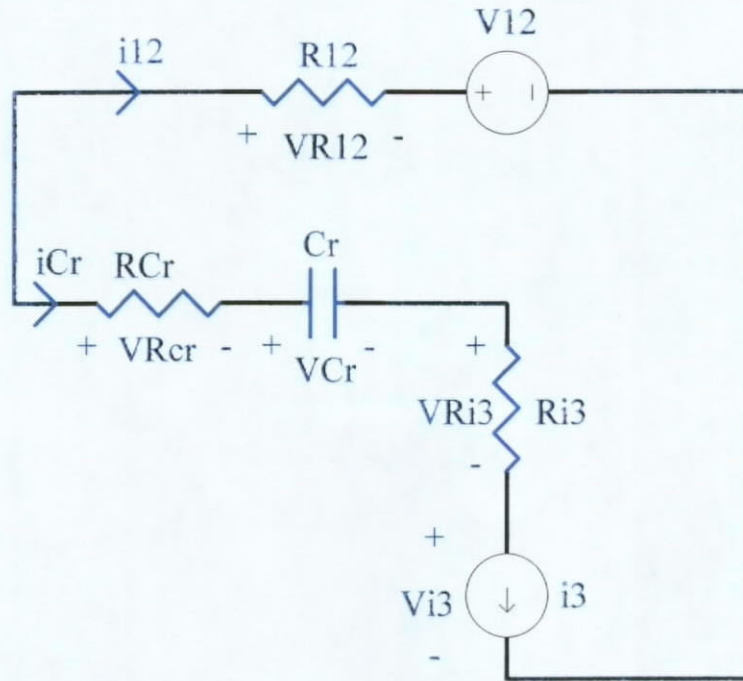


Fig. 4.2. Capacitor Charging Stage $[T_0, T_1]$ of FM ZVS QR Buck Converter.

At time T_1 , the diode S_D starts to conduct. The voltage on the diode S_D should be zero. Therefore, T_1 can be found by this equation,

$$v_{Cr}(T_1) + i_{Cr}(T_1) \cdot R_{Cr} = i_{12}(T_1) \cdot R_{12} + V_{12} . \quad (4.5)$$

Having solved the equation, we can write T_1 explicitly:

$$T_1 = \left(\frac{\alpha}{w_r} - C_r \cdot R_{CT} \right), \text{ where } R_{CT} = R_{12} + R_{Cr} . \quad (4.6)$$

4.2 Resonant Stage $[T_1, T_2]$

The diode S_D turns on at time T_1 , the capacitor voltage $v_{Cr}(t)$ resonates with the inductor current $i_{Lr}(t)$. However, there is an exponential damping factor associated with the switching waveforms. They are not purely sinusoidal. Fig. 4.3 shows the equivalent circuit of FM ZVS QRSW in resonant stage $[T_1, T_2]$.

Initial conditions:

$$\begin{cases} i_{Lr}(0) = 0 , \\ v_{Cr}(0) = \frac{i_3}{C_r} \cdot T_1 = V_{12} - i_3 \cdot R_{CT} . \end{cases} \quad (4.7)$$

State equations:

$$\begin{bmatrix} -L_r & R_{CT} \cdot C_r \\ 0 & C_r \end{bmatrix} \cdot \begin{bmatrix} \frac{di_{Lr}(t)}{dt} \\ \frac{dv_{Cr}(t)}{dt} \end{bmatrix} = \begin{bmatrix} R_{LT} & -1 \\ -1 & 0 \end{bmatrix} \cdot \begin{bmatrix} i_{Lr}(t) \\ v_{Cr}(t) \end{bmatrix} + \begin{bmatrix} V_{FSD} + V_{12} \\ i_3 \end{bmatrix}, \quad (4.8)$$

where

$$R_{CT} = R_{Cr} + R_{12} , \quad R_{LT} = R_{Lr} + R_{SD} . \quad (4.9)$$

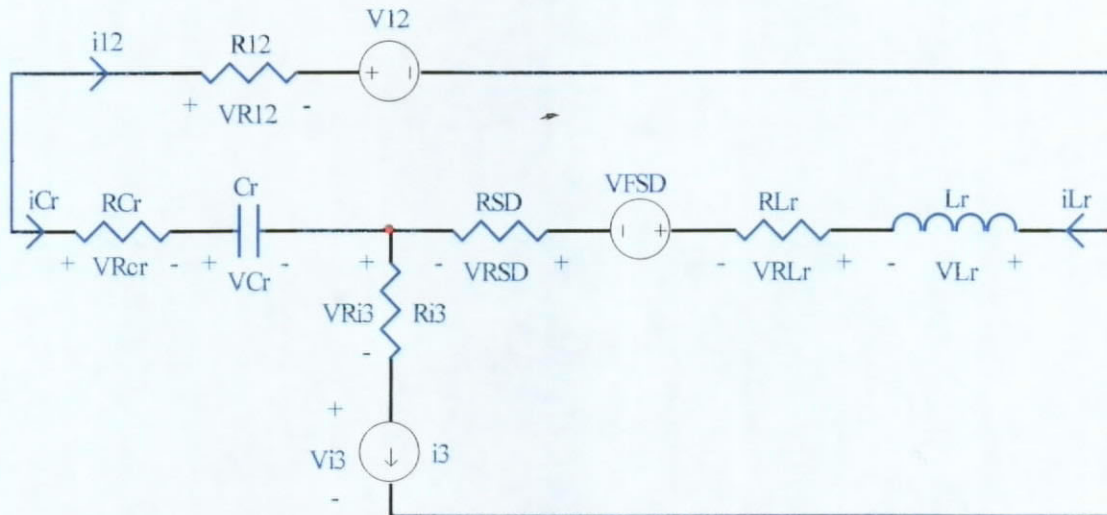


Fig. 4.3. Resonant Stage $[T_1, T_2]$ of FM ZVS QR Buck Converter.

The switching waveforms in resonant stage are:

$$\begin{cases} v_{Cr}(t) = C_1 + K_1 \cdot e^{-a(t-T_1)} \cdot \sin(\omega_o(t-T_1) + \theta_1) , \\ i_{Cr}(t) = K_2 \cdot e^{-a(t-T_1)} \cdot \sin(\omega_o(t-T_1) + \theta_2) , \\ i_{Lr}(t) = i_3 \cdot [1 - K_3 \cdot e^{-a(t-T_1)} \cdot \sin(\omega_o(t-T_1) + \theta_3)] , \\ v_{Lr}(t) = K_4 \cdot e^{-a(t-T_1)} \cdot \sin(\omega_o(t-T_1) + \theta_4) , \end{cases} \quad (4.10)$$

where

$$\begin{aligned}
 C_1 &= V_{12} + \frac{V_{12}}{\alpha} \left(\beta + \frac{R_{LT}}{Z_r} \right), \quad \beta = \frac{V_{FSD}}{Z_r \cdot i_3}, \\
 K_1 &= \frac{V_{12}}{\alpha} \sqrt{1 + \left(\frac{w_r}{w_o} \right)^2 \cdot \left(\frac{R_{ALL}}{2Z_r} + \beta \right)^2}, \\
 \theta_1 &= 2\pi - \tan^{-1} \left(\frac{\frac{R_{ALL}}{Z_r} + \beta}{\frac{w_r}{w_o} - \frac{a}{w_o} \cdot \left(\frac{R_{ALL}}{Z_r} + \beta \right)} \right), \\
 K_2 &= \frac{K_1}{Z_r}, \quad \theta_2 = \theta_1 + \pi - \tan^{-1} \left(\frac{w_o}{a} \right), \\
 K_3 &= \sqrt{1 + \left(\frac{1}{w_o} (\beta + a) \right)^2}, \quad \theta_3 = \tan^{-1} \left(\frac{w_o}{\beta + a} \right), \\
 K_4 &= i_3 \cdot Z_r \cdot K_3, \quad \theta_4 = \theta_3 + 2\pi - \tan^{-1} \left(\frac{w_o}{a} \right), \\
 a &= \frac{R_{ALL}}{2L_r}, \quad w_o = \sqrt{\frac{1}{L_r C_r} - \frac{R_{ALL}^2}{4L_r^2}} = \sqrt{w_r^2 - a^2}, \\
 R_{CT} &= R_{Cr} + R_{12}, \quad R_{LT} = R_{Lr} + R_{SD}, \\
 R_{ALL} &= R_{CT} + R_{LT} = R_{Cr} + R_{12} + R_{Lr} + R_{SD}. \tag{4.11}
 \end{aligned}$$

From the equations (4.10), we know that the switching waveforms have a damping factor “ a ” = $R_{ALL}/(2L_r)$. They are not purely sinusoidal because of the internal resistance of each component. Moreover, the damping factor “ a ” shifts the resonant angular frequency from w_r to w_o . Obviously, the real resonant angular frequency w_o is smaller than the ideal resonant angular frequency w_r .

At time T_2 , the switch S_M starts to conduct. In order to achieve ZVS, the voltage on the switch S_M should be zero. Therefore, T_2 can be found by this equation,

$$v_{Cr}(T_2) + i_{Cr}(T_2) \cdot R_{Cr} = 0. \tag{4.12}$$

The equation is simplified to

$$C_1 + K_{T2} \cdot e^{-a(T_2-T_1)} \cdot \sin(w_o(T_2 - T_1) + \theta_{T2}) = 0 , \quad (4.13)$$

where

$$K_{T2} = K_1 R_{Cr} C_r \sqrt{\left(\frac{1}{R_{Cr} C_r} - a\right)^2 + w_o^2} \quad (4.14)$$

and

$$\theta_{T2} = \theta_1 + \tan^{-1} \left(\frac{\frac{w_o}{1}}{\frac{1}{R_{Cr} C_r} - a} \right) . \quad (4.15)$$

Unfortunately, the time T_2 cannot be written explicitly because of the exponential term in equation (4.13). We have to solve it by using numerical method.

4.3 Inductor Discharging Stage [T₂, T₃]

After the time T_2 , the capacitor voltage $v_{Cr}(t)$ reaches zero and the switch S_M turns on. The inductor current $i_L(t)$ decreases to zero at time T_3 . During this stage, the capacitor voltage $v_{Cr}(t)$ in the practical circuits will not keep zero but very small, therefore, the power loss in the capacitor C_r is negligible.

Since S_M is a current bi-directional switch, the forward bias voltage drop will be different. Equation (4.17) and (4.24) describe the inductor current $i_{Lr}(t)$ for $i_{SM}(t) < 0$ and $i_{SM}(t) > 0$ respectively. It is necessary to add an intermediate stage T_a between T_2 and T_3 . Therefore, the first inductor discharging stage in section 4.3.1 considers the time between T_2 and T_a when the current $i_{SM}(t) < 0$. Then, the second discharging stage in section 4.3.2 considers the time between T_a and T_3 when the current $i_{SM}(t) > 0$. The results are summarized in the equation (4.30).

4.3.1 First Inductor Discharging Stage [T₂, T_a]

Fig. 4.4 shows the equivalent circuit of FM ZVS QRSW in first inductor discharging stage [T₂, T_a].

Initial conditions:

$$i_{Lr}(0) = i_3 \cdot [1 - K_3 \cdot e^{-a(T_2-T_1)} \cdot \sin(w_o(T_2 - T_1) + \theta_3)] . \quad (4.16)$$

State equation:

$$\begin{aligned} \frac{di_{Lr}(t)}{dt} &= -\frac{R_{SD} + R_{Lr} + R_{12} + R_{SMa}}{L_r} \cdot i_{Lr}(t) \\ &\quad - \frac{V_{FSD} + V_{FSMa} + V_{12} - i_3 \cdot (R_{12} + R_{SMa})}{L_r}, \text{ for } i_{SM}(t) < 0 . \end{aligned} \quad (4.17)$$

Therefore,

$$i_{Lr}(t) = C_{sa} + K_{sa} \cdot e^{-Aa(t-T_2)} \quad (4.18)$$

where

$$\begin{aligned} C_{sa} &= \frac{i_3 \cdot (R_{12} + R_{SMa}) - V_{FSD} - V_{FSMa} - V_{12}}{R_{SD} + R_{Lr} + R_{12} + R_{SMa}} , \\ K_{sa} &= i_3 \cdot [1 - K_3 \cdot e^{-a(T_2-T_1)} \cdot \sin(w_o(T_2 - T_1) + \theta_3)] - C_{sa} \end{aligned} \quad (4.19)$$

and

$$A_a = \frac{R_{SD} + R_{Lr} + R_{12} + R_{SMa}}{L_r} . \quad (4.20)$$

The switch S_M changes the direction of forward bias voltage when i_{SM}(t) = 0 at time T_a. Then, the time T_a can be found by solving

$$i_{SM}(T_a) = i_3 - i_{Lr}(T_a) = 0 . \quad (4.21)$$

Therefore,

$$T_a = T_2 - \frac{1}{A_a} \cdot \ln \left(\frac{i_3 - C_{sa}}{K_{sa}} \right) . \quad (4.22)$$

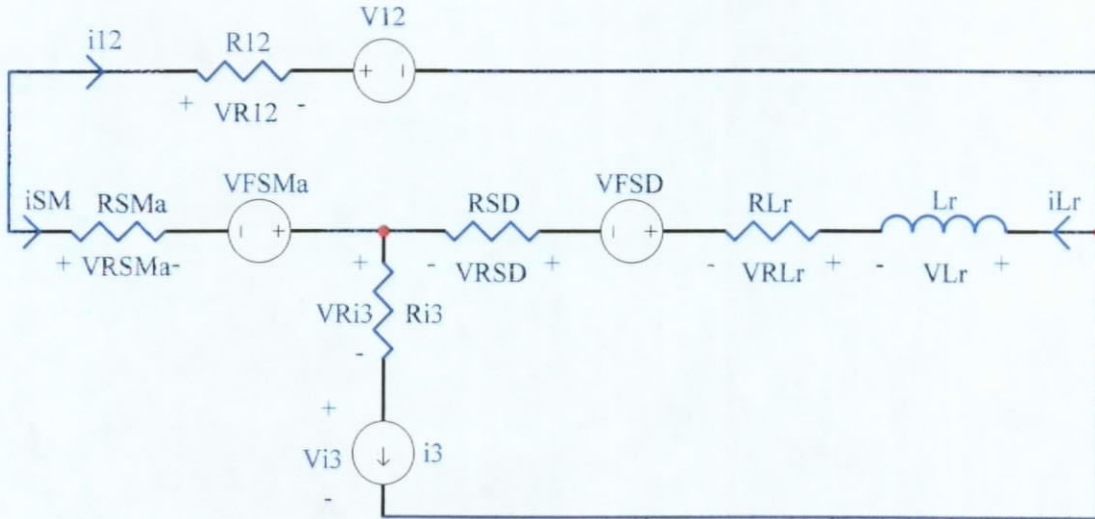


Fig. 4.4. Inductor Discharging Stage $[T_2, T_a]$ of FM ZVS QR Buck Converter.

4.3.2 Second Inductor Discharging Stage $[T_a, T_3]$

Fig. 4.5 shows the equivalent circuit of FM ZVS QRSW in second inductor discharging stage $[T_a, T_3]$.

Initial conditions:

$$i_{Lr}(0) = C_{5a} + K_{5a} \cdot e^{-Aa \cdot (Ta - T_2)} = i_3 . \quad (4.23)$$

State equation:

$$\begin{aligned} \frac{di_{Lr}(t)}{dt} &= -\frac{R_{SD} + R_{Lr} + R_{12} + R_{SMb}}{L_r} \cdot i_{Lr}(t) \\ &\quad - \frac{V_{FSD} - V_{FSMb} + V_{12} - i_3 \cdot (R_{12} + R_{SMb})}{L_r}, \text{ for } i_{SM}(t) > 0 . \end{aligned} \quad (4.24)$$

Therefore,

$$i_{Lr}(t) = C_{5b} + K_{5b} \cdot e^{-Ab \cdot (t - Ta)} \quad (4.25)$$

where

$$\begin{aligned} C_{5b} &= \frac{i_3 \cdot (R_{12} + R_{SMb}) - V_{FSD} + V_{FSMb} - V_{12}}{R_{SD} + R_{Lr} + R_{12} + R_{SMb}} , \\ K_{5b} &= i_3 - C_{5b} \end{aligned} \quad (4.26)$$

and

$$A_b = \frac{R_{SD} + R_{Lr} + R_{12} + R_{SMb}}{L_r} . \quad (4.27)$$

At time T_3 , the inductor current $i_{Lr}(t)$ reaches zero. Then, T_3 can be found by this equation

$$i_{Lr}(T_3) = C_{5b} + K_{5b} \cdot e^{-Ab \cdot (T_3 - T_a)} = 0 . \quad (4.28)$$

Therefore,

$$T_3 = T_a - \frac{1}{A_b} \cdot \ln\left(\frac{-C_{5b}}{K_{5b}}\right) . \quad (4.29)$$

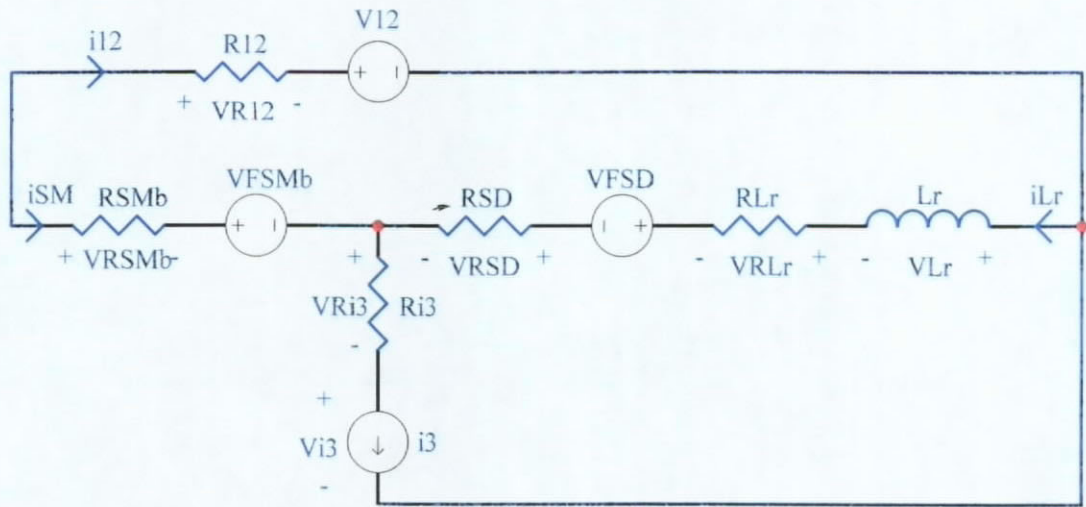


Fig. 4.5. Inductor Discharging Stage [T_a, T_3] of FM ZVS QR Buck Converter.

The switching waveforms in inductor discharging stage are:

$$\begin{cases} v_{Cr}(t) = 0 \text{ and } i_{Cr}(t) = 0 , \\ i_{Lr}(t) = \begin{cases} C_{5a} + K_{5a} \cdot e^{-Aa(t-T_2)} , & \text{for } T_2 < t < T_a \\ C_{5b} + K_{5b} \cdot e^{-Ab(t-T_a)} , & \text{for } T_a < t < T_3 \end{cases} , \\ v_{Lr}(t) = \begin{cases} K_{6a} \cdot e^{-Aa(t-T_2)} , & \text{for } T_2 < t < T_a \\ K_{6b} \cdot e^{-Ab(t-T_a)} , & \text{for } T_a < t < T_3 \end{cases} , \\ i_{SM}(t) = i_3 - i_{Lr}(t) , \end{cases} \quad (4.30)$$

where

$$K_{6a} = -L_r \cdot K_{5a} \cdot A_a \quad \text{and} \quad K_{6b} = -L_r \cdot K_{5b} \cdot A_b . \quad (4.31)$$

4.4 Free-Wheeling Stage $[T_3, T_s]$

After the time T_3 , both capacitor voltage $v_{Cr}(t)$ and inductor current $i_{Lr}(t)$ reach zero and the diode S_D turns off. The switch S_M still turns on and the constant current i_3 flows through S_M . Fig. 4.6 shows the equivalent circuit of FM ZVS QRSW in free-wheeling stage $[T_3, T_s]$.

The switching waveforms in free-wheeling stage are:

$$\begin{cases} v_{Cr}(t) = 0 , \\ i_{Cr}(t) = 0 , \\ i_{Lr}(t) = 0 , \\ v_{Lr}(t) = 0 , \\ i_{SM}(t) = i_3 . \end{cases} \quad (4.32)$$

At time T_s , the switch S_M will turn off and the capacitor C_r will be charged linearly again because one switching cycle is complete at T_s .

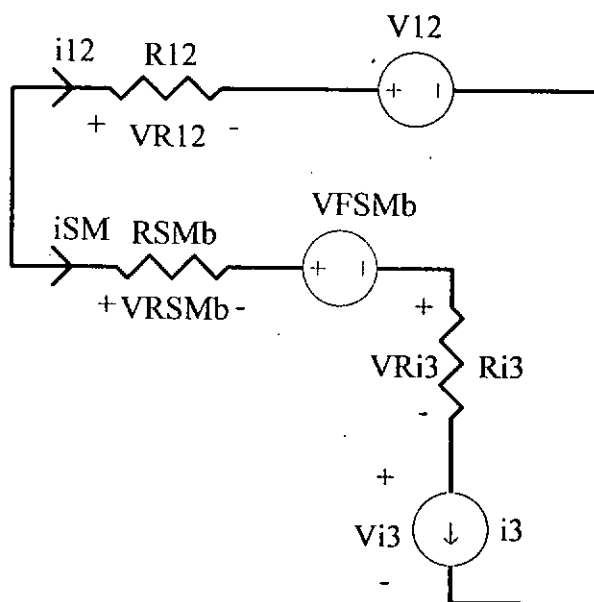


Fig. 4.6. Free-Wheeling Stage $[T_3, T_s]$ of FM ZVS QR Buck Converter.

Chapter 5 Modeling of Practical FM

ZVS QR Boost Converter

In the following chapters, all the equations were developed and derived by the author. They are the major contributions to the new analysis in this thesis.

5.1 Capacitor Charging Stage [T₀, T₁]

The diode S_D and the transistor S_M turn off at T₀, current i_{Cr}(t) flows through the capacitor C_r with internal resistance R_{Cr}.

Initial conditions:

$$\begin{cases} i_{Lr}(0) = 0 , \\ v_{Cr}(0) = 0 . \end{cases} \quad (5.1)$$

State equations:

$$\begin{bmatrix} \frac{di_{Lr}(t)}{dt} \\ \frac{dv_{Cr}(t)}{dt} \end{bmatrix} = \begin{bmatrix} \frac{v_{Lr}(t)}{L_r} \\ \frac{i_{Cr}(t)}{C_r} \end{bmatrix} = \begin{bmatrix} 0 \\ \frac{i_3}{C_r} \end{bmatrix}. \quad (5.2)$$

Because the current i₃ is assumed to be constant, the capacitor voltage V_{Cr}(t) rises

linearly. Fig. 5.1 shows the equivalent circuit of FM ZVS QRSW in capacitor charging stage $[T_0, T_1]$. The switching waveforms in capacitor charging stage are:

$$\begin{cases} v_{Cr}(t) = \frac{i_3}{C_r} \cdot t = \frac{V_{12} \cdot w_r}{\alpha} \cdot t , \\ i_{Cr}(t) = C_r \cdot \frac{dv_{Cr}(t)}{dt} = i_3 , \\ i_{Lr}(t) = 0 , \\ v_{Lr}(t) = L_r \cdot \frac{di_{Lr}(t)}{dt} = 0 , \end{cases} \quad (5.3)$$

where

$$\alpha = \frac{V_{12}}{Z_r \cdot i_3} . \quad (5.4)$$

At time T_1 , the diode S_D starts to conduct. The voltage on the diode S_D should be zero. Therefore, T_1 can be found by this equation,

$$v_{Cr}(T_1) + i_3 \cdot R_{Cr} = V_{12} . \quad (5.5)$$

Having solved the equation, we can write T_1 explicitly:

$$T_1 = \left(\frac{\alpha}{w_r} - C_r \cdot R_{Cr} \right) . \quad (5.6)$$

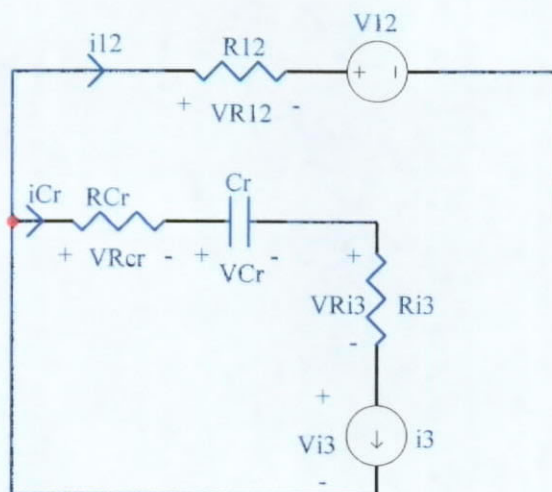


Fig. 5.1. Capacitor Charging Stage $[T_0, T_1]$ of FM ZVS QR Boost Converter.

5.2 Resonant Stage [T₁, T₂]

The diode S_D turns on at time T₁, the capacitor voltage v_{Cr}(t) resonates with the inductor current i_{Lr}(t). However, there is an exponential damping factor associated with the switching waveforms. They are not purely sinusoidal. Fig. 5.2 shows the equivalent circuit of FM ZVS QRSW in resonant stage [T₁, T₂].

Initial conditions:

$$\begin{cases} i_{Lr}(0) = 0 , \\ v_{Cr}(0) = \frac{i_3}{C_r} \cdot T_1 = V_{12} - i_3 \cdot R_{Cr} . \end{cases} \quad (5.7)$$

State equations:

$$\begin{bmatrix} -L_r & R_{Cr} \cdot C_r \\ 0 & C_r \end{bmatrix} \begin{bmatrix} \frac{di_{Lr}(t)}{dt} \\ \frac{dv_{Cr}(t)}{dt} \end{bmatrix} = \begin{bmatrix} R_{LT} + R_{12} & -1 \\ -1 & 0 \end{bmatrix} \begin{bmatrix} i_{Lr}(t) \\ v_{Cr}(t) \end{bmatrix} + \begin{bmatrix} V_{FSD} + V_{12} \\ i_3 \end{bmatrix}, \quad (5.8)$$

where

$$R_{LT} = R_{Lr} + R_{SD} . \quad (5.9)$$

The switching waveforms in resonant stage are:

$$\begin{cases} v_{Cr}(t) = C_1 + K_1 \cdot e^{-a(t-T_1)} \cdot \sin(w_o(t-T_1) + \theta_1) , \\ i_{Cr}(t) = K_2 \cdot e^{-a(t-T_1)} \cdot \sin(w_o(t-T_1) + \theta_2) , \\ i_{Lr}(t) = i_3 \cdot [1 - K_3 \cdot e^{-a(t-T_1)} \cdot \sin(w_o(t-T_1) + \theta_3)] , \\ v_{Lr}(t) = K_4 \cdot e^{-a(t-T_1)} \cdot \sin(w_o(t-T_1) + \theta_4) , \end{cases} \quad (5.10)$$

where

$$\begin{aligned}
 C_1 &= V_{12} + \frac{V_{12}}{\alpha} \left(\beta + \frac{R_{LT} + R_{12}}{Z_r} \right), \quad \beta = \frac{V_{FSD}}{Z_r \cdot i_3}, \\
 K_1 &= \frac{V_{12}}{\alpha} \sqrt{1 + \left(\frac{w_r}{w_o} \right)^2 \cdot \left(\frac{R_{ALL}}{2Z_r} + \beta \right)^2}, \\
 \theta_1 &= 2\pi - \tan^{-1} \left(\frac{\frac{R_{ALL}}{Z_r} + \beta}{\frac{w_r}{w_o} - \frac{\alpha}{w_o} \cdot \left(\frac{R_{ALL}}{Z_r} + \beta \right)} \right), \\
 K_2 &= \frac{K_1}{Z_r}, \quad \theta_2 = \theta_1 + \pi - \tan^{-1} \left(\frac{w_o}{a} \right), \\
 K_3 &= \sqrt{1 + \left(\frac{1}{w_o} (\beta + a) \right)^2}, \quad \theta_3 = \tan^{-1} \left(\frac{w_o}{\beta + a} \right), \\
 K_4 &= i_3 \cdot Z_r \cdot K_3, \quad \theta_4 = \theta_3 + 2\pi - \tan^{-1} \left(\frac{w_o}{a} \right), \\
 a &= \frac{R_{ALL}}{2L_r}, \quad w_o = \sqrt{\frac{1}{L_r C_r} - \frac{R_{ALL}^2}{4L_r^2}} = \sqrt{w_r^2 - a^2}, \\
 R_{CT} &= R_{Cr} + R_{12}, \quad R_{LT} = R_{Lr} + R_{SD}, \\
 R_{ALL} &= R_{CT} + R_{LT} = R_{Cr} + R_{12} + R_{Lr} + R_{SD}. \tag{5.11}
 \end{aligned}$$

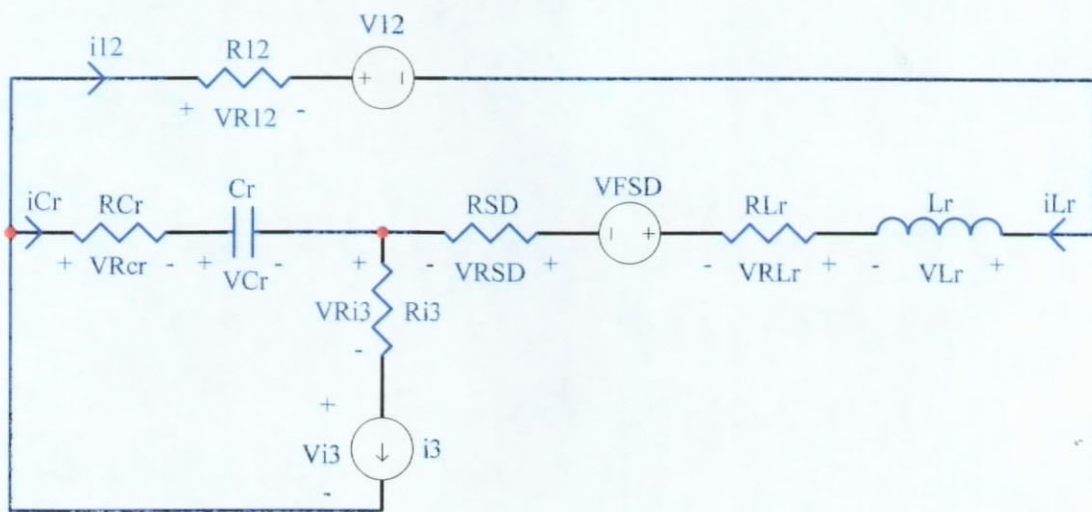


Fig. 5.2. Resonant Stage $[T_1, T_2]$ of FM ZVS QR Boost Converter.

From the equations (5.10), we know that the switching waveforms have a damping factor $a = R_{\text{ALL}} / (2L_r)$. They are not purely sinusoidal because of the internal resistance of each component. Moreover, the damping factor a shifts the resonant angular frequency from w_r to w_o . Obviously, the real resonant angular frequency w_o is smaller than the ideal resonant angular frequency w_r .

At time T_2 , the switch S_M starts to conduct. In order to achieve ZVS, the voltage on the switch S_M should be zero. Therefore, T_2 can be found by this equation,

$$v_{Cr}(T_2) + i_{Cr}(T_2) \cdot R_{Cr} = 0 . \quad (5.12)$$

The equation is simplified to

$$C_1 + K_{T2} \cdot e^{-a(T_2-T_1)} \cdot \sin(w_o(T_2 - T_1) + \theta_{r2}) = 0 , \quad (5.13)$$

where

$$K_{T2} = K_1 R_{Cr} C_r \sqrt{\left(\frac{1}{R_{Cr} C_r} - a \right)^2 + w_o^2} \quad (5.14)$$

and

$$\theta_{T2} = \theta_1 + \tan^{-1} \left(\frac{\frac{w_o}{1}}{\frac{1}{R_{Cr} C_r} - a} \right) . \quad (5.15)$$

Unfortunately, the time T_2 cannot be written explicitly because of the exponential term in equation (5.13). We have to solve it by using numerical method.

5.3 Inductor Discharging Stage [T₂, T₃]

After the time T_2 , the capacitor voltage $v_{Cr}(t)$ reaches zero and the switch S_M turns on. The inductor current $i_{Lr}(t)$ decreases to zero at time T_3 . During this stage, the

capacitor voltage $v_{Cr}(t)$ in the practical circuits will not keep zero but very small, therefore, the power loss in the capacitor C_r is negligible.

Since S_M is a current bi-directional switch, the forward bias voltage drop will be different. Equation (5.17) and (5.24) describe the inductor current $i_{Lr}(t)$ for $i_{SM}(t)<0$ and $i_{SM}(t)>0$ respectively. It is necessary to add an intermediate stage T_a between T_2 and T_3 .

5.3.1 First Inductor Discharging Stage [T_2, T_a]

Fig. 5.3 shows the equivalent circuit of FM ZVS QRSW in first inductor discharging stage [T_2, T_a].

Initial conditions:

$$i_{Lr}(0) = i_3 \cdot [1 - K_3 \cdot e^{-a(T_2-T_1)} \cdot \sin(w_o(T_2 - T_1) + \theta_3)] . \quad (5.16)$$

State equation:

$$\begin{aligned} \frac{di_{Lr}(t)}{dt} &= -\frac{R_{SD} + R_{Lr} + R_{12} + R_{SMa}}{L_r} \cdot i_{Lr}(t) \\ &\quad - \frac{V_{FSD} + V_{FSMa} + V_{12} - i_3 \cdot R_{SMa}}{L_r}, \text{ for } i_{SM}(t) < 0. \end{aligned} \quad (5.17)$$

Therefore,

$$i_{Lr}(t) = C_{sa} + K_{sa} \cdot e^{-Aa \cdot (t-T_2)} \quad (5.18)$$

where

$$C_{5a} = \frac{i_3 \cdot R_{SMA} - V_{FSD} - V_{FSMA} - V_{12}}{R_{SD} + R_{Lr} + R_{12} + R_{SMA}},$$

$$K_{5a} = i_3 \cdot [1 - K_3 \cdot e^{-\alpha(T_2 - T_1)} \cdot \sin(\omega_o(T_2 - T_1) + \theta_3)] - C_{5a} \quad (5.19)$$

and

$$A_a = \frac{R_{SD} + R_{Lr} + R_{12} + R_{SMA}}{L_r}. \quad (5.20)$$

The switch S_M changes the direction of forward bias voltage when $i_{SM}(t) = 0$ at time T_a . Then, the time T_a can be found by solving

$$i_{SM}(T_a) = i_3 - i_{Lr}(T_a) = 0. \quad (5.21)$$

Therefore,

$$T_a = T_2 - \frac{1}{A_a} \cdot \ln \left(\frac{i_3 - C_{5a}}{K_{5a}} \right). \quad (5.22)$$

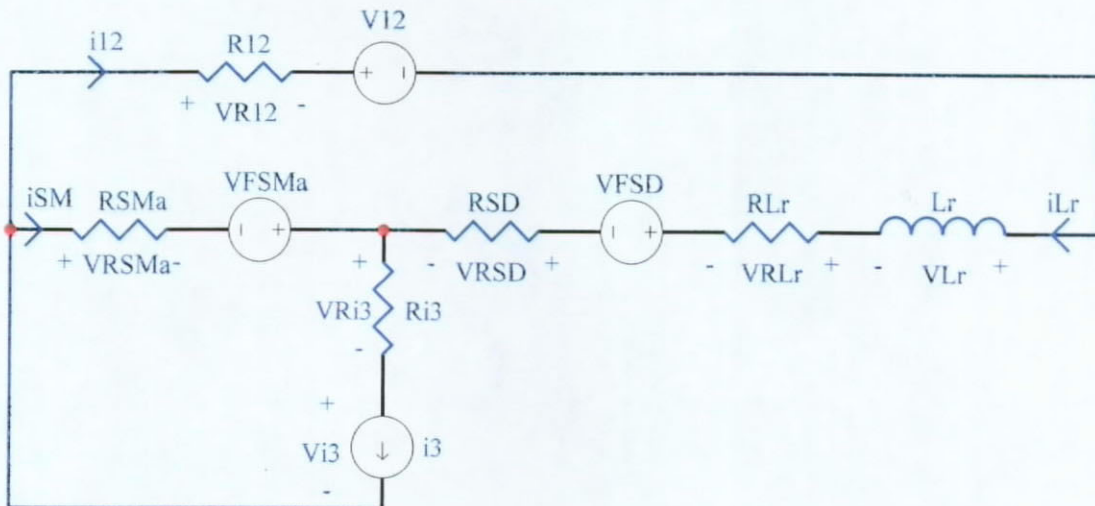


Fig. 5.3. Inductor Discharging Stage $[T_2, T_a]$ of FM ZVS QR Boost Converter.

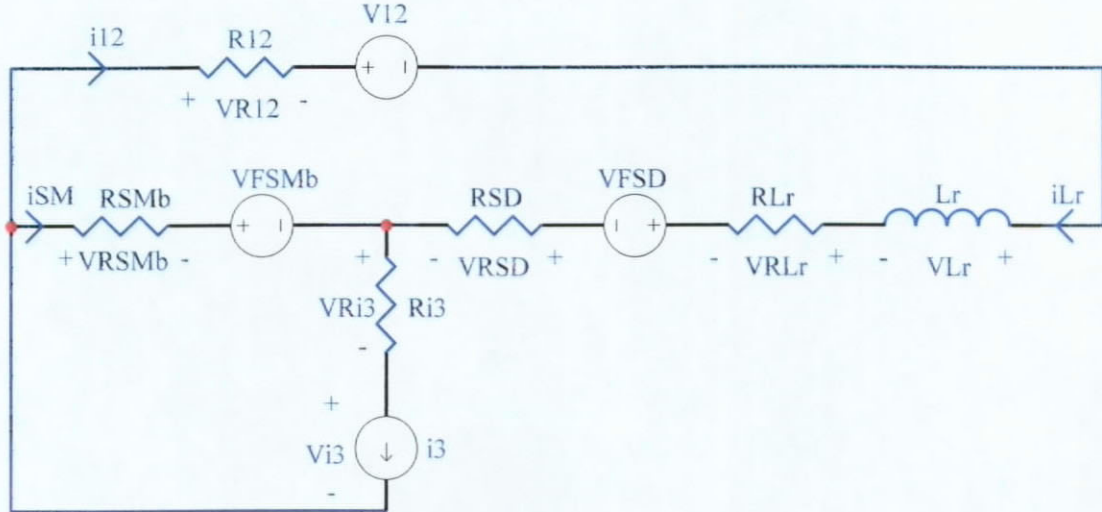


Fig. 5.4. Inductor Discharging Stage [T_a, T_3] of FM ZVS QR Boost Converter.

5.3.2 Second Inductor Discharging Stage [T_a, T_3]

Fig. 5.4 shows the equivalent circuit of FM ZVS QRSW in second inductor discharging stage [T_a, T_3].

Initial conditions:

$$i_{Lr}(0) = C_{5a} + K_{5a} \cdot e^{-Aa(Ta-T_2)} = i_3 . \quad (5.23)$$

State equation:

$$\begin{aligned} \frac{di_{Lr}(t)}{dt} &= -\frac{R_{SD} + R_{Lr} + R_{12} + R_{SMB}}{L_r} \cdot i_{Lr}(t) \\ &\quad - \frac{V_{FSD} - V_{FSMb} + V_{12} - i_3 \cdot R_{SMB}}{L_r}, \text{ for } i_{SM}(t) > 0 . \end{aligned} \quad (5.24)$$

Therefore,

$$i_{Lr}(t) = C_{5b} + K_{5b} \cdot e^{-Ab(t-Ta)} \quad (5.25)$$

where

$$\begin{aligned} C_{5b} &= \frac{i_3 \cdot R_{SMB} - V_{FSD} + V_{FSMb} - V_{12}}{R_{SD} + R_{Lr} + R_{12} + R_{SMB}} , \\ K_{5b} &= i_3 - C_{5b} \end{aligned} \quad (5.26)$$

and

$$A_b = \frac{R_{SD} + R_{Lr} + R_{12} + R_{SMb}}{L_r} . \quad (5.27)$$

At time T_3 , the inductor current $i_{Lr}(t)$ reaches zero. Then, T_3 can be found by this equation

$$i_{Lr}(T_3) = C_{5b} + K_{5b} \cdot e^{-Ab \cdot (T_3 - T_a)} = 0 . \quad (5.28)$$

Therefore,

$$T_3 = T_a - \frac{1}{A_b} \cdot \ln\left(\frac{-C_{5b}}{K_{5b}}\right) . \quad (5.29)$$

The switching waveforms in inductor discharging stage are:

$$\begin{cases} v_{Cr}(t) = 0 \text{ and } i_{Cr}(t) = 0 , \\ i_{Lr}(t) = \begin{cases} C_{5a} + K_{5a} \cdot e^{-Aa \cdot (t-T_2)} , & \text{for } T_2 < t < T_a \\ C_{5b} + K_{5b} \cdot e^{-Ab \cdot (t-T_a)} , & \text{for } T_a < t < T_3 \end{cases} , \\ v_{Lr}(t) = \begin{cases} K_{6a} \cdot e^{-Aa \cdot (t-T_2)} , & \text{for } T_2 < t < T_a \\ K_{6b} \cdot e^{-Ab \cdot (t-T_a)} , & \text{for } T_a < t < T_3 \end{cases} , \\ i_{SM}(t) = i_3 - i_{Lr}(t) , \end{cases} \quad (5.30)$$

where,

$$K_{6a} = -L_r \cdot K_{5a} \cdot A_a \quad \text{and} \quad K_{6b} = -L_r \cdot K_{5b} \cdot A_b . \quad (5.31)$$

5.4 Free-Wheeling Stage [T₃, T_s]

After the time T_3 , both capacitor voltage $v_{Cr}(t)$ and inductor current $i_{Lr}(t)$ reach zero and the diode S_D turns off. The switch S_M still turns on and the constant current i_3 flows through S_M . Fig. 5.5 shows the equivalent circuit of FM ZVS QRSW in free-wheeling stage [T_3, T_s].

The switching waveforms in free-wheeling stage are:

$$\begin{cases} v_{Cr}(t) = 0 \\ i_{Cr}(t) = 0 \\ i_{Lr}(t) = 0 \\ v_{Lr}(t) = 0 \\ i_{SM}(t) = i_3 \end{cases} \quad (5.32)$$

At time T_s , the switch S_M will turn off and the capacitor C_r will be charged linearly again because one switching cycle is complete at T_s .

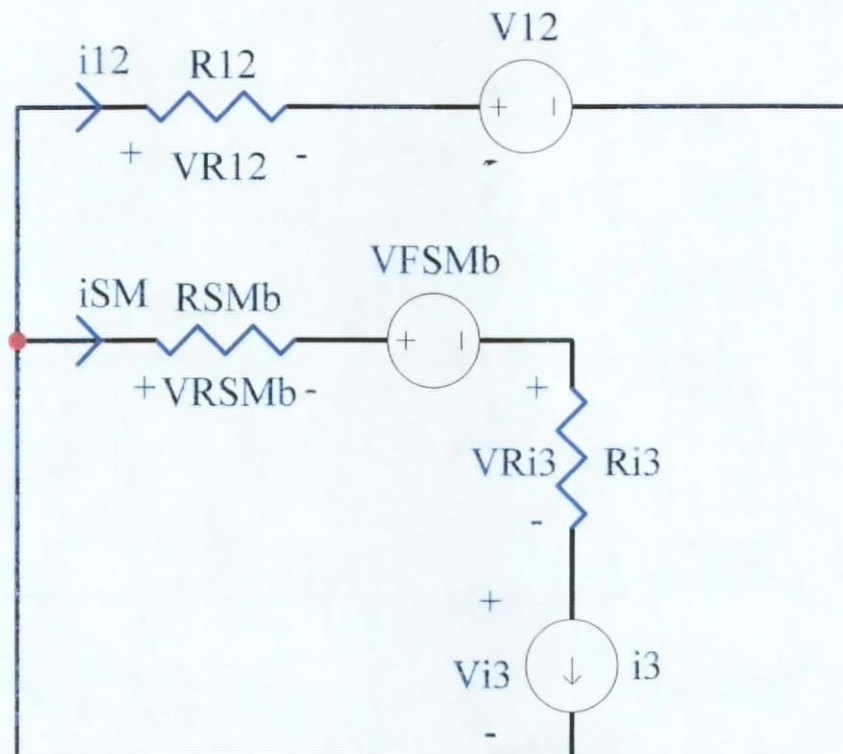


Fig. 5.5. Free-Wheeling Stage $[T_3, T_s]$ of FM ZVS QR Boost Converter.

Chapter 6 Modeling of FM ZVS

Converters Using Unified Model

In this chapter, all the equations were developed and derived by the author. They are the major contributions to the new analysis in this thesis. Chapter 4 and Chapter 5 have already derived the FM ZVS QR Buck and Boost Converters respectively. This chapter is going to summarize the techniques used in Chapter 4 and Chapter 5. The large signal regulated unified model shown in Fig. 6.1 is used to summarize all equations in Buck, Boost, Buck-Boost, Cuk, Sepic and Zeta converters. The switching frequency f_s is a variable to be determined by numerical method so that the DC operating points in the large signal method are solved and the output load voltage is kept constant. The MATLAB tools [6] will be used in Chapter 7.

There are four switching stages: capacitor charging stage, resonant stage, inductor discharging stage and free-wheeling stage. The following sections analyze and solve the system equations in each switching stage.

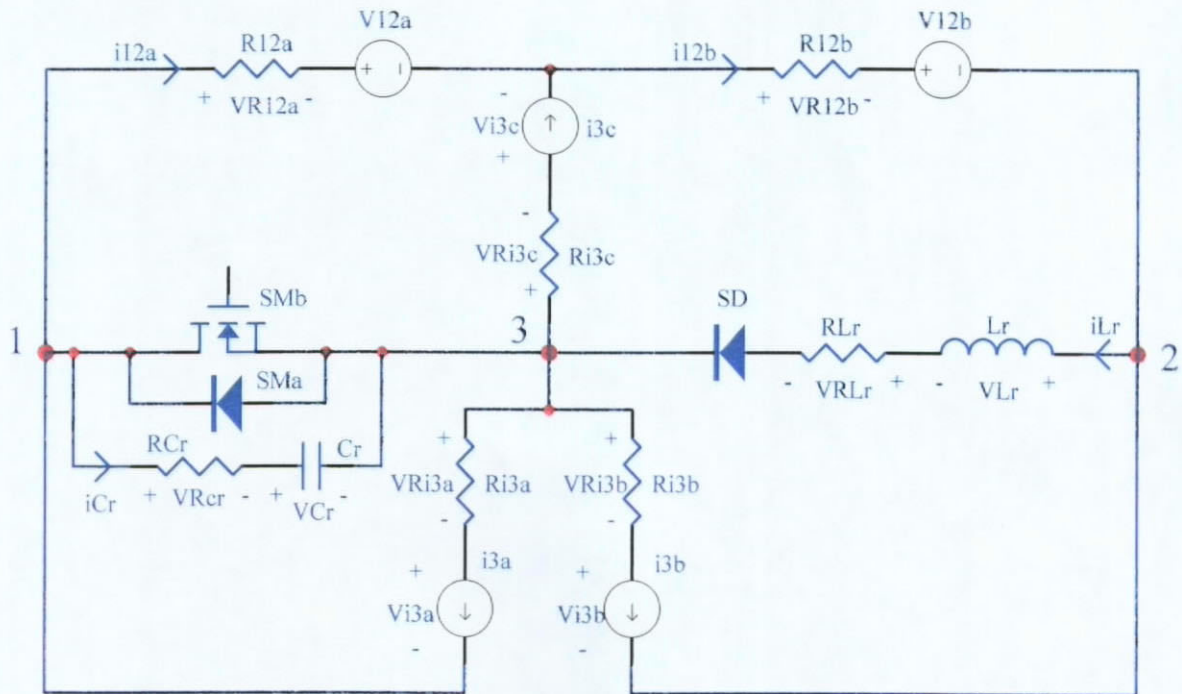


Fig. 6.1. Unified Practical Model of FM ZVS QR Converter.

6.1 Capacitor Charging Stage [T₀, T₁]

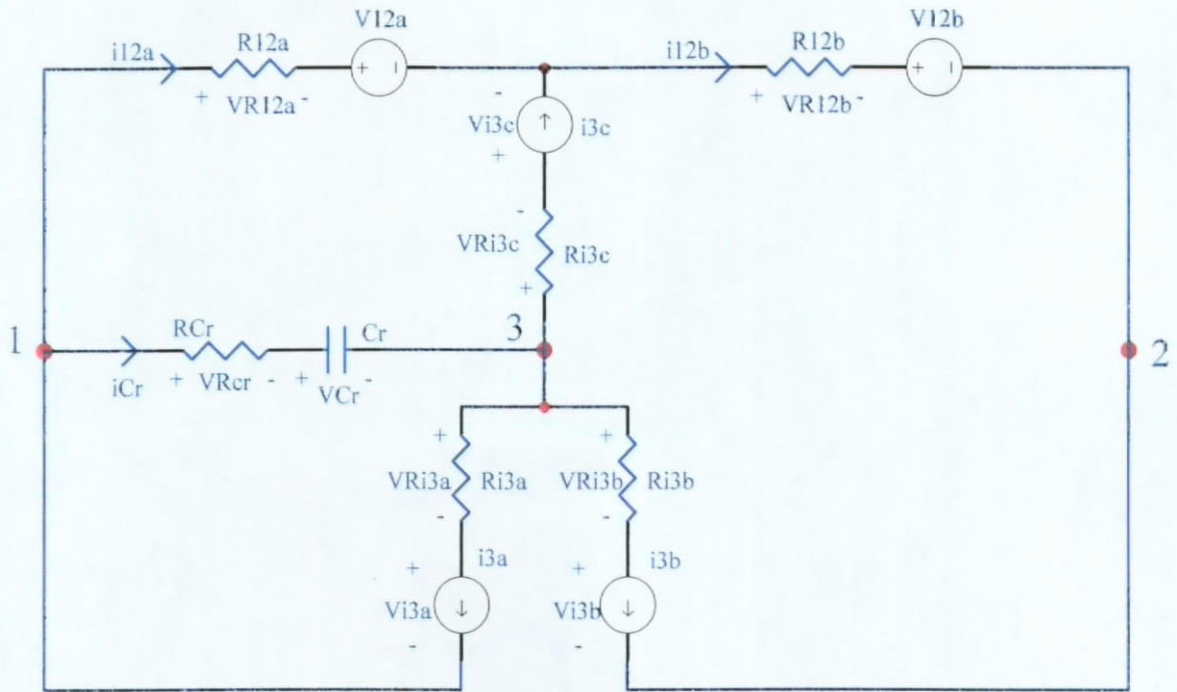
The diode S_D and the transistor S_M turn off at T_0 . The current $i_{Cr}(t)$ flows through the capacitor C_r with an internal resistance R_{Cr} . Because the current $i_3 = i_{3a} + i_{3b} + i_{3c}$ is assumed to be constant, the capacitor voltage $V_{Cr}(t)$ rises linearly. Fig. 6.2 shows the equivalent circuit of FM ZVS QRCs in capacitor charging stage $[T_0, T_1]$.

Initial conditions:

$$\begin{cases} i_{Lr}(0^-) = 0 , \\ v_{Cr}(0^-) = 0 . \end{cases} \quad (6.1)$$

State equations:

$$\begin{bmatrix} \frac{di_{Lr}(t)}{dt} \\ \frac{dv_{Cr}(t)}{dt} \end{bmatrix} = \begin{bmatrix} \frac{v_{Lr}(t)}{L_r} \\ \frac{i_{Cr}(t)}{C_r} \end{bmatrix} = \begin{bmatrix} 0 \\ \frac{i_{3a} + i_{3b} + i_{3c}}{C_r} \end{bmatrix}. \quad (6.2)$$

Fig. 6.2. Capacitor Charging Stage $[T_0, T_1]$ of FM ZVS QR Unified Model.

The switching waveforms in capacitor charging stage are:

$$\begin{cases} v_{Cr}(t) = \frac{i_{3a} + i_{3b} + i_{3c}}{C_r} \cdot t = \frac{V_{12} \cdot w_r}{\alpha} \cdot t , \\ i_{Cr}(t) = C_r \cdot \frac{dv_{Cr}(t)}{dt} = i_{3a} + i_{3b} + i_{3c} , \\ i_{Lr}(t) = 0 , \\ v_{Lr}(t) = L_r \cdot \frac{di_{Lr}(t)}{dt} = 0 , \end{cases} \quad (6.3)$$

where

$$\alpha = \frac{V_{12}}{Z_r \cdot (i_{3a} + i_{3b} + i_{3c})} . \quad (6.4)$$

At time T_1 , the diode S_D starts to conduct. The voltage on the diode S_D should be zero. Therefore, T_1 can be found by this equation,

$$v_{Cr}(T_1) + i_{Cr}(T_1) \cdot R_{Cr} = V_{12a} + V_{12b} + i_{12a} \cdot R_{12a} + i_{12b} \cdot R_{12b} . \quad (6.5)$$

Having solved the equation, we can write T_1 explicitly:

$$T_1 = \left(\frac{C_r}{i_{3a} + i_{3b} + i_{3c}} (V_{12} - i_{3b} \cdot R_{12} - i_{3c} \cdot R_{12a}) - C_r \cdot R_{Cr} \right), \quad (6.6)$$

where

$$V_{12} = V_{12a} + V_{12b} \text{ and } R_{12} = R_{12a} + R_{12b}. \quad (6.7)$$

6.2 Resonant Stage [T_1, T_2]

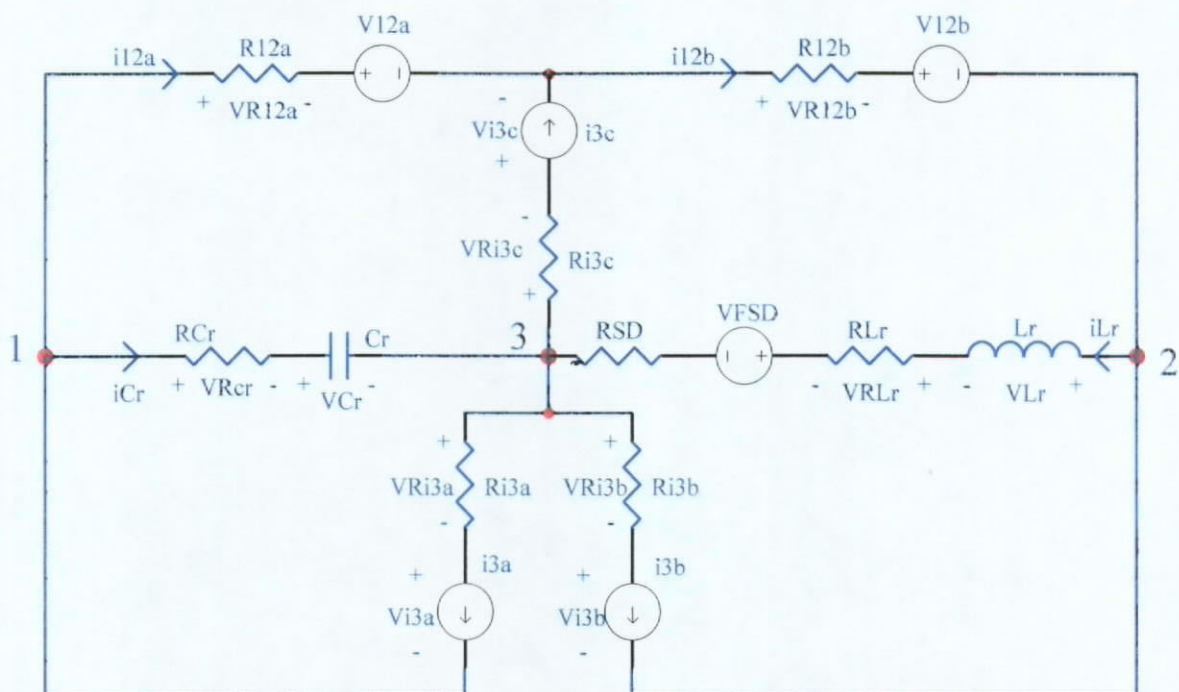


Fig. 6.3. Resonant Stage [T_1, T_2] of FM ZVS QR Unified Model.

The diode S_D turns on at time T_1 , the capacitor voltage $v_{Cr}(t)$ resonates with the inductor current $i_{Lr}(t)$. However, there is an exponential damping factor associated with the switching waveforms. They are not purely sinusoidal. Fig. 6.3 shows the equivalent unified circuit of FM ZVS QRSW in resonant stage between the time $[T_1, T_2]$.

Initial conditions:

$$\begin{cases} i_{Lr}(0^-) = 0, \\ v_{Cr}(0^-) = \frac{i_{3a} + i_{3b} + i_{3c}}{C_r} \cdot T_1 = V_{12a} + V_{12b} - (i_{3a} + i_{3b} + i_{3c}) \cdot R_{Cr} - (i_{3b} + i_{3c}) \cdot R_{12a} - i_{3b} \cdot R_{12b} \end{cases} \quad (6.8)$$

State equations:

$$\begin{bmatrix} -L_r & R_{Cr} \cdot C_r + R_{12a} \cdot C_r \\ 0 & C_r \end{bmatrix} \begin{bmatrix} \frac{di_{Lr}(t)}{dt} \\ \frac{dv_{Cr}(t)}{dt} \end{bmatrix} = \begin{bmatrix} R_{LT} + R_{12b} & -1 \\ -1 & 0 \end{bmatrix} \begin{bmatrix} i_{Lr}(t) \\ v_{Cr}(t) \end{bmatrix} + \begin{bmatrix} V_{FSD} + V_{12a} + V_{12b} + i_{3a} \cdot R_{12a} - i_{3b} \cdot R_{12b} \\ i_{3a} + i_{3b} + i_{3c} \end{bmatrix}, \quad (6.9)$$

where

$$R_{LT} = R_{Lr} + R_{SD} \quad (6.10)$$

The switching waveforms in resonant stage between the time $[T_1, T_2]$ are:

$$\begin{cases} v_{Cr}(t) = V_{12} \cdot (C_1 + K_1 \cdot e^{-\alpha(t-T_1)} \cdot \sin(w_o(t-T_1) + \theta_1)), \\ i_{Cr}(t) = V_{12} \cdot (K_2 \cdot e^{-\alpha(t-T_1)} \cdot \sin(w_o(t-T_1) + \theta_2)), \\ i_{Lr}(t) = i_3 \cdot [1 - K_3 \cdot e^{-\alpha(t-T_1)} \cdot \sin(w_o(t-T_1) + \theta_3)], \\ v_{Lr}(t) = i_3 \cdot K_4 \cdot e^{-\alpha(t-T_1)} \cdot \sin(w_o(t-T_1) + \theta_4), \end{cases} \quad (6.11)$$

where

$$C_1 = 1 + \frac{1}{\alpha} \left(\beta + \frac{R_{LT}}{Z_r} \right) + \frac{i_{3a} \cdot R_{12} + i_{3c} \cdot R_{12b}}{V_{12}}, \quad \beta = \frac{V_{FSD}}{Z_r \cdot i_3},$$

$$K_1 = \frac{1}{\alpha} \sqrt{1 + \left(\frac{w_r}{w_o} \right)^2 \cdot \left(\frac{R_{ALL}}{2Z_r} + \beta \right)^2},$$

$$\begin{aligned}
\theta_1 &= 2\pi - \tan^{-1} \left(\frac{\frac{R_{ALL}}{Z_r} + \beta}{\frac{w_r}{w_o} - \frac{a}{w_o} \cdot \left(\frac{R_{ALL}}{Z_r} + \beta \right)} \right), \\
K_2 &= \frac{K_1}{Z_r}, \quad \theta_2 = \theta_1 + \pi - \tan^{-1} \left(\frac{w_o}{a} \right), \\
K_3 &= \sqrt{1 + \left(\frac{\beta \cdot w_r + a}{w_o} \right)^2}, \quad \theta_3 = \tan^{-1} \left(\frac{w_o}{\beta \cdot w_r + a} \right), \\
K_4 &= Z_r \cdot K_3, \quad \theta_4 = \theta_3 + 2\pi - \tan^{-1} \left(\frac{w_o}{a} \right), \\
a &= \frac{R_{ALL}}{2L_r}, \quad w_o = \sqrt{\frac{1}{L_r C_r} - \frac{R_{ALL}^2}{4L_r^2}} = \sqrt{w_r^2 - a^2}, \\
R_{CT} &= R_{Cr} + R_{12} = R_{Cr} + R_{12a} + R_{12b}, \quad R_{LT} = R_{Lr} + R_{SD}, \\
R_{ALL} &= R_{CT} + R_{LT} = R_{Cr} + R_{12} + R_{Lr} + R_{SD} \\
i_3 &= i_{3a} + i_{3b} + i_{3c}, \quad V_{12} = V_{12a} + V_{12b}. \tag{6.12}
\end{aligned}$$

From the equations (6.11), we know that the switching waveforms have a damping factor "a" = $R_{ALL}/(2L_r)$ in the exponential index. They are not purely sinusoidal because of the accumulative value of the internal resistance of each component. Moreover, the damping factor "a" shifts the resonant angular frequency from w_r to w_o . Obviously, the shifted resonant angular frequency w_o is smaller than the ideal resonant angular frequency w_r .

At time T_2 , the switch S_M starts to conduct. In order to achieve ZVS, the voltage on the switch S_M should be zero. Therefore, T_2 can be found by this equation,

$$v_{Cr}(T_2) + i_{Cr}(T_2) \cdot R_{Cr} = 0. \tag{6.13}$$

The equation is simplified to

$$C_1 + K_{T2} \cdot e^{-a(T_2-T_1)} \cdot \sin(w_o(T_2 - T_1) + \theta_{T2}) = 0 , \quad (6.14)$$

where

$$K_{T2} = K_1 R_{Cr} C_r \sqrt{\left(\frac{1}{R_{Cr} C_r} - a\right)^2 + w_o^2} \quad (6.15)$$

and

$$\theta_{T2} = \theta_1 + \tan^{-1} \left(\frac{\frac{w_o}{1}}{\frac{1}{R_{Cr} C_r} - a} \right) . \quad (6.16)$$

Unfortunately, the time T_2 cannot be written explicitly because of the exponential term in equation (6.14). We have to solve it by using numerical method.

6.3 Inductor Discharging Stage [T₂, T₃]

After the time T_2 , the capacitor voltage $v_{Cr}(t)$ reaches zero and the switch S_M turns on. The inductor current $i_{Lr}(t)$ decreases to zero at time T_3 . During this stage, the capacitor voltage $v_{Cr}(t)$ in the practical circuits will not keep zero but very small, therefore, the power loss in the capacitor C_r is negligible.

Since S_M is a current bi-directional switch, the forward bias voltage drop will be different. Equation (6.18) and (6.25) describe the inductor current $i_{Lr}(t)$ for $i_{SM}(t) < 0$ and $i_{SM}(t) > 0$ respectively. It is necessary to add an intermediate stage T_a between T_2 and T_3 .

6.3.1 First Inductor Discharging Stage [T₂, T_a]

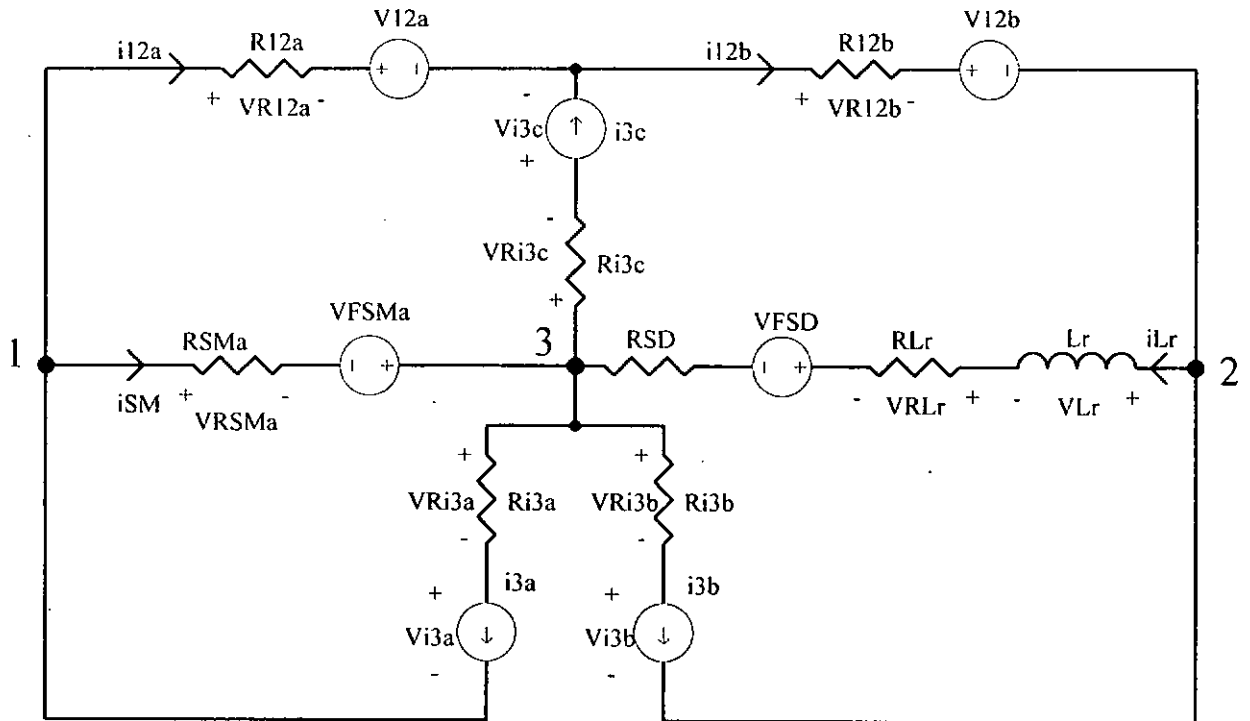


Fig. 6.4. First Inductor Discharging Stage [T₂, T_a] of FM ZVS QR Unified Model.

Fig. 6.4 shows the equivalent circuit of FM ZVS QR unified model in first inductor discharging stage [T₂, T_a].

Initial conditions:

$$i_{Lr}(0) = i_3 \cdot [1 - K_3 \cdot e^{-\alpha(T_2 - T_1)} \cdot \sin(w_o(T_2 - T_1) + \theta_3)] . \quad (6.17)$$

State equation:

$$\begin{aligned} \frac{di_{Lr}(t)}{dt} &= -\frac{R_{SD} + R_{Lr} + R_{12} + R_{SMA}}{L_r} \cdot i_{Lr}(t) \\ &\quad - \frac{V_{FSD} + V_{FSMa} + V_{12} - i_{3b}R_{12} - i_{3c}R_{12a} - i_3 \cdot R_{SMA}}{L_r}, \text{ for } i_{SM}(t) < 0. \end{aligned} \quad (6.18)$$

Therefore,

$$i_{Lr}(t) = C_{5a} + K_{5a} \cdot e^{-\alpha(t-T_2)} \quad (6.19)$$

where

$$\begin{aligned} C_{5a} &= \frac{i_{3b}R_{12} + i_{3c}R_{12a} + i_3 \cdot R_{SMa} - V_{FSD} - V_{FSMa} - V_{12}}{R_{SD} + R_{Lr} + R_{12} + R_{SMa}}, \\ K_{5a} &= i_3 \cdot [1 - K_3 \cdot e^{-a(T_2 - T_1)} \cdot \sin(w_o(T_2 - T_1) + \theta_3)] - C_{5a} \end{aligned} \quad (6.20)$$

and

$$A_a = \frac{R_{SD} + R_{Lr} + R_{12} + R_{SMa}}{L_r} \quad (6.21)$$

The switch S_M changes the direction of forward bias voltage when $i_{SM}(t) = 0$ at time T_a . Then, the time T_a can be found by solving

$$i_{SM}(T_a) = i_3 - i_{Lr}(T_a) = 0 \quad (6.22)$$

Therefore,

$$T_a = T_2 - \frac{1}{A_a} \cdot \ln\left(\frac{i_3 - C_{5a}}{K_{5a}}\right) \quad (6.23)$$

6.3.2 Second Inductor Discharging Stage [T_a, T_3]

Fig. 6.5 shows the equivalent circuit of FM ZVS QR unified model in second inductor discharging stage [T_a, T_3].

Initial conditions:

$$i_{Lr}(0) = C_{5a} + K_{5a} \cdot e^{-Aa(Ta-T_2)} = i_3 \quad (6.24)$$

State equation:

$$\begin{aligned} \frac{di_{Lr}(t)}{dt} &= -\frac{R_{SD} + R_{Lr} + R_{12} + R_{SMb}}{L_r} \cdot i_{Lr}(t) \\ &- \frac{V_{FSD} + V_{12} - i_{3b}R_{12} - i_{3c}R_{12a} - V_{FSMb} - i_3 \cdot R_{SMb}}{L_r}, \text{ for } i_{SM}(t) > 0 \end{aligned} \quad (6.25)$$

Therefore,

$$i_{Lr}(t) = C_{5b} + K_{5b} \cdot e^{-Ab \cdot (t-Ta)} \quad (6.26)$$

where

$$\begin{aligned} C_{5b} &= \frac{i_{3b}R_{12} + i_{3c}R_{12a} + V_{FSMb} + i_3 \cdot R_{SMb} - V_{FSD} - V_{12}}{R_{SD} + R_{Lr} + R_{12} + R_{SMb}}, \\ K_{5b} &= i_3 - C_{5b} \end{aligned} \quad (6.27)$$

and

$$A_b = \frac{R_{SD} + R_{Lr} + R_{12} + R_{SMb}}{L_r}. \quad (6.28)$$

At time T_3 , the inductor current $i_{Lr}(t)$ reaches zero. Then, T_3 can be found by this equation

$$i_{Lr}(T_3) = C_{5b} + K_{5b} \cdot e^{-Ab \cdot (T_3-Ta)} = 0. \quad (6.29)$$

Therefore,

$$T_3 = T_a - \frac{1}{A_b} \cdot \ln\left(\frac{-C_{5b}}{K_{5b}}\right). \quad (6.30)$$

The switching waveforms in inductor discharging stage $[T_2, T_3]$ are:

$$\begin{cases} v_{Cr}(t) = 0 \text{ and } i_{Cr}(t) = 0, \\ i_{Lr}(t) = \begin{cases} C_{5a} + K_{5a} \cdot e^{-Aa \cdot (t-T_2)}, & \text{for } T_2 < t < Ta, \\ C_{5b} + K_{5b} \cdot e^{-Ab \cdot (t-Ta)}, & \text{for } Ta < t < T_3, \end{cases}, \\ v_{Lr}(t) = \begin{cases} K_{6a} \cdot e^{-Aa \cdot (t-T_2)}, & \text{for } T_2 < t < Ta, \\ K_{6b} \cdot e^{-Ab \cdot (t-Ta)}, & \text{for } Ta < t < T_3, \end{cases}, \\ i_{SM}(t) = i_3 - i_{Lr}(t), \end{cases} \quad (6.31)$$

where

$$K_{6a} = -L_r \cdot K_{5a} \cdot A_a \quad \text{and} \quad K_{6b} = -L_r \cdot K_{5b} \cdot A_b. \quad (6.32)$$

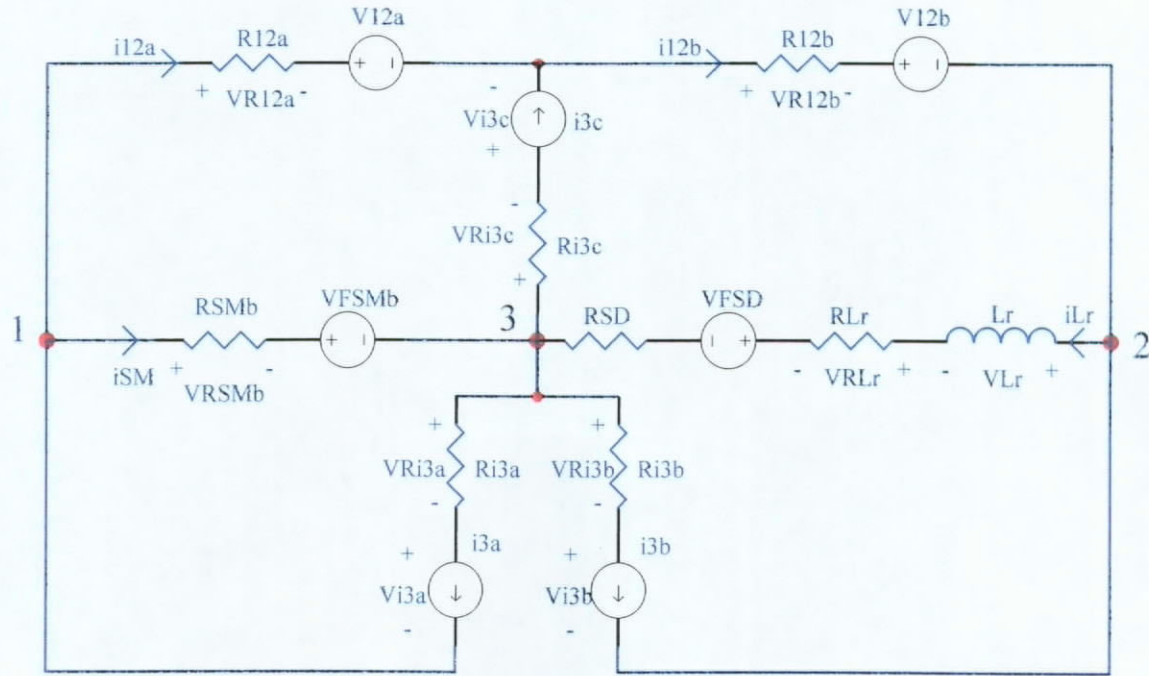


Fig. 6.5. Second Inductor Discharging Stage $[T_a, T_3]$ of FM ZVS QR Unified Model.

6.4 Free-Wheeling Stage $[T_3, T_s]$

After the time T_3 , both capacitor voltage $v_{Cr}(t)$ and inductor current $i_{Lr}(t)$ reach zero and the diode S_D turns off. The switch S_M still turns on and the constant current i_3 flows through S_M . Fig. 6.6 shows the equivalent circuit of FM ZVS QRSW in free-wheeling stage $[T_3, T_s]$.

The switching waveforms in free-wheeling stage are:

$$\begin{cases} v_{Cr}(t) = 0 \\ i_{Cr}(t) = 0 \\ i_{Lr}(t) = 0 \\ v_{Lr}(t) = 0 \\ i_{SM}(t) = i_3 \end{cases} \quad (6.33)$$

At time T_s , the switch S_M will turn off and the capacitor C_r will be charged linearly again because one switching cycle is complete at T_s .

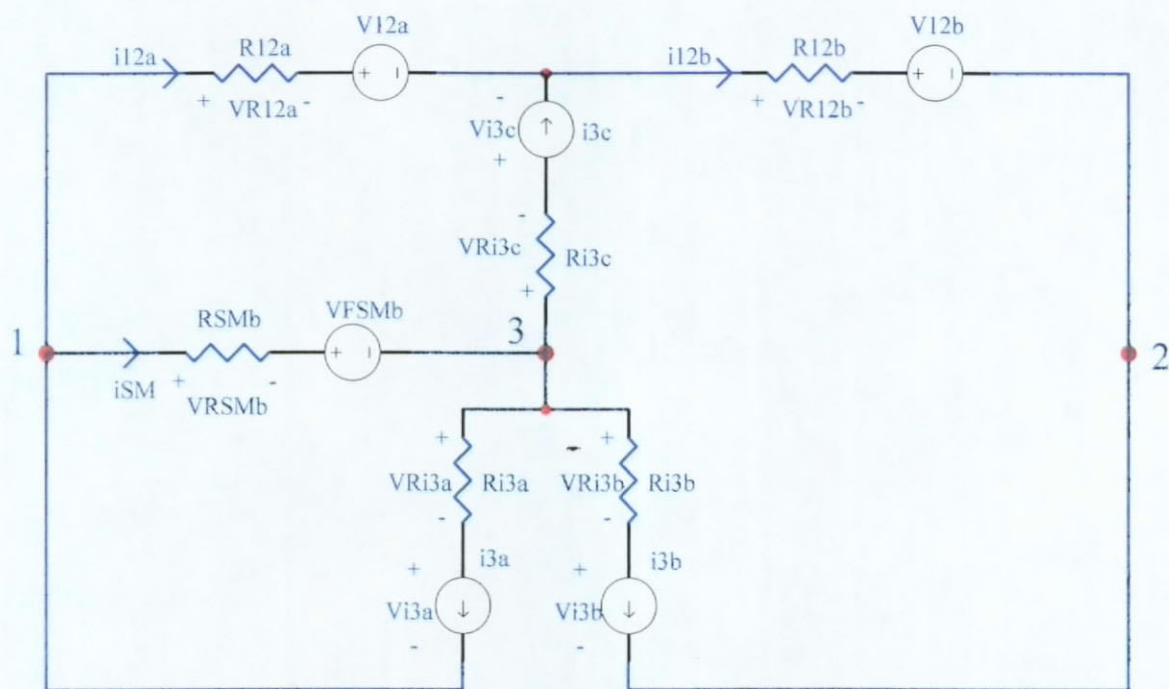


Fig. 6.6. Free-Wheeling Stage [T₃, T_s] of FM ZVS QR Unified Model.

Chapter 7 Power Distribution and Efficiency Analysis

The switching mode power supply industry is developing some small size, low switching noise and high efficiency power converters. The zero switching condition in the quasi-resonant topology can decrease the switching noise [2].

The derivation in the previous chapters is assumed that the zero switching condition can be attained. Therefore, the switching loss due to non-zero switching effect is minimized and negligible.

By using the equations (6.3), (6.11), (6.31) and (6.33) in Chapter 6, we can predict the power distribution in the near-practical model of a Buck Converter and a Boost Converter. In order to simplify the analysis, we define that all internal equivalent resistance is 0.1Ω and all forward bias voltages are $0.7V$, which are reasonable practical parameters. Actually, these simulation conditions can be arbitrarily chosen and the simulation operations are repeatable. The section 7.1 shows the results under non-regulated operating mode. The results predicted from near-practical unified model are comparable with the results shown in Fig. 3.1 - Fig.

3.6 predicted from the ideal unified model depicted in Fig. 2.9. The used parameters are referred from TABLE II shown in [2]. On the other hand, the section 7.2 describes the results of a Buck Converter under regulated operating mode. The output voltage will be under regulation by adjusting the switching frequency of the switch.

7.1 Non-regulated Operating Mode

Fig. 7.1 shows the power distribution of the source power and the load power in Half-wave Type of FM ZVS QR Buck Converter. The positive value P_B is load power, which means that the load is dissipating the power. The negative value P_{V12} is source power, which means that the source is providing the power. The absolute values of a positive curve and a negative curve in the same condition of supply voltage V_{12} are not the same. Hence, the source power (input power) is not the same as the load power (output power). Actually, the source power is larger than the load power. Obviously, there is some power loss within the non-ideal devices defined in Chapter 4. After comparing them with Fig. 3.1, it is noted that they are different because of the power loss in non-ideal components. The load power in the near-practical lossy model shown in Fig. 4.1 is lower than the one in the ideal model shown in Fig. 2.4.

Similarly, Fig. 7.2 shows the simulation results of the power distribution in Half-wave Type of FM ZVS QR Boost Converter.

Fig. 7.3 shows the power loss of each component. It is interesting to note that the loss in diode S_D is very significant, especially, when i_3 is large. We also know that the power loss in R_C is the least significant.

The efficiency of this model is plotted in Fig. 7.5 and Fig. 7.6. Because the

conduction power loss is considered only, it shows the maximum value of the efficiency that can be achieved under different operating points. In order to verify the analytical results, the experiments mentioned in [2] are used to compared. It is confirmed that the efficiency of a boost QRC is around 94 % when the output voltage is 28.7V, the output current is 0.58A and the input voltage is 20V respectively in the experiments. They are the guidelines for the engineers to design an optimal converter for some given conditions and components. For example, for some chosen circuit components, the on-state resistance of IRF-730 MOSFET is 1Ω and the internal equivalent resistances of other components can be measured so that all parameters can be entered into the simulation tools that is listed in Appendix A.1-A.10. The simulation can predict the efficiency and the power loss in each component without building the circuit.

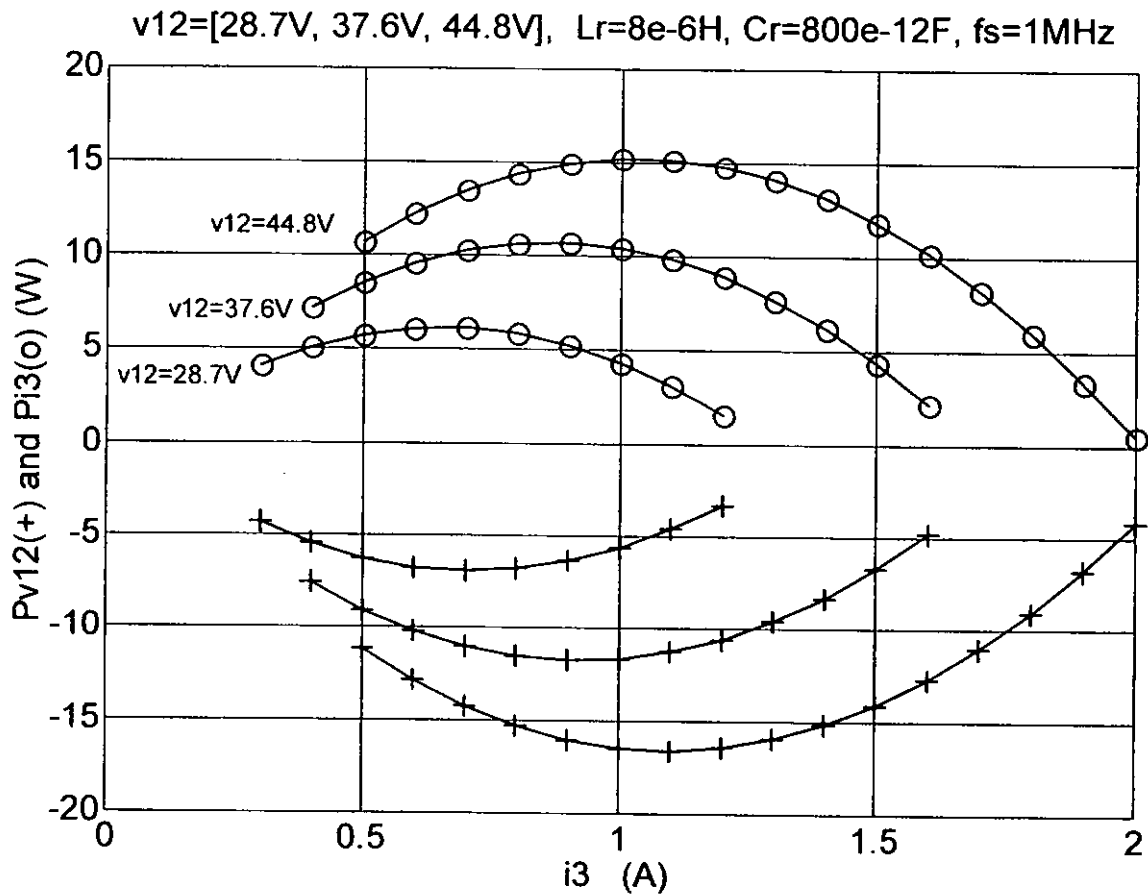


Fig. 7.1. Power Distribution of Half-wave Type of FM ZVS QR Buck Converter.

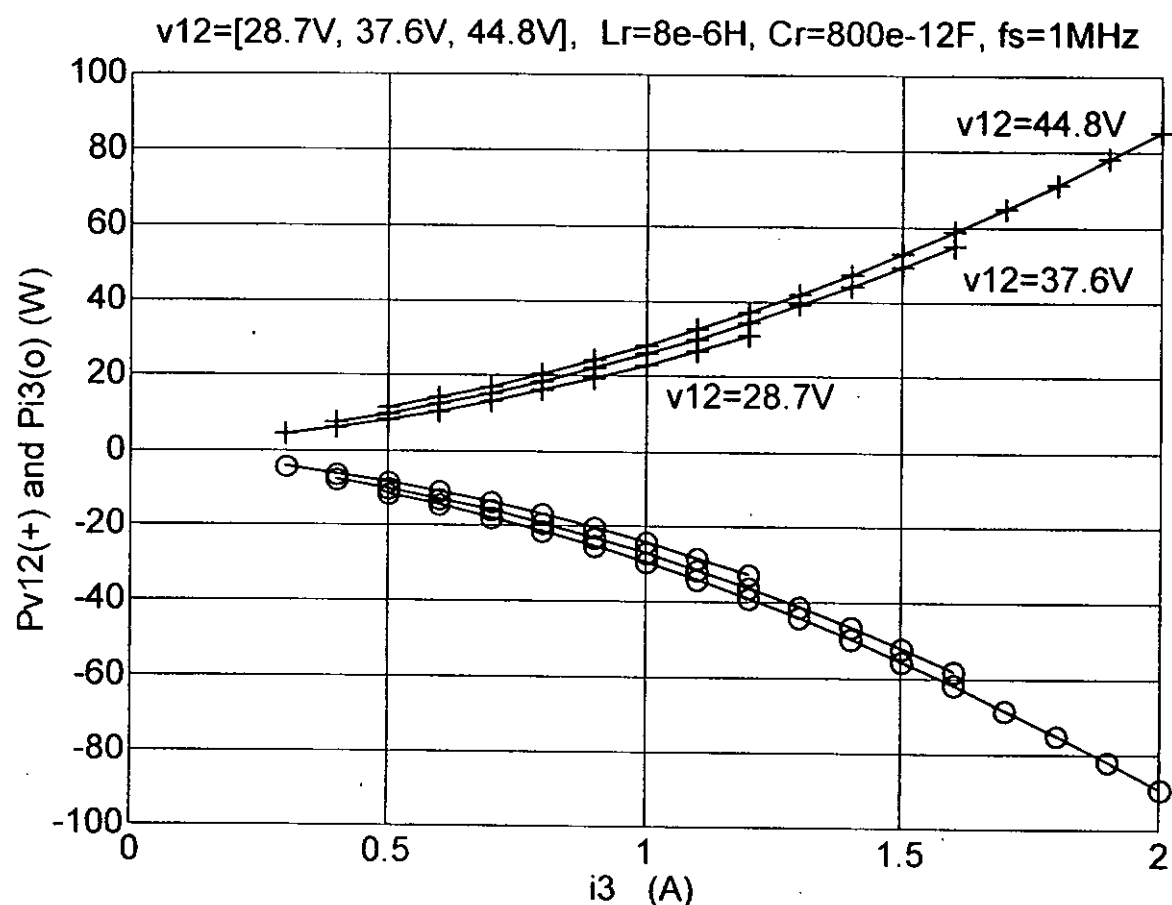


Fig. 7.2. Power Distribution of Half-wave Type of FM ZVS QR Boost Converter.

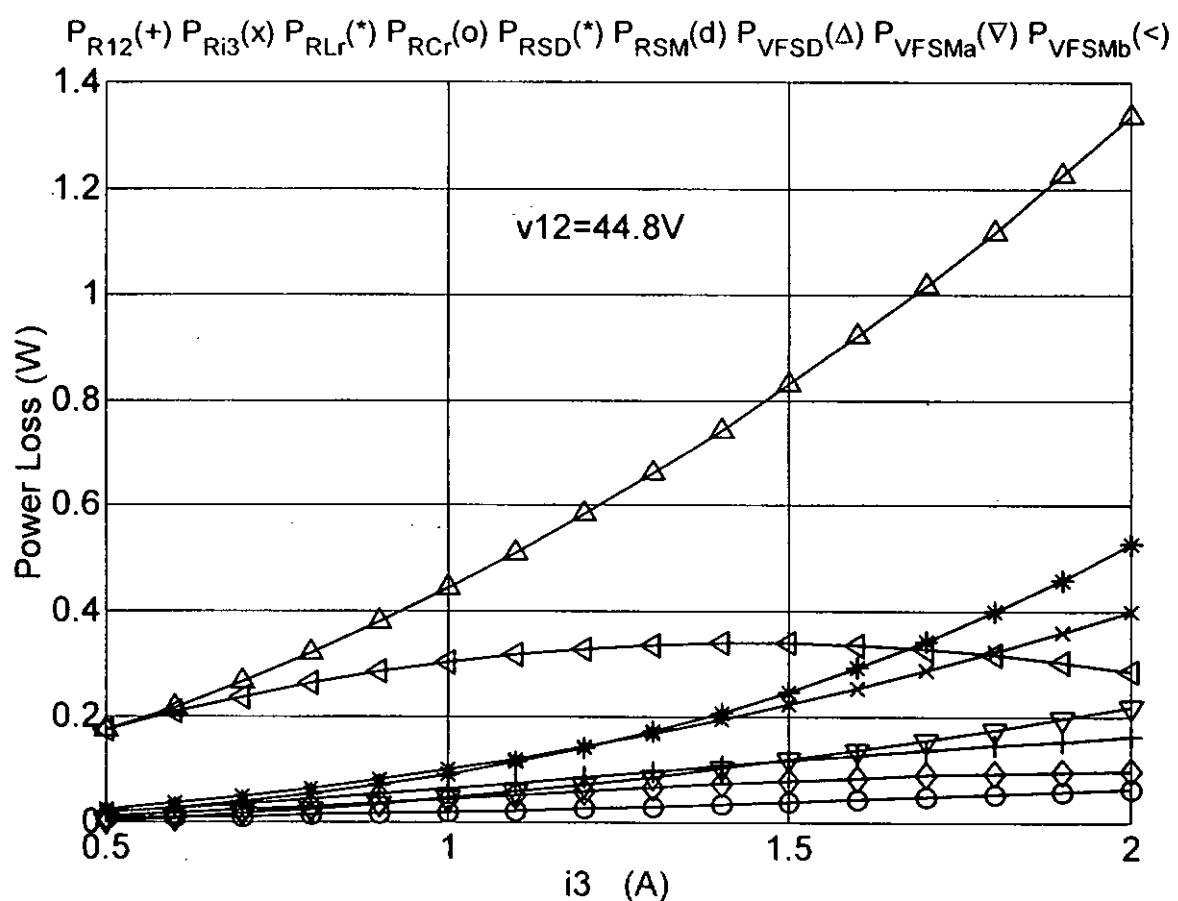


Fig. 7.3. Power Loss of Each Component in FM ZVS QR Buck Converter.

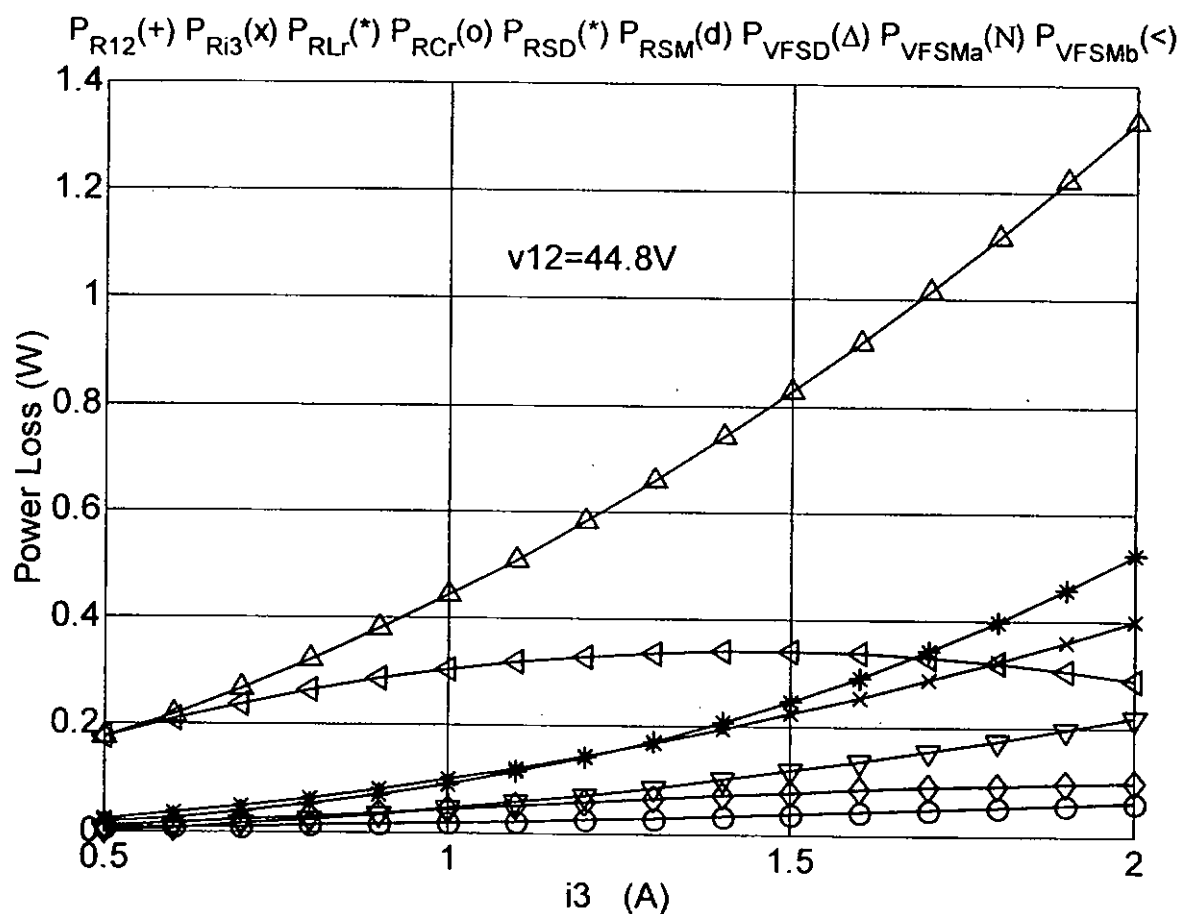


Fig. 7.4. Power Loss of Each Component in FM ZVS QR Boost Converter.

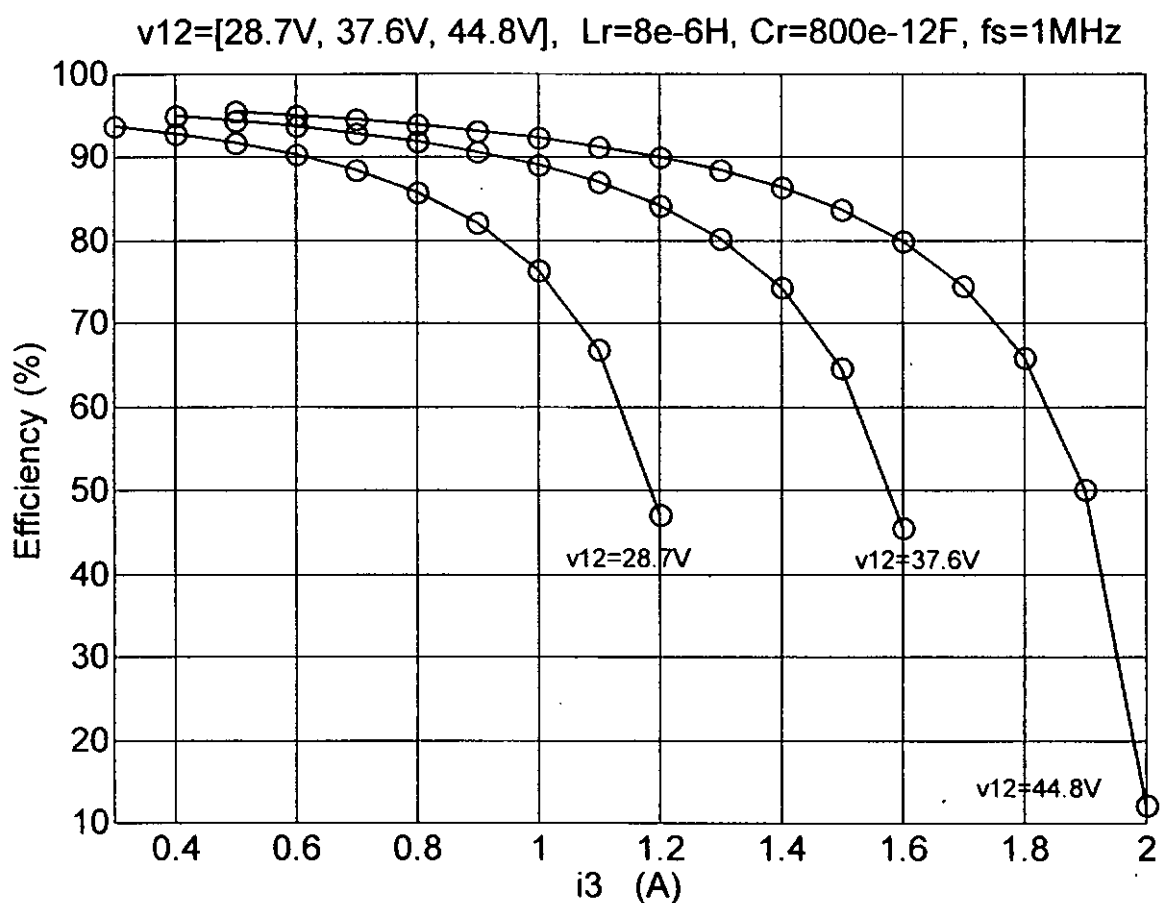


Fig. 7.5. Efficiency of Half-wave Type of FM ZVS QR Buck Converter.

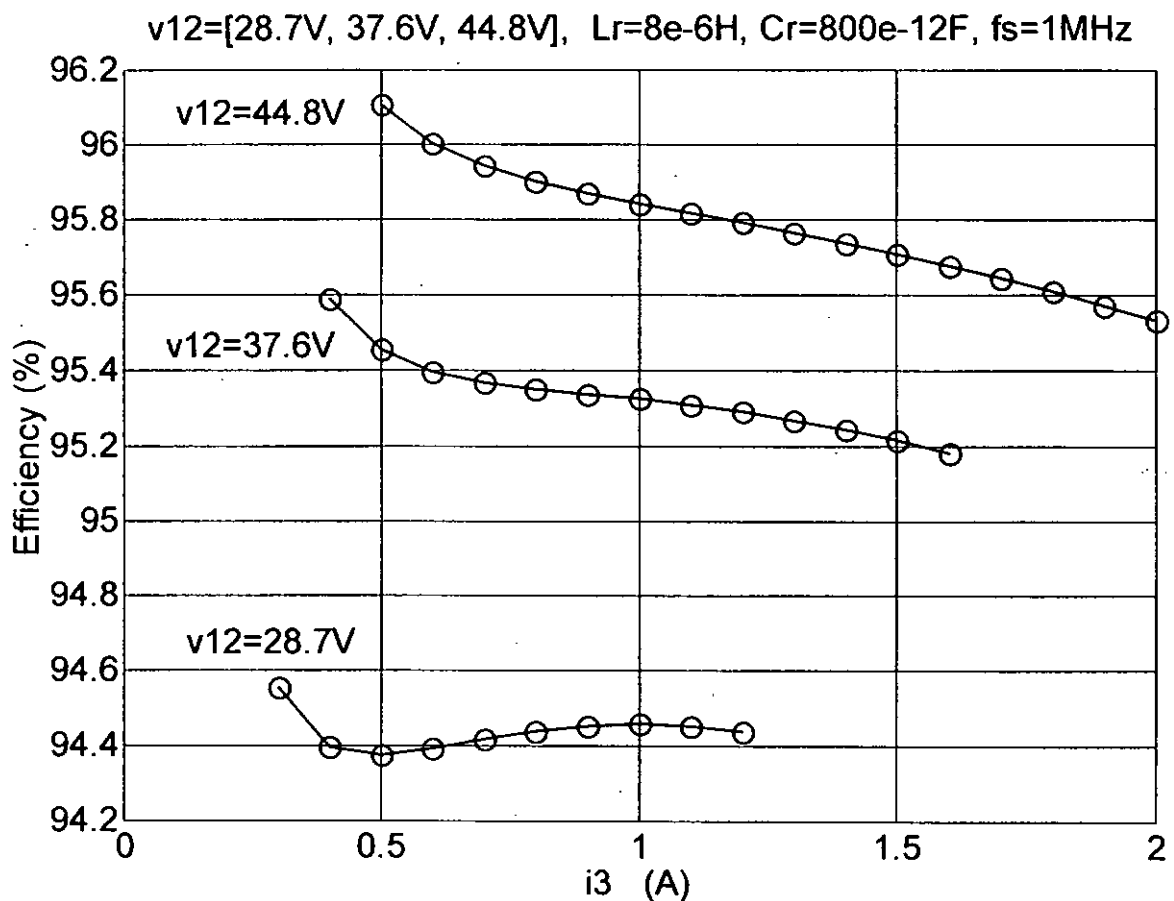


Fig. 7.6. Efficiency of Half-wave Type of FM ZVS QR Boost Converter.

7.2 Regulated Operating Mode

By using the equations (6.3), (6.11), (6.19), (6.26), (6.31) and (6.33) in Chapter 6, the power distribution in the large signal model of quasi-resonant unified model is predicted numerically by using averaging technique. In order to simplify the analysis, we define that all internal equivalent resistance is 0.1Ω and all forward bias voltages are 0.7V, which are reasonable practical parameters. Actually, these simulation conditions can be arbitrarily chosen and the simulation operations are repeatable. In order to verify the analytical results, the experiments mentioned in [2] are used to compared. It is assumed that the supply voltage and load current are varied but the load voltage is kept regulating at 30V. The load voltage can be regulated because the switching frequency f_s is kept changing under different operating conditions. The optimal switching frequency f_s is found by numerical iteration. For example, the function scalar minimization “fminbnd” in MATLAB [6] is used.

Fig. 7.7 - Fig. 7.12 show the results of power distribution analysis of QR regulated Buck, Boost, Buck-Boost, Cuk, Sepic and Zeta converters by using large signal regulated unified model. All the analyzed converters in this section are operating in the regulated operating mode. The results shown in Fig. 7.7 - Fig. 7.12 are using the MATLAB simulation algorithms that are listed in Appendix A.1 – A.6.

Fig. 7.13 shows the power loss of each component in a quasi-resonant buck converter under regulated operating mode of a large signal regulated unified model. It is interesting to note that the loss in the inductor L_r , the diode S_D and the output equivalent resistance are very significant, especially, when the output current i_3 is large. On the other hand, the power loss in the R_{Cr} is the least significant. The results in Fig. 7.13 and Fig. 7.14 are using the MATLAB simulation tools that are listed in

Appendix A.7. The others simulation algorithms for unified large signal model are listed in Appendix A.8 – A.10.

The efficiency of the large signal regulated unified model of a quasi-resonant buck converter is plotted in Fig. 7.14. Because the conduction power loss is considered only, it shows the maximum value of the efficiency that can be achieved under different operating points. They are the guidelines for the engineers to design an optimal converter for some given conditions and components. For example, for some chosen circuit components, the on-state resistance of IRF-730 MOSFET is 1Ω and the internal equivalent resistances of other components can be measured so that all parameters can be entered into the simulation tools that is listed in Appendix A.1 – A.10. The simulation can predict the efficiency and the power loss in each component without building the circuit.

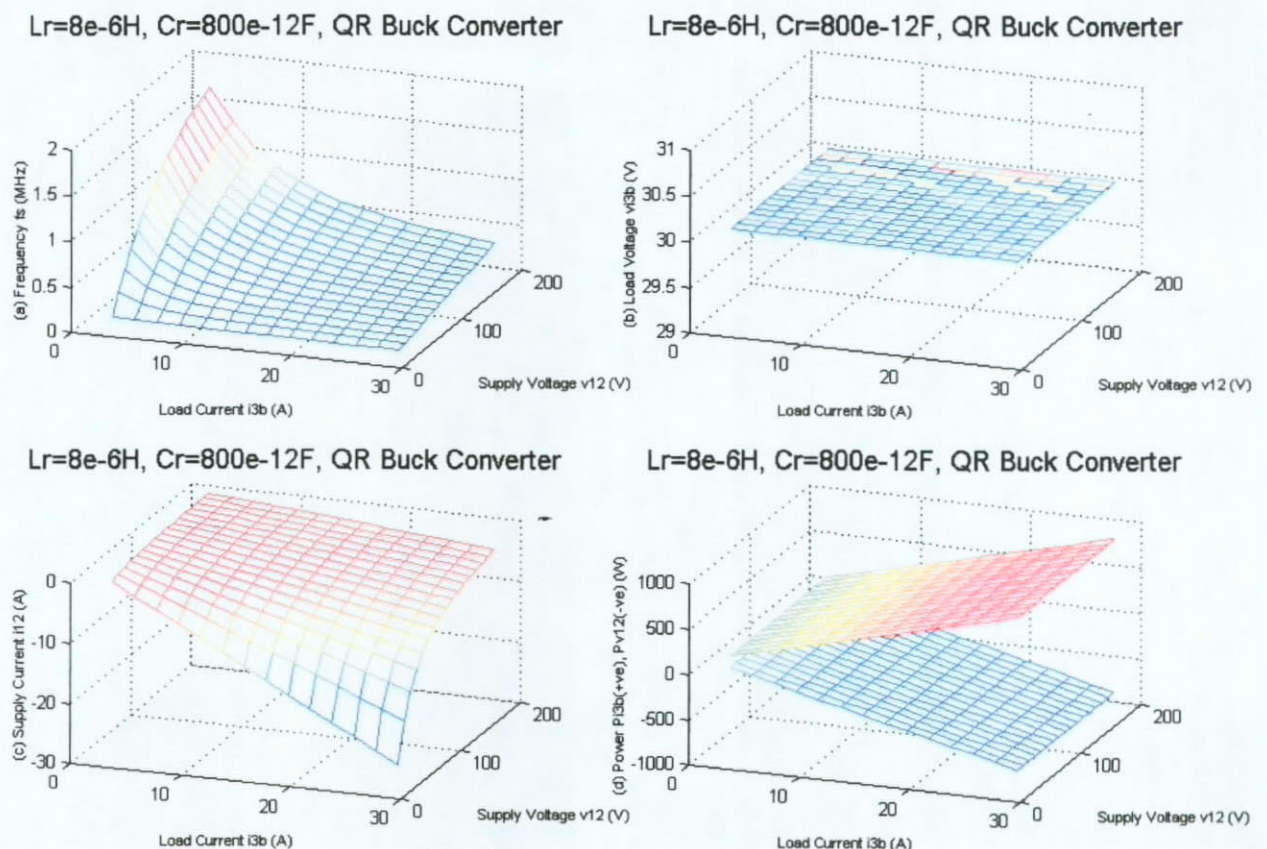


Fig. 7.7. QR Regulated Buck Converter (a) Switching Frequency f_s , (b) Regulated Load Voltage V_{i3} , (c) Supply Current I_{12} , (d) Supply Power P_{v12} and Load Power P_{i3} .

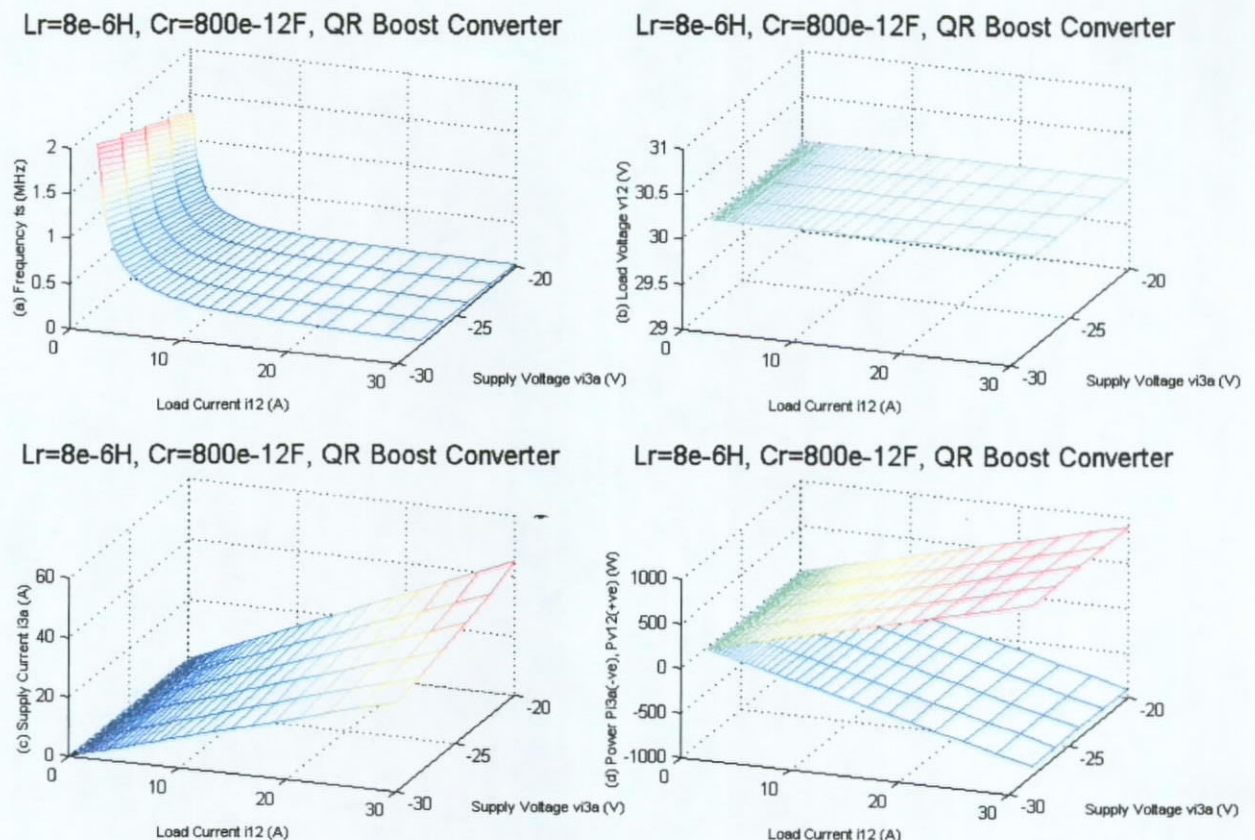


Fig. 7.8. QR Regulated Boost Converter (a) Switching Frequency f_s , (b) Regulated Load Voltage V_{12} , (c) Supply Current I_{3a} , (d) Supply Power P_{i3a} and Load Power P_{V12} .

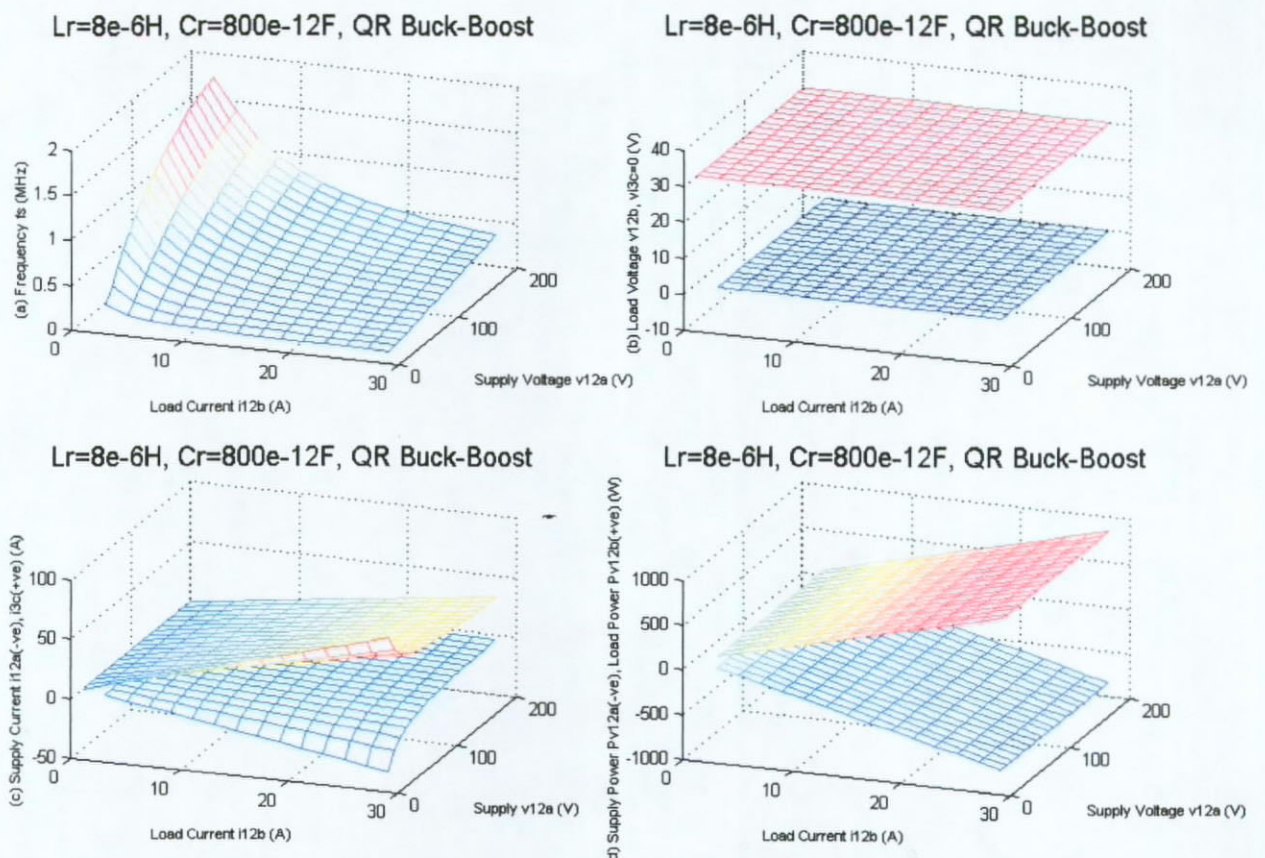


Fig. 7.9. QR Regulated Buck-Boost Converter (a) Switching Frequency f_s , (b) Regulated Load Voltage V_{12b} & Intermediate Voltage Branch V_{i3c} , (c) Supply Current I_{12a} & Intermediate Current Branch I_{3c} , (d) Supply Power P_{v12a} and Load Power P_{v12} .

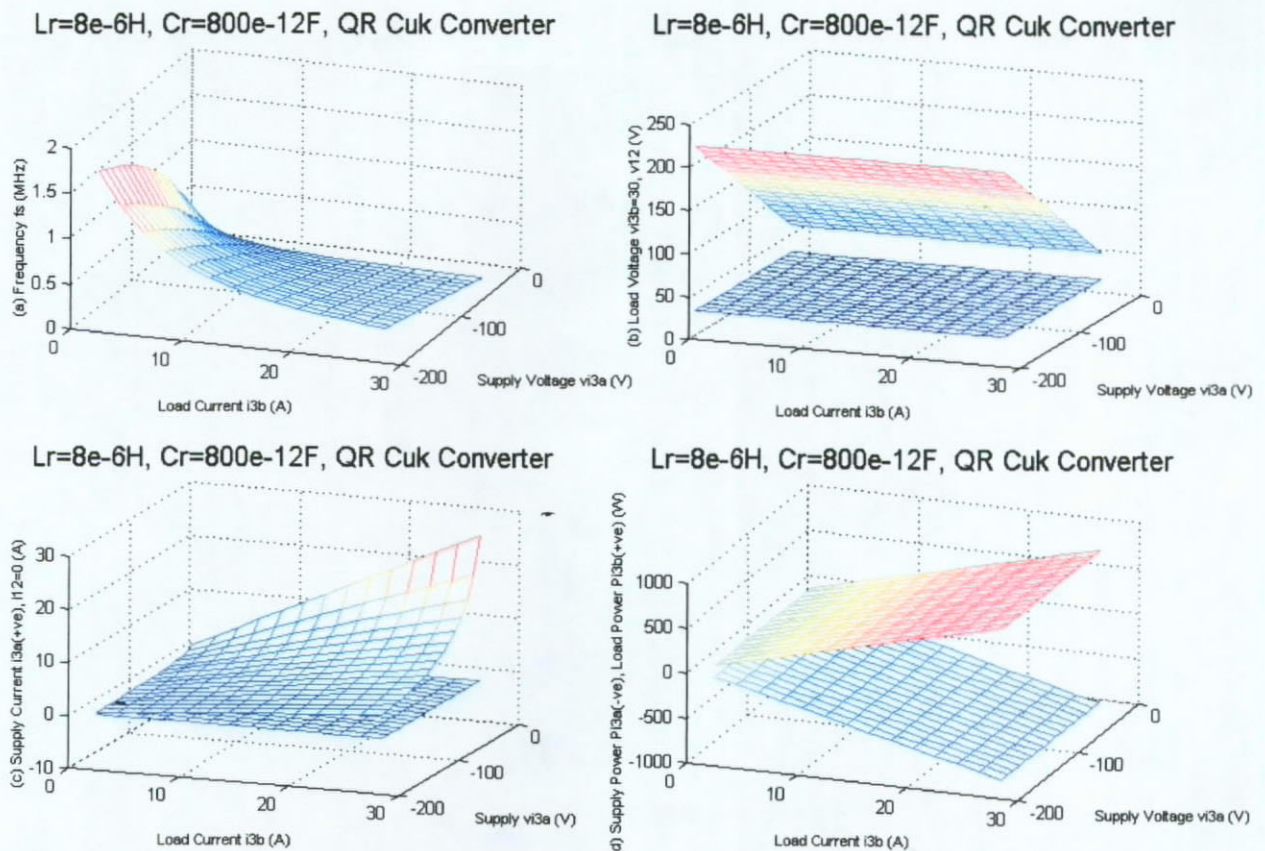


Fig. 7.10. QR Regulated Cuk Converter (a) Switching Frequency f_s , (b) Regulated Load Voltage V_{i3b} & Intermediate Voltage Branch V_{12} , (c) Supply Current I_{3a} & Intermediate Current Branch Iv_{12} , (d) Supply Power P_{i3a} and Load Power P_{i3b} .

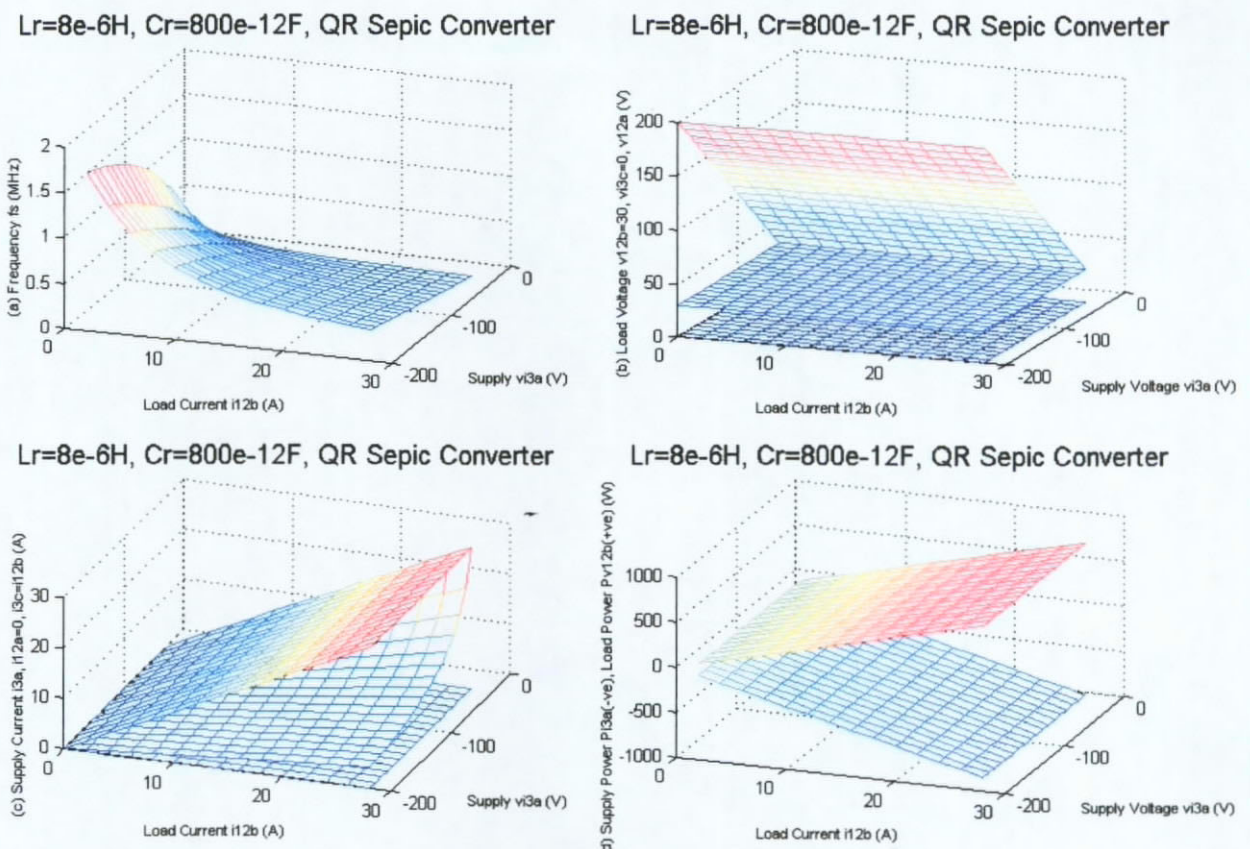


Fig. 7.11. QR Regulated Sepic Converter (a) Switching Frequency f_s , (b) Regulated Load Voltage V_{12b} & Intermediate Voltage Branch V_{12a} , V_{i3c} (c) Supply Current I_{3a} & Intermediate Current Branch I_{12a} , I_{3c} (d) Supply Power P_{i3a} and Load Power P_{v12b} .

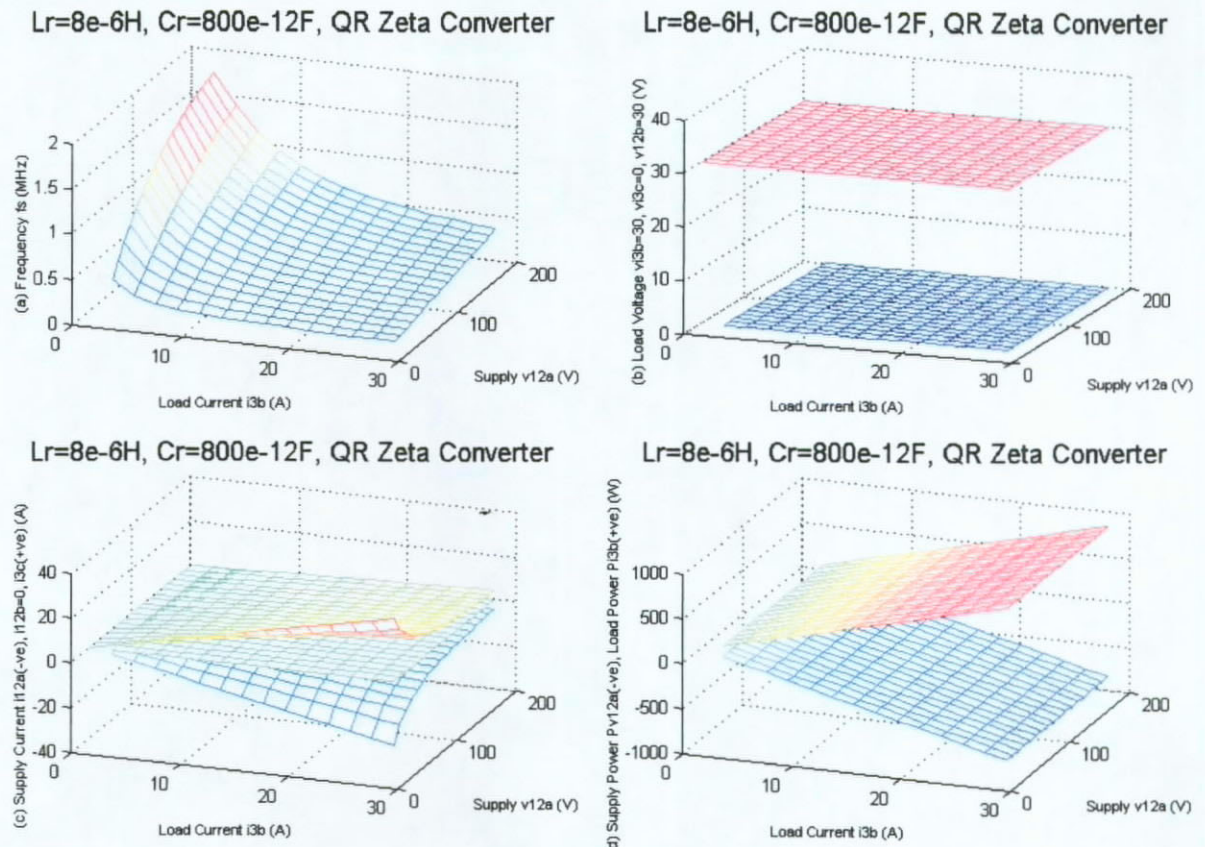


Fig. 7.12. QR Regulated Zeta Converter (a) Switching Frequency f_s , (b) Regulated Load Voltage V_{i3b} & Intermediate Voltage Branch V_{12b} , V_{i3c} (c) Supply Current Iv_{12a} & Intermediate Current Branch Iv_{12b} , I_{3c} (d) Supply Power Pv_{12a} and Load Power P_{i3b} .

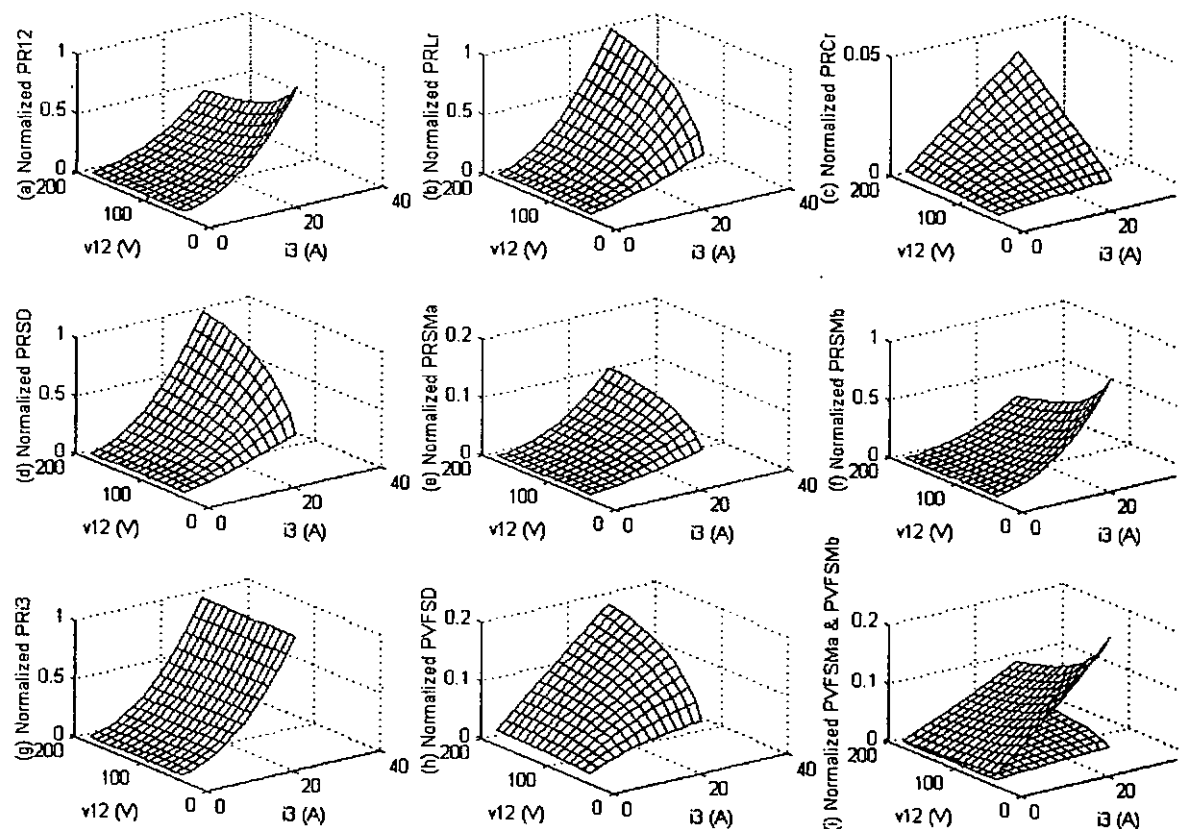


Fig. 7.13. Power Loss of Each Component in FM ZVS QR Buck Converter.

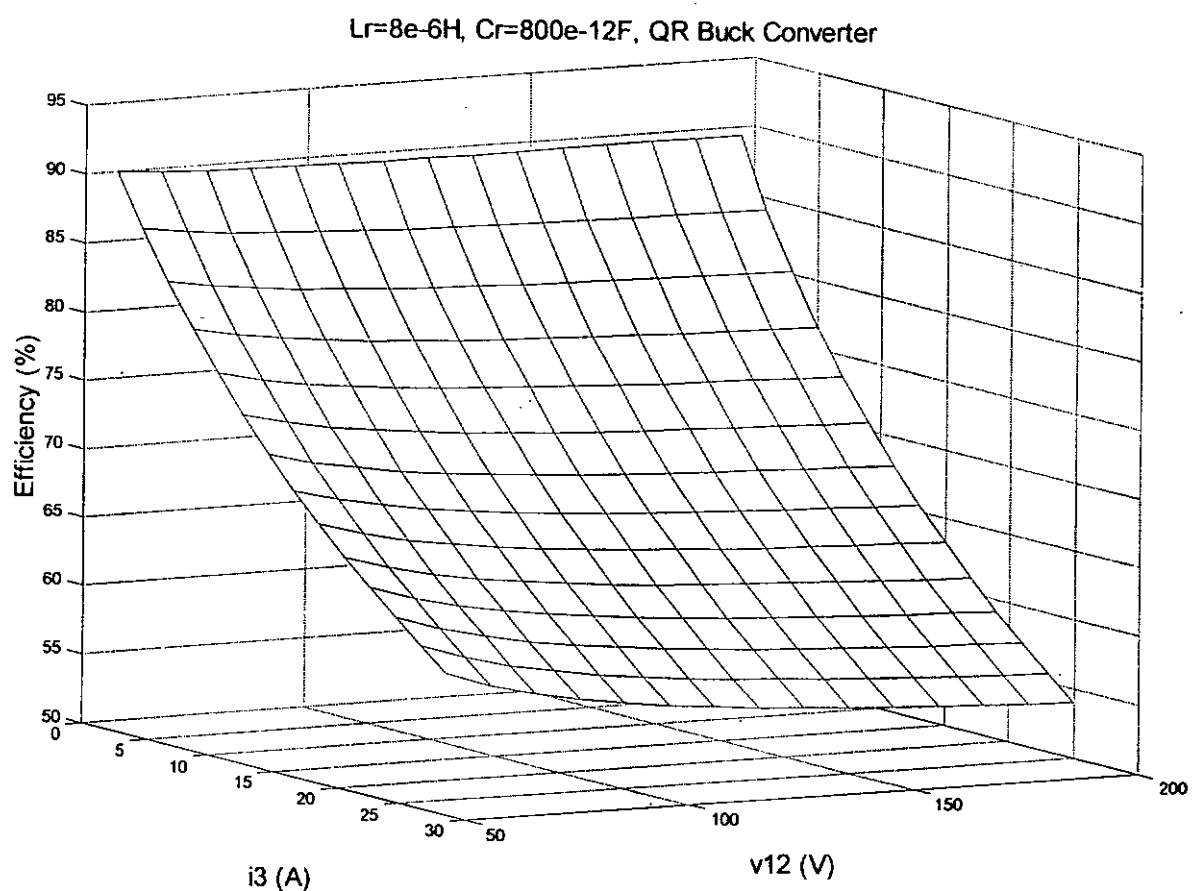


Fig. 7.14. Efficiency of Half-wave Type FM ZVS QR Buck Converter.

Chapter 8 Conclusion

This paper has already reviewed the ideal model of pulse-width modulated switch (PWMSW) and quasi-resonant switch (QRSW) in Chapter 2. It is also indicated that the PWMSW can be unified in a basic circuit: a switch and a diode. The analysis of PWM converters is simplified because the topology consists of a current branch and a voltage loop. Each operation model of Buck, Boost, Buck-Boost, Cuk, Sepic and Zeta Converter can be generalized into one general operation model that is shown in Fig. 2.3. Adding a capacitor in parallel with the switch and an inductor in series with the diode to the PWMSW can form the QRSW that is shown in Fig. 2.4. One example of the half-wave frequency-modulated zero-voltage switching quasi-resonant switch (FM ZVS QRSW) has been mentioned. Analogously, other types of quasi-resonant converters (QRCs) shown in Fig. 2.8 have been derived from the basic model of QRSW shown in Fig. 2.4. In Chapter 3, the power distribution in the ideal half-wave FM ZVS QR Converters is chosen to be analyzed but it is assumed that they are not operating in the regulation mode because the frequency is fixed. The purpose of this analysis is mainly to verify the power attributes derived in Chapter 2. Starting from Chapter 4 is the major contributions to this thesis. Chapter 4 and

Chapter 5 have already derived the switching waveforms of the near-practical model of Buck and Boost Converter respectively. Chapter 6 mathematically summarizes the techniques used in Chapter 4 and Chapter 5. It shows the capability of using unified model to simplify the analysis of the different quasi-resonant models. Finally, in Chapter 7, the power efficiency of the lossy model has been considered.

This paper analyzes the power distribution of the ideal half-wave FM ZVS QRSW. Voltage nodes and current branches will change their power attributes when the operating point is changed. Some special operating points of the converters can be found. A near-practical model is derived.

The power dissipation and the efficiency of the QRCs can be estimated. It is known that the most critical components are in making the high efficiency converters. Most power is lost in the equivalent resistance of the current branch, the inductor and the main diode. The conduction power loss of each component can be predicted and the most significant component in power dissipation can be found. Therefore, in order to improve the efficiency, the internal resistance of these components should be eliminated first.

The power distribution in the FM ZVS QRCs is found by using some numerical methods and large signal regulated unified model. Some MATLAB functions such as “fminbnd” and “fzero” are used to solve the explicit equation.

Furthermore, the power efficiency of the derived lossy models is considered and studied. It is verified that the efficiency will change when the operating point is varied but the output load voltage is kept regulating by adjusting the switching frequency. The theoretical maximum efficiency under different operating points is known. The maximum efficiency under varying operating conditions is known without doing cycle-by-cycle simulation. Although the FM ZVS QR Converters are

derived only in this paper, this analytical method can be applied in other converters.

The major difficulty is that the time T_2 in equation (4.13) or (5.13) cannot be written explicitly because of the exponential term. Therefore, using numerical method to plot the power distribution and efficiency is a must. It is difficult to find the explicit form of constant V_{Cr} and I_{lr} by using the averaging method shown in equation (2.5).

Although the FM ZVS QR Buck and Boost Converters are considered only in this thesis, this new analytical method can be further generalized by using the other unified near-practical model.

Moreover, this approach can be used to analyze other switching modes such as ZVS Cyclic Quasi-Resonant Switch (ZVS-CQRSW), PWM ZVS-QRSW, PWM ZVS-CQRSW and Active-Clamp Quasi-Resonant Switch (AC ZVS-QRSW).

Finally, these models for efficiency analysis can be collected into a simulation package, for example Simulink in MATLAB [7], that can be used by engineers to evaluate the optimal operating conditions of the converters.

Glossary

AC	Actively clamped
Active Power	Real part P of an apparent power $P+jQ$
Apparent Power	$P+jQ$ where includes the real part P and imaginary part Q of a power
BJT	Bipolar junction transistor
Cr	Resonant capacitor, which is much smaller than the filter capacitor(s)
Capacitor Charging Stage	A period between T_0 and T_1 where S_D and S_M are off and V_{Cr} rises linearly
CBS	Current-bidirectional switch in which current can flow bidirectionally
CCM	Continuous conduction mode, which the filter inductor is large enough to act as a constant current source
CQR	Cyclic QR
CQRC's	Cyclic QRC's
Current Load	A current controlled device acts as a load which dissipates power
Current Source	A current controlled device acts as a source which supplies

power

Damping Factor "a" The resonant amplitude or the stress is smaller if the damping factor "a" ($=R_{ALL} / 2 L_r$) is larger because it is in the index of the exponential component with sinusoidal switching waveform during the resonant stage

f_{max} Maximum switching frequency

f_s Switching frequency

FM Frequency modulation

First Inductor Discharging Stage

A period between T_2 and T_a where both S_D and S_{Ma} are on and I_{Lr} is decreasing. The I_{SMa} will reach zero at T_a .

Free Wheeling Stage

A period between T_3 and T_s where V_{Cr} and I_{Lr} reach zero after T_3 . The diode S_D is off but S_{Mb} is still on. The switch S_M will turn off and C_r will be charged linearly again after T_s because one switching cycle is complete at T_s .

g(α) Transfer function

gmax(α) Maximum transfer function when the condition is at maximum switching frequency fmax

I₁₂ A current flows through V_{12}

I_{12a} A current flows through V_{12a}

I_{12b} A current flows through V_{12b}

I₃ A current branch ($=I_{3a}+I_{3b}+I_{3c}$) shown in Fig. 2.3

I_{3a} A current branch in parallel with S_M shown in Fig. 2.3

I_{3b} A current branch in parallel with S_D shown in Fig. 2.3

I_{3c} A current branch in connectiong to both V_{12a} and V_{12b} shown in Fig. 2.3

I_{Cr} A current flows through C_r

I_{Lr} A current flows through L_r

I_{SD} A current flows through S_D

I_{SM} A current flows through S_M

I_{SMa} A current flows through S_{Ma}

I_{SMb} A current flows through S_{Mb}

Inductor Discharging Stage

A period between T_2 and T_3 where both S_D and S_M are on and I_{Lr} will decrease to zero at T_3 . However, it is divided into first inductor discharging stage and second inductor discharging stage. An intermediate stage T_a is added between T_2 and T_3

Intermediate Current Branch

A current controlled device which is transformed from an inductor where acts as an energy transfer device. Store energy from the source in the first switching cycle and deliver energy to the load in the other switching cycle

Intermediate Voltage Node

A voltage controlled device which is transformed from a capacitor where acts as an energy transfer device. Store energy from the source in the first switching cycle and deliver energy to the load in the other switching cycle

KCL Kirchhoff's current law

KVL Kirchhoff's voltage law

L_r	Resonant inductor, which is much smaller than the filter inductor(s)
Large Signal Model	A model is to represent the circuit in stable operating points
LC resonant network	Inductor capacitor resonant network that forms the quasi-resonant operating condition
MOSFET	Metal Oxide Semiconductor Field Effect Transistor
Power Distribution	It is an analysis to know that each component will either supply or dissipate how much power in the circuit
PWM	Pulse-width modulation, with fixed switching frequency
PWMSW	PWM switch model
QR	Quasi-resonant
QRC	Quasi-resonant converter
QRC's	Quasi-resonant converters
QRCs	Quasi-resonant converters
QRSW	Quasi-resonant switch model
R₁₂	Internal equivalent resistance of V ₁₂
R_{12a}	Internal equivalent resistance of V _{12a}
R_{12b}	Internal equivalent resistance of V _{12b}
R_{C_r}	Internal equivalent resistance of C _r
R_{L_r}	Internal equivalent resistance of L _r
R_{i3}	Internal equivalent resistance of I ₃
R_{i3a}	Internal equivalent resistance of I _{3a}
R_{i3b}	Internal equivalent resistance of I _{3b}
R_{i3c}	Internal equivalent resistance of I _{3c}

R_{LT}	$R_{LT}=R_{Lr}+R_{SD}$
R_{SD}	Internal equivalent resistance of S_D
R_{SMa}	Internal equivalent resistance of S_{Ma}
R_{SMb}	Internal equivalent resistance of S_{Mb}
Reactive Power	Imaginary part Q of an apparent power $P+jQ$
Regulated Model	Output voltage or current is kept constant even though some operating conditions are changed
Resonant Stage	A period between T_1 and T_2 where S_D is on but S_M is off and V_{Cr} resonates with I_{Lr}
S_D	Switching diode
S_M	Switching transistor
S_{Ma}	Reverse current flow diode in parallel with S_{Mb} that forms a bi-directional switching transistor
S_{Mb}	Positive current flow transistor in parallel with S_{Ma} that forms a bi-directional switching transistor
Second Inductor Discharging Stage	
	A period between T_a and T_3 where both S_D and S_{Mb} are on and I_{Lr} is decreasing. The I_{SMb} will increase from zero after T_a . I_{Lr} will reach zero at T_3 .
Small Signal Model	A model is to represent the small change varying operating points. It is mostly created by adding small perturbations and using state-space averaging technique. It is used to analyze the dynamic behaviour and stability of QRC.
T_0	The time when both diode S_D and transistor S_M are off at T_0
T_1	The time when diode S_D will start to conduct at T_1

T_2	The time when capacitor voltage V_{Cr} reaches zero and switch S_M will start to conduct at T_2
T_a	The time when I_{SM} changes from negative value to positive value. The S_{Ma} is conducted before T_a and S_{Mb} is conducted after T_a
T_3	I_{Lr} reaches to zero at T_3
T_s	Switching period of converter ($=1/f_s$)
V_{12}	A voltage node ($= V_{12a} + V_{12b}$)
V_{12a}	A voltage node connecting to S_M directly shown in Fig. 2.3
V_{12b}	A voltage node connecting to S_D directly shown in Fig. 2.3
V_{Cr}	A voltage across C_r
V_{FSD}	Forward bias voltage of S_D
V_{FSMa}	Forward bias voltage of S_{Ma}
V_{FSMb}	Forward bias voltage of S_{Mb}
V_{i3}	A voltage across I_3
V_{i3a}	A voltage across I_{3a}
V_{i3b}	A voltage across I_{3b}
V_{i3c}	A voltage across I_{3c}
V_{Lr}	A voltage across L_r
V_{R12}	A voltage across the R_{12}
V_{R12a}	A voltage across the R_{12a}
V_{R12b}	A voltage across the R_{12b}
V_{RCr}	A voltage across the R_{Cr}
V_{Ri3}	A voltage across the R_{i3}
V_{Ri3a}	A voltage across the R_{i3a}

V_{Ri3b}	A voltage across the R_{i3b}
V_{Ri3c}	A voltage across the R_{i3c}
V_{RLr}	A voltage across the R_{Lr}
V_{RSD}	A voltage across the R_{SD}
V_{RSM}	A voltage across the R_{SM}
V_{RSMa}	A voltage across the R_{SMa}
V_{RSMb}	A voltage across the R_{SMb}
V_{BS}	Voltage-bi-directional switch, the voltage across which can vary bi-directionally
Voltage Load	A voltage controlled device acts as a load which dissipates power
Voltage Source	A voltage controlled device acts as a source which supplies power
w_o	Shifted Resonant angular frequency ($= \sqrt{W_r^2 - a^2}$) with considering internal equivalent resistance in the circuit
w_r	Ideal Resonant angular frequency ($= 1/\sqrt{L_r C_r}$) without considering internal equivalent resistance in the circuit
Z_r	Resonant characteristic impedance ($= \sqrt{L_r/C_r}$)
ZCS	Zero-current switching or, more specifically, zero-current turn-off
ZVS	Zero-voltage switching or, more specifically, zero-voltage turn-on

Appendix A:MATLAB Scripts

A.1 Regulated Buck QRC

These MATLAB scripts are used to simulate the regulated Buck QRC.

```
%Define the components' parameters
clear all
Lr=8e-6; %Define the inductance of Inductor
Cr=800e-12; %Define the capacitance of Capacitor
wr=1/sqrt(Lr*Cr);
Zr=sqrt(Lr/Cr);
vi3b_target=30; %Define the output voltage

%Define the analysis range
v12=1:10:200; %Define the voltage range
i3b=0.1:2:30; %Define the current range

%Calculate the output at each operating point
for i=1:length(v12),
    for j=1:length(i3b),
        alpha=v12(i)./Zr/i3b(j);
        if (alpha<=1)&(alpha>0),
            fs(i,j)=wr*(1-vi3b_target/v12(i))/(pi+asin(alpha)+alpha/2+(1+sqrt(1-alpha.^2))/alpha);
            T1=alpha./wr;
            T2=T1+(pi+asin(alpha))./wr;
            T3=T2+(1+sqrt(1-alpha.^2))./alpha/wr;
            if ((1/T3)<=fs(i,j))|(fs(i,j)<=0),
                fs(i,j)=nan;
                i12(i,j)=nan;
                Pv12(i,j)=nan;
                vi3b(i,j)=nan;
                Pi3b(i,j)=nan;
                g(i,j)=nan;
            else
                Ts=1/fs(i,j);
                Simulation_Time=Ts;
            end
        end
    end
end
```

```

Time_axis=0:Time_step:Simulation_Time;
Time_length=length(Time_axis);
iLr=zeros(Time_length,1);
vCr=zeros(Time_length,1);

%Calculate the output at each time interval
for k=1:Time_length,
    if (rem(Time_axis(k),Ts)>T1)&(rem(Time_axis(k),Ts)<=T2)
        iLr(k)=i3b(j).*(1-cos(wr*(rem(Time_axis(k),Ts)-T1)));
    elseif (rem(Time_axis(k),Ts)>T2)&(rem(Time_axis(k),Ts)<=T3)
        iLr(k)=i3b(j).*(1+sqrt(1-alpha.^2)-alpha.*wr*(rem(Time_axis(k),Ts)-T2));
    end
    if (rem(Time_axis(k),Ts)>0)&(rem(Time_axis(k),Ts)<=T1)
        vCr(k)=v12(i).*wr/alpha*rem(Time_axis(k),Ts);
    elseif (rem(Time_axis(k),Ts)>T1)&(rem(Time_axis(k),Ts)<=T2)
        vCr(k)=v12(i)/alpha*sin(wr*(rem(Time_axis(k),Ts)-T1))+v12(i);
    end
    end
    g(i,j)=fs(i,j)/wr*(pi+asin(alpha)+alpha/2+(1+sqrt(1-alpha^2))/alpha);
%    i12(i,j)=mean(iLr)-i3b(j);
%    i12(i,j)=(g(i,j)-1)*i3b(j);
    Pv12(i,j)=v12(i).*i12(i,j);
%    vi3b(i,j)=v12(i)-mean(vCr);
%    vi3b(i,j)=(1-g(i,j))*v12(i);
    Pi3b(i,j)=vi3b(i,j)*i3b(j);
    end
    else
        fs(i,j)=nan;
        i12(i,j)=nan;
        Pv12(i,j)=nan;
        vi3b(i,j)=nan;
        Pi3b(i,j)=nan;
        g(i,j)=nan;
    end
end
end

%Drow the figures
figure(1);
subplot(2,2,1);
H=mesh(i3b,v12,fs./1e6);
set(H,'markersize',15);
view(20,30);
xlabel('i3b (A)', 'fontsize', 15);
ylabel('v12 (V)', 'fontsize', 15);
zlabel('fs (MHz)', 'fontsize', 15);
title('Lr=8e-6H, Cr=800e-12F, QR Buck Converter', 'fontsize', 15);

%Drow the figures

```

```
subplot(2,2,2);
mesh(i3b,v12,vi3b);
view(20,30);
xlabel('i3b (A)','fontsize',15);
ylabel('v12 (V)','fontsize',15);
zlabel('vi3b (V)','fontsize',15);
title('Lr=8e-6H, Cr=800e-12F, QR Buck Converter','fontsize',15);

%Draw the figures
subplot(2,2,3);
mesh(i3b,v12,i12);
view(20,30);
xlabel('i3b (A)','fontsize',15);
ylabel('v12 (V)','fontsize',15);
zlabel('i12 (A)','fontsize',15);
title('Lr=8e-6H, Cr=800e-12F, QR Buck Converter','fontsize',15);

%Draw the figures
subplot(2,2,4);
mesh(i3b,v12,Pi3b);
hold on;
mesh(i3b,v12,Pv12);
hold off;
view(20,30);
xlabel('i3b (A)','fontsize',15);
ylabel('v12 (V)','fontsize',15);
zlabel('Pi3b(+ve) Pv12(-ve) (W)','fontsize',15);
title('Lr=8e-6H, Cr=800e-12F, QR Buck Converter','fontsize',15);
```

A.2 Regulated Boost QRC

These MATLAB scripts are used to simulate the regulated Boost QRC.

```
%Define the components' parameters
clear all
Lr=8e-6;
Cr=800e-12;
wr=1/sqrt(Lr*Cr);
Zr=sqrt(Lr/Cr);
v12_target=30;

%Define the analysis range
vi3a=-20:-2:-30;
i12=logspace(-1,1.477);

%Calculate the output at each operating point
for i=1:length(vi3a),
    for j=1:length(i12),
        i3a(i,j)=i12(j)*(-v12_target)/vi3a(i);
        alpha=v12_target./Zr/i3a(i,j);
        if (alpha<=1)&(alpha>0),
            fs(i,j)=wr*(-vi3a(i)/v12_target)/(pi+asin(alpha)+alpha/2+(1+sqrt(1-alpha^2))/alpha);
            T1=alpha./wr;
            T2=T1+(pi+asin(alpha))./wr;
            T3=T2+(1+sqrt(1-alpha.^2))./alpha/wr;
            if ((1/T3)<=fs(i,j))|(fs(i,j)<=0),
                fs(i,j)=nan;
                v12(i,j)=nan;
                Pv12(i,j)=nan;
                Pi3a(i,j)=nan;
                g(i,j)=nan;
            else
                g(i,j)=fs(i,j)/wr*(pi+asin(alpha)+alpha/2+(1+sqrt(1-alpha^2))/alpha);
                v12(i,j)=v12_target;
                Pv12(i,j)=v12_target.*i12(j);
                Pi3a(i,j)=vi3a(i)*i3a(i,j);
            end
        else
            fs(i,j)=nan;
            v12(i,j)=nan;
            Pv12(i,j)=nan;
            Pi3a(i,j)=nan;
            g(i,j)=nan;
        end
    end
end
```

```
%Draw the figures
figure(1);
subplot(2,2,1);
mesh(i12,vi3a,fs./1e6);
view(20,30);
xlabel('i12 (A)', 'fontsize', 15);
ylabel('vi3a (V)', 'fontsize', 15);
zlabel('fs (MHz)', 'fontsize', 15);
title('Lr=8e-6H, Cr=800e-12F', 'fontsize', 15);

%Draw the figures
subplot(2,2,2);
mesh(i12,vi3a,v12);
%set(gca,'ZLim',[-30 -28]);
view(20,30);
xlabel('i12 (A)', 'fontsize', 15);
ylabel('vi3a (V)', 'fontsize', 15);
zlabel('v12 (V)', 'fontsize', 15);
title('Lr=8e-6H, Cr=800e-12F', 'fontsize', 15)

%Draw the figures
subplot(2,2,3);
mesh(i12,vi3a,i3a);
view(20,30);
xlabel('i12 (A)', 'fontsize', 15);
ylabel('vi3a (V)', 'fontsize', 15);
zlabel('i3a (A)', 'fontsize', 15);
title('Lr=8e-6H, Cr=800e-12F', 'fontsize', 15)

%Draw the figures
subplot(2,2,4);
mesh(i12,vi3a,Pi3a);
hold on;
mesh(i12,vi3a,Pv12);
hold off;
view(20,30);
xlabel('i12 (A)', 'fontsize', 15);
ylabel('vi3a (V)', 'fontsize', 15);
zlabel('Pi3a(-ve) Pv12(+ve) (W)', 'fontsize', 15);
title('Lr=8e-6H, Cr=800e-12F', 'fontsize', 15);
```

A.3 Regulated Buck-Boost QRC

These MATLAB scripts are used to simulate the regulated Buck-Boost QRC.

```
%Define the components' parameters
clear all
Lr=8e-6;
Cr=800e-12;
wr=1/sqrt(Lr*Cr);
Zr=sqrt(Lr/Cr);
v12b_target=30;

%Define the analysis range
v12=50:10:230;
v12a=v12-v12b_target;
i12b=0.1:2:30;

%Calculate the output at each operating point
for i=1:length(v12a),
    for j=1:length(i12b),
        i3c(i,j)=i12b(j)*v12(i)/v12a(i);
        v12b(i,j)=v12b_target;
        alpha=v12(i)./Zr/i3c(i,j);
        if (alpha<=1)&(alpha>0),
            fs(i,j)=wr*(v12a(i)/v12(i))/(pi+asin(alpha)+alpha/2+(1+sqrt(1-alpha^2))/alpha);
            T1=alpha./wr;
            T2=T1+(pi+asin(alpha))./wr;
            T3=T2+(1+sqrt(1-alpha.^2))./alpha./wr;
            if ((1/T3)<=fs(i,j))|(fs(i,j)<=0),
                fs(i,j)=nan;
                g(i,j)=nan;
                Pv12b(i,j)=nan;
                i12a(i,j)=nan;
                Pv12a(i,j)=nan;
                vi3c(i,j)=nan;
                Pi3c(i,j)=nan;
            else
                g(i,j)=fs(i,j)/wr*(pi+asin(alpha)+alpha/2+(1+sqrt(1-alpha^2))/alpha);
                Pv12b(i,j)=v12b(i,j).*i12b(j);
                i12a(i,j)=i12b(j)-i3c(i,j);
                Pv12a(i,j)=v12a(i).*i12a(i,j);
                vi3c(i,j)=v12a(i)-g(i,j)*v12(i);
                Pi3c(i,j)=vi3c(i,j)*i3c(i,j);
            end
        else
            fs(i,j)=nan;
            g(i,j)=nan;
            Pv12b(i,j)=nan;
```

```
i12a(i,j)=nan;
Pv12a(i,j)=nan;
vi3c(i,j)=nan;
Pi3c(i,j)=nan;
end
end
end

%Draw the figures
figure(1);
subplot(2,2,1);
mesh(i12b,v12a,fs./1e6);
view(20,30);
xlabel('i12b (A)','fontsize',15);
ylabel('v12a (V)','fontsize',15);
zlabel('fs (MHz)','fontsize',15);
title('Lr=8e-6H, Cr=800e-12F','fontsize',15);

%Draw the figures
subplot(2,2,2);
mesh(i12b,v12a,vi3c);
hold on;
mesh(i12b,v12a,v12b);
hold off;
%set(gca,'ZLim',[-30 -28]);
view(20,30);
xlabel('i12b (A)','fontsize',15);
ylabel('v12a (V)','fontsize',15);
zlabel('vi3c=0 v12b (V)','fontsize',15);
title('Lr=8e-6H, Cr=800e-12F','fontsize',15)

%Draw the figures
subplot(2,2,3);
mesh(i12b,v12a,i12a);
hold on;
mesh(i12b,v12a,i3c);
hold off;
view(20,30);
xlabel('i12b (A)','fontsize',15);
ylabel('v12a (V)','fontsize',15);
zlabel('i12a(-ve) i3c(+ve) (A)','fontsize',15);
title('Lr=8e-6H, Cr=800e-12F','fontsize',15)

%Draw the figures
subplot(2,2,4);
mesh(i12b,v12a,Pv12a);
hold on;
%mesh(i12b,v12a,Pi3c);
mesh(i12b,v12a,Pv12b);
```

```
hold off;
view(20,30);
xlabel('i12b (A)', 'fontsize', 15);
ylabel('v12a (V)', 'fontsize', 15);
zlabel('Pv12a(-ve) Pv12b(+ve) (W)', 'fontsize', 15);
title('Lr=8e-6H, Cr=800e-12F', 'fontsize', 15);
```

A.4 Regulated Cuk QRC

These MATLAB scripts are used to simulate the regulated Cuk QRC.

```
%Define the components' parameters
clear all
Lr=8e-6;
Cr=800e-12;
wr=1/sqrt(Lr*Cr);
Zr=sqrt(Lr/Cr);
vi3b_target=30;

%Define the analysis range
vi3a=-31:-10:-200;
i3b=0.1:2:30;

%Calculate the output at each operating point
for i=1:length(vi3a),
    for j=1:length(i3b),
        vi3b(i,j)=vi3b_target;
        v12(i,j)=vi3b(i,j)-vi3a(i);
        i3(i,j)=-v12(i,j)*i3b(j)/vi3a(i);
        alpha=v12(i,j)./Zr/i3(i,j);
        if (alpha<=1)&(alpha>0),
            fs(i,j)=wr*(i3b(j)/i3(i,j))/(pi+asin(alpha)+alpha/2+(1+sqrt(1-alpha^2))/alpha);
            T1=alpha./wr;
            T2=T1+(pi+asin(alpha))./wr;
            T3=T2+(1+sqrt(1-alpha.^2))./alpha/wr;
            if ((1/T3)<=fs(i,j))|(fs(i,j)<=0),
                fs(i,j)=nan;
                g(i,j)=nan;
                i12(i,j)=nan;
                Pv12(i,j)=nan;
                i3a(i,j)=nan;
                Pi3a(i,j)=nan;
                Pi3b(i,j)=nan;
            else
                g(i,j)=fs(i,j)/wr*(pi+asin(alpha)+alpha/2+(1+sqrt(1-alpha^2))/alpha);
                i12(i,j)=g(i,j)*i3(i,j)-i3b(j);
                Pv12(i,j)=v12(i,j).*i12(i,j);
                i3a(i,j)=i3(i,j)-i3b(j);
                Pi3a(i,j)=vi3a(i)*i3a(i,j);
                Pi3b(i,j)=vi3b(i,j)*i3b(j);
            end
        else
            fs(i,j)=nan;
            g(i,j)=nan;
            i12(i,j)=nan;
```

```
Pv12(i,j)=nan;
i3a(i,j)=nan;
Pi3a(i,j)=nan;
Pi3b(i,j)=nan;
end
end
end

%Draw the figures
figure(1);
subplot(2,2,1);
mesh(i3b,vi3a,fs./1e6);
view(20,30);
xlabel('Load Current i3b (A)', 'fontsize', 10);
ylabel('Supply vi3a (V)', 'fontsize', 10);
zlabel('fs (MHz)', 'fontsize', 15);
title('Lr=8e-6H, Cr=800e-12F, QR Cuk Converter', 'fontsize', 15);

%Draw the figures
subplot(2,2,2);
mesh(i3b,vi3a,vi3b);
hold on;
mesh(i3b,vi3a,v12);
hold off;
view(20,20);
xlabel('Load Current i3b (A)', 'fontsize', 10);
ylabel('Supply vi3a (V)', 'fontsize', 10);
zlabel('vi3b=30, v12 (V)', 'fontsize', 15);
title('Lr=8e-6H, Cr=800e-12F, QR Cuk Converter', 'fontsize', 15);

%Draw the figures
subplot(2,2,3);
mesh(i3b,vi3a,i12);
hold on;
mesh(i3b,vi3a,i3a);
hold off;
view(20,20);
xlabel('Load Current i3b (A)', 'fontsize', 10);
ylabel('Supply vi3a (V)', 'fontsize', 10);
zlabel('i12=0, i3a(+ve) (A)', 'fontsize', 15);
title('Lr=8e-6H, Cr=800e-12F, QR Cuk Converter', 'fontsize', 15);

%Draw the figures
subplot(2,2,4);
mesh(i3b,vi3a,Pi3a);
hold on;
mesh(i3b,vi3a,Pi3b);
hold off;
view(20,30);
```

```
xlabel('Load Current i3b (A)', 'fontsize', 10);
ylabel('Supply vi3a (V)', 'fontsize', 10);
zlabel('Pi3a(-ve) Pi3b(+ve) (W)', 'fontsize', 15);
title('Lr=8e-6H, Cr=800e-12F, QR Cuk Converter', 'fontsize', 15);
```

A.5 Regulated Sepic QRC

These MATLAB scripts are used to simulate the regulated Sepic QRC.

```
%Define the components' parameters
clear all
Lr=8e-6;
Cr=800e-12;
wr=1/sqrt(Lr*Cr);
Zr=sqrt(Lr/Cr);
v12b_target=30;

%Define the analysis range
vi3a=-30:-10:-200;
i12b=0.1:2:30;

%Calculate the output at each operating point
for i=1:length(vi3a),
    for j=1:length(i12b),
        v12b(i,j)=v12b_target;
        v12a(i,j)=-vi3a(i);
        v12(i,j)=v12a(i,j)+v12b(i,j);
        i3c(i,j)=i12b(j);
        i3a(i,j)=i12b(j)*((vi3a(i)-v12b(i,j))/vi3a(i)-1);
        i3(i,j)=i3a(i,j)+i3c(i,j);
        alpha=v12(i,j)./Zr/i3(i,j);
        if (alpha<=1)&(alpha>0),
            fs(i,j)=wr*(i3c(i,j)/i3(i,j))/(pi+asin(alpha)+alpha/2+(1+sqrt(1-alpha^2))/alpha);
            T1=alpha./wr;
            T2=T1+(pi+asin(alpha))./wr;
            T3=T2+(1+sqrt(1-alpha.^2))./alpha/wr;
            if ((1/T3)<=fs(i,j))|(fs(i,j)<=0),
                fs(i,j)=nan;
                g(i,j)=nan;
                i12a(i,j)=nan;
                Pv12a(i,j)=nan;
                Pv12b(i,j)=nan;
                Pi3a(i,j)=nan;
                Pi3c(i,j)=nan;
            else
                g(i,j)=fs(i,j)/wr*(pi+asin(alpha)+alpha/2+(1+sqrt(1-alpha^2))/alpha);
                i12a(i,j)=i12b(j)-i3c(i,j);
                Pv12a(i,j)=v12a(i,j)*i12a(i,j);
                Pv12b(i,j)=v12b(i,j)*i12b(j);
                Pi3a(i,j)=vi3a(i)*i3a(i,j);
                vi3c(i,j)=v12a(i,j)+vi3a(i);
                Pi3c(i,j)=vi3c(i,j)*i3c(i,j);
            end
        end
    end
end
```



```
    end
else
    fs(i,j)=nan;
    g(i,j)=nan;
    i12a(i,j)=nan;
    Pv12a(i,j)=nan;
    Pv12b(i,j)=nan;
    Pi3a(i,j)=nan;
    Pi3c(i,j)=nan;
end
end
end

%Draw the figures
figure(1);
subplot(2,2,1);
mesh(i12b,vi3a,fs./1e6);
view(20,30);
xlabel('i12b (A)','fontsize',15);
ylabel('vi3a (V)','fontsize',15);
zlabel('fs (MHz)','fontsize',15);
title('Lr=8e-6H, Cr=800e-12F','fontsize',15);

%Draw the figures
subplot(2,2,2);
mesh(i12b,vi3a,v12a);
hold on;
mesh(i12b,vi3a,v12b);
mesh(i12b,vi3a,vi3c);
hold off;
view(20,20);
xlabel('i12b (A)','fontsize',15);
ylabel('vi3a (V)','fontsize',15);
zlabel('vi3c=0, v12b=30, v12a (V)','fontsize',15);
title('Lr=8e-6H, Cr=800e-12F','fontsize',15)

%Draw the figures
subplot(2,2,3);
mesh(i12b,vi3a,i3a);
hold on;
mesh(i12b,vi3a,i12a);
mesh(i12b,vi3a,i3c);
hold off;
view(20,40);
xlabel('i12b (A)','fontsize',15);
ylabel('vi3a (V)','fontsize',15);
zlabel('i12a=0, i3a, i3c=i12b (A)','fontsize',15);
title('Lr=8e-6H, Cr=800e-12F','fontsize',15)
```

```
%Draw the figures
subplot(2,2,4);
mesh(i12b,vi3a,Pi3a);
hold on;
mesh(i12b,vi3a,Pv12b);
hold off;
view(20,30);
xlabel('i12b (A)', 'fontsize', 15);
ylabel('vi3a (V)', 'fontsize', 15);
zlabel('Pi3a(-ve) Pv12b(+ve) (W)', 'fontsize', 15);
title('Lr=8e-6H, Cr=800e-12F', 'fontsize', 15);
```

A.6 Regulated Zeta QRC

These MATLAB scripts are used to simulate the regulated Zeta QRC.

```
%Define the components' parameters
clear all
Lr=8e-6;
Cr=800e-12;
wr=1/sqrt(Lr*Cr);
Zr=sqrt(Lr/Cr);
vi3b_target=30;

%Define the analysis range
v12a=30:10:200;
i3b=0.1:2:30;

%Calculate the output at each operating point
for i=1:length(v12a),
    for j=1:length(i3b),
        vi3b(i,j)=vi3b_target;
        v12b(i,j)=vi3b_target;
        v12(i,j)=v12a(i)+v12b(i,j);
        i3c(i,j)=i3b(j)*((v12a(i)+vi3b_target)/v12a(i)-1);
        i12a(i,j)=-i3c(i,j);
        i3(i,j)=i3b(j)+i3c(i,j);
        alpha=v12(i,j)./Zr/i3(i,j);
        if (alpha<=1)&(alpha>0),
            fs(i,j)=wr*(i3b(j)/i3(i,j))/(pi+asin(alpha)+alpha/2+(1+sqrt(1-alpha^2))/alpha);
            T1=alpha./wr;
            T2=T1+(pi+asin(alpha))./wr;
            T3=T2+(1+sqrt(1-alpha.^2))./alpha/wr;
            if ((1/T3)<=fs(i,j))|(fs(i,j)<=0),
                fs(i,j)=nan;
                g(i,j)=nan;
                i12a(i,j)=nan;
                Pv12a(i,j)=nan;
                i12b(i,j)=nan;
                Pv12b(i,j)=nan;
                Pi3b(i,j)=nan;
                vi3c(i,j)=nan;
                Pi3c(i,j)=nan;
            else
                g(i,j)=fs(i,j)/wr*(pi+asin(alpha)+alpha/2+(1+sqrt(1-alpha^2))/alpha);
                Pv12a(i,j)=v12a(i)*i12a(i,j);
                i12b(i,j)=i12a(i,j)+i3c(i,j);
                Pv12b(i,j)=v12b(i,j)*i12b(i,j);
                Pi3b(i,j)=vi3b_target*i3b(j);
                vi3c(i,j)=vi3b_target-v12b(i,j);
            end
        end
    end
end
```

```

Pi3c(i,j)=vi3c(i,j)*i3c(i,j);
end
else
    fs(i,j)=nan;
    g(i,j)=nan;
    i12a(i,j)=nan;
    Pv12a(i,j)=nan;
    i12b(i,j)=nan;
    Pv12b(i,j)=nan;
    Pi3b(i,j)=nan;
    vi3c(i,j)=nan;
    Pi3c(i,j)=nan;
end
end
end

%Draw the figures
figure(1);
subplot(2,2,1);
mesh(i3b,v12a,fs./1e6);
view(20,30);
xlabel('i3b (A)','fontsize',15);
ylabel('v12a (V)','fontsize',15);
zlabel('fs (MHz)','fontsize',15);
title('Lr=8e-6H, Cr=800e-12F','fontsize',15);

%Draw the figures
subplot(2,2,2);
mesh(i3b,v12a,v12b);
hold on;
mesh(i3b,v12a,vi3b);
mesh(i3b,v12a,vi3c);
hold off;
view(20,20);
xlabel('i3b (A)','fontsize',15);
ylabel('v12a (V)','fontsize',15);
zlabel('vi3b=30, vi3c=0, v12b=30 (V)','fontsize',15);
title('Lr=8e-6H, Cr=800e-12F','fontsize',15)

%Draw the figures
subplot(2,2,3);
mesh(i3b,v12a,i12a);
hold on;
mesh(i3b,v12a,i12b);
mesh(i3b,v12a,i3c);
hold off;
view(20,30);
xlabel('i3b (A)','fontsize',15);
ylabel('v12a (V)','fontsize',15);

```

```
zlabel('i12a(-ve), i12b=0, i3c(+ve) (A)', 'fontsize', 15);
title('Lr=8e-6H, Cr=800e-12F', 'fontsize', 15)

%Draw the figures
subplot(2,2,4);
mesh(i3b,v12a,Pi3b);
hold on;
mesh(i3b,v12a,Pv12a);
%mesh(i3b,v12a,Pv12b);
%mesh(i3b,v12a,Pi3c);
hold off;
view(20,30);
xlabel('i3b (A)', 'fontsize', 15);
ylabel('v12a (V)', 'fontsize', 15);
zlabel('Pv12a(-ve) Pi3b(+ve) (W)', 'fontsize', 15);
title('Lr=8e-6H, Cr=800e-12F', 'fontsize', 15);
```

A.7 Regulated Lossy Buck QRC

These MATLAB scripts are used to simulate the regulated Lossy Buck QRC.

```
%Define the global variables
clear all
global Lr Cr wr Zr vi3b_target
global R12 RLr RCr RSD RSMA RSMB Ri3b VFSD VFSMa VFSMb
global RCT RLT RALL a wo Aa Ab v12 i3b

global i j
global alpha beta T1 C1 K1 phase1 K2 phase2 K3 phase3 K4 phase4 KT2 phaseT2
T2
global C5a K5a Ta C5b K5b T3 K6a K6b

%Define the components' parameters
syms x
Lr=8e-6;
Cr=800e-12;
wr=1/sqrt(Lr*Cr);
Zr=sqrt(Lr/Cr);
vi3b_target=30;

R12=0.1;
RLr=0.1;
RCr=0.1;
RSD=0.1;
RSMA=0.1;
RSMB=0.1;
Ri3b=0.1;
VFSD=0.7;
VFSMa=0.7;
VFSMb=0.7;

RCT=RCr+R12;
RLT=RLr+RSD;
RALL=RLT+RCT;
a=RALL/2/Lr;
wo=sqrt(wr^2-a^2);
Aa=(RLT+R12+RSMA)/Lr;
Ab=(RLT+R12+RSMB)/Lr;

%Define the analysis range
v12=51:10:200;
i3b=0.1:2:30;

%Calculate the output at each operating point
for i=1:length(v12),
```

```

for j=1:length(i3b),
    alpha=v12(i)./Zr./i3b(j);
    beta=VFSD./Zr./i3b(j);
    if (alpha<=1)&(alpha>0),
        T1=Cr./i3b(j)*(-i3b(j)*R12+v12(i)-i3b(j)*RCr);
        C1=VFSD+v12(i)+i3b(j)*RLT;
        K1=v12(i)/alpha*sqrt(1+(wr^2/wo^2)*(RALL/2/Zr+beta)^2);
        phase1=2*pi-atan((RALL/Zr+beta)/(wr/wo-a/wo*(RALL/Zr+beta)));
        K2=K1/Zr;
        phase2=phase1+pi-atan(wo/a);
        K3=sqrt(1+(beta+a)^2/wo^2);
        phase3=atan(wo/(beta+a));
        K4=i3b(j)*K3*Zr;
        phase4=phase3+2*pi-atan(wo/a);
        KT2=K1*RCr*Cr*sqrt((1/RCr/Cr-a)^2+wo^2);
        phaseT2=phase1+atan(wo/(1/RCr/Cr-a));
        funf=char(eval('C1+KT2*exp(-a*x)*sin(wo*x+phaseT2)')); 
        T2=fzero(funf,[2*pi/wo/4 2*pi*3/wo/4])+T1;
        if ((T2-T1)<0),
            error('error: T2<T1');
        end

C5a=(i3b(j)*R12+i3b(j)*RSMa-VFSD-VFSMa-v12(i))/(RLT+R12+RSMa);
K5a=i3b(j)*(1-K3*exp(-a*(T2-T1))*sin(wo*(T2-T1)+phase3))-C5a;
Ta=T2-1/Aa*log((i3b(j)-C5a)/K5a);

C5b=(i3b(j)*R12+i3b(j)*RSMb-VFSD+VFSMb-v12(i))/(RLT+R12+RSMb);
K5b=i3b(j)-C5b;
T3=Ta-1/Ab*log(-C5b/K5b);

K6a=-Lr*K5a*Aa;
K6b=-Lr*K5b*Ab;

fs_init=wr*(1-vi3b_target/v12(i))/(pi+asin(alpha)+alpha/2+(1+sqrt(1-alpha^2))/alpha);
fs_org(i,j)=fs_init;
if fs_init>0
    options=optimset('Display','off');
    fs(i,j)=fminbnd('obj_v12',0.5*fs_init,fs_init,options);
else
    fs(i,j)=0;
end

if ((1/T3)<=fs(i,j))|(fs(i,j)<=0),
    fs(i,j)=nan;
    fs_org(i,j)=nan;
    Pv12(i,j)=nan;
    Pi3b(i,j)=nan;
    PR12(i,j)=nan;

```

```

PRj3b(i,j)=nan;
PRCr(i,j)=nan;
PRLr(i,j)=nan;
PRSD(i,j)=nan;
PRSMa(i,j)=nan;
PRSMb(i,j)=nan;
PRSM(i,j)=nan;
PVFSD(i,j)=nan;
PVFSMa(i,j)=nan;
PVFSMb(i,j)=nan;
PVFSM(i,j)=nan;
PCr(i,j)=nan;
PLr(i,j)=nan;
i12(i,j)=nan;
vi3b(i,j)=nan;
else
    Ts=1/fs(i,j);
    Simulation_Time=Ts;
    resolution=10000;
    Time_step=Simulation_Time/resolution;
    Time_axis=Time_step:Time_step:Time_step*(resolution-1);
    Time_length=length(Time_axis);
    vCr=zeros(Time_length,1);
    iCr=zeros(Time_length,1);
    iLr=zeros(Time_length,1);
    vLr=zeros(Time_length,1);
    iSMA=zeros(Time_length,1);
    iSMB=zeros(Time_length,1);
    i12_t=zeros(Time_length,1);
    vi3b_t=zeros(Time_length,1);

    for k=1:Time_length,
        Time_now=rem(Time_axis(k),Ts);
        if (Time_now>0)&(Time_now<=T1)
            vCr(k)=v12(i)/alpha*wr*Time_now;
            iCr(k)=i3b(j);
            i12_t(k)=-i3b(j);
            vi3b_t(k)=-i3b(j)*Ri3b-vCr(k)-iCr(k)*RCr+v12(i)-i3b(j)*R12;
        elseif (Time_now>T1)&(Time_now<=T2)
            vCr(k)=C1+K1*exp(-a*(Time_now-T1))*sin(wo*(Time_now-
T1)+phase1);
            iCr(k)=K2*exp(-a*(Time_now-T1))*sin(wo*(Time_now-
T1)+phase2);
            iLr(k)=i3b(j)*(1-K3*exp(-a*(Time_now-T1)))*sin(wo*(Time_now-
T1)+phase3));
            vLr(k)=K4*exp(-a*(Time_now-T1))*sin(wo*(Time_now-
T1)+phase4);
            i12_t(k)=iLr(k)-i3b(j);
            vi3b_t(k)=-i3b(j)*Ri3b-iLr(k)*RLT-VFSD-vLr(k);
        else
            vCr(k)=v12(i)/alpha*wr*Time_now;
            iCr(k)=i3b(j);
            i12_t(k)=-i3b(j);
            vi3b_t(k)=-i3b(j)*Ri3b-vCr(k)-iCr(k)*RCr+v12(i)-i3b(j)*R12;
        end;
    end;
end;

```

```

elseif (Time_now>T2)&(Time_now<=Ta)
    iLr(k)=C5a+K5a*exp(-Aa*(Time_now-T2));
    vLr(k)=K6a*exp(-Aa*(Time_now-T2));
    iSMA(k)=i3b(j)-iLr(k);
    i12_t(k)=iLr(k)-i3b(j);
    vi3b_t(k)=-i3b(j)*Ri3b-iLr(k)*RLT-VFSD-vLr(k);
elseif (Time_now>Ta)&(Time_now<=T3)
    iLr(k)=C5b+K5b*exp(-Ab*(Time_now-Ta));
    vLr(k)=K6b*exp(-Ab*(Time_now-Ta));
    iSMb(k)=i3b(j)-iLr(k);
    i12_t(k)=iLr(k)-i3b(j);
    vi3b_t(k)=-i3b(j)*Ri3b-iLr(k)*RLT-VFSD-vLr(k);
elseif (Time_now>T3)&(Time_now<=Ts)
    iSMb(k)=i3b(j);
    i12_t(k)=-i3b(j);
    vi3b_t(k)=-i3b(j)*Ri3b-iSMb(k)*RSMb-VFSMb+v12(i)-i3b(j)*R12;
end
end
mean_vCr=mean(vCr);
mean_iCr=mean(iCr);
rms_iCr=sqrt(mean(iCr.^2));
mean_iLr=mean(iLr);
rms_iLr=sqrt(mean(iLr.^2));
mean_vLr=mean(vLr);
mean_iSMA=mean(iSMA);
rms_iSMA=sqrt(mean(iSMA.^2));
mean_iSMb=mean(iSMb);
rms_iSMb=sqrt(mean(iSMb.^2));
mean_i12=mean(i12_t);
rms_i12=sqrt(mean(i12_t.^2));
mean_vi3b=mean(vi3b_t);

Pv12(i,j)=v12(i)*mean_i12;
Pi3b(i,j)=i3b(j)*mean_vi3b;
PR12(i,j)=R12*rms_i12^2;
PRi3b(i,j)=Ri3b*i3b(j)^2;
PRCr(i,j)=RCr*rms_iCr^2;
PRLr(i,j)=RLr*rms_iLr^2;
PRSD(i,j)=RSD*rms_iLr^2;
PRSMa(i,j)=RSMa*rms_iSMA^2;
PRSMB(i,j)=RSMB*rms_iSMb^2;
PRSM(i,j)=PRSMa(i,j)+PRSMB(i,j);
PVFSD(i,j)=VFSD*mean_iLr;
PVFSMa(i,j)=-VFSMa*mean_iSMA;
PVFSMb(i,j)=VFSMb*mean_iSMb;
PVFSM(i,j)=PVFSMa(i,j)+PVFSMb(i,j);
PCr(i,j)=mean_iCr*mean_vCr;
PLr(i,j)=mean_iLr*mean_vLr;
i12(i,j)=mean_i12;

```

```

    vi3b(i,j)=mean_vvi3b;
    end
else
    fs(i,j)=nan;
    fs_org(i,j)=nan;
    Pv12(i,j)=nan;
    Pi3b(i,j)=nan;
    PR12(i,j)=nan;
    PRi3b(i,j)=nan;
    PRCr(i,j)=nan;
    PRLr(i,j)=nan;
    PRSD(i,j)=nan;
    PRSMa(i,j)=nan;
    PRSMb(i,j)=nan;
    PRSM(i,j)=nan;
    PVFSD(i,j)=nan;
    PVFSMa(i,j)=nan;
    PVFSMb(i,j)=nan;
    PVFSM(i,j)=nan;
    PCr(i,j)=nan;
    PLr(i,j)=nan;
    i12(i,j)=nan;
    vi3b(i,j)=nan;
end
end
end

%Draw the figures
figure(1);
colormap([0 0 0]);
subplot(2,2,1);
H=mesh(i3b,v12,fs./1e6);
set(H,'markersize',15);
view(20,30);
xlabel('i3 (A)', 'fontsize', 15);
ylabel('v12 (V)', 'fontsize', 15);
zlabel('fs (MHz)', 'fontsize', 15);
title('Lr=8e-6H, Cr=800e-12F, QR Buck Converter', 'fontsize', 15);

%Draw the figures
subplot(2,2,2);
mesh(i3b,v12,vi3b);
%hold on;
%mesh(i3b,v12,Pv12);
%hold off;
view(20,30);
xlabel('i3 (A)', 'fontsize', 15);
ylabel('v12 (V)', 'fontsize', 15);
zlabel('vi3 (V)', 'fontsize', 15);

```

```
axis([0 30 50 200 29.999 30.001]);
title('Lr=8e-6H, Cr=800e-12F, QR Buck Converter','fontsize',15);

%Draw the figures
subplot(2,2,3);
mesh(i3b,v12,i12);
view(20,30);
xlabel('i3 (A)','fontsize',15);
ylabel('v12 (V)','fontsize',15);
zlabel('i12 (A)','fontsize',15);
title('Lr=8e-6H, Cr=800e-12F, QR Buck Converter','fontsize',15);

%Draw the figures
subplot(2,2,4);
mesh(i3b,v12,Pi3b);
hold on;
mesh(i3b,v12,Pv12);
hold off;
view(20,30);
xlabel('i3 (A)','fontsize',15);
ylabel('v12 (V)','fontsize',15);
zlabel('Pi3(+ve) Pv12(-ve) (W)','fontsize',15);
title('Lr=8e-6H, Cr=800e-12F, QR Buck Converter','fontsize',15);

%Draw the figures
figure(2)
colormap([0 0 0]);
subplot(3,3,1);
mesh(i3b,v12,PR12./max(max(PRLr)));
xlabel('i3 (A)');
ylabel('v12 (V)');
zlabel('Normalized PR12');
subplot(3,3,2);
mesh(i3b,v12,PRLr./max(max(PRLr)));
xlabel('i3 (A)');
ylabel('v12 (V)');
zlabel('Normalized PRLr');
subplot(3,3,3);
mesh(i3b,v12,PRCr./max(max(PRLr)));
xlabel('i3 (A)');
ylabel('v12 (V)');
zlabel('Normalized PRCr');
subplot(3,3,4);
mesh(i3b,v12,PRSD./max(max(PRLr)));
xlabel('i3 (A)');
ylabel('v12 (V)');
zlabel('Normalized PRSD');
subplot(3,3,5);
mesh(i3b,v12,PRSMA./max(max(PRLr)));

```

```

xlabel('i3 (A)');
ylabel('v12 (V)');
zlabel('Normalized PRSMa');
subplot(3,3,6);
mesh(i3b,v12,PRSMb./max(max(PRLr)));
xlabel('i3 (A)');
ylabel('v12 (V)');
zlabel('Normalized PRSMb');
subplot(3,3,7);
mesh(i3b,v12,PRi3b./max(max(PRLr)));
xlabel('i3 (A)');
ylabel('v12 (V)');
zlabel('Normalized PRi3');
subplot(3,3,8);
mesh(i3b,v12,PVFSD./max(max(PRLr)));
xlabel('i3 (A)');
ylabel('v12 (V)');
zlabel('Normalized PVFSD');
subplot(3,3,9);
mesh(i3b,v12,PVFSMa./max(max(PRLr)));
hold on;
mesh(i3b,v12,PVFSMb./max(max(PRLr)));
hold off;
xlabel('i3 (A)');
ylabel('v12 (V)');
zlabel('Normalized PVFSMa & PVFSMb','VerticalAlignment','bottom');

%Draw the figures
figure(3)
colormap([0 0 0]);
Ploss=PR12+PRLr+PRCr+PRSD+PRSMa+PRSMb+PRi3b+PVFSD+PVFSMa+PV
FSMb;
H=mesh(i3b,v12,Pi3b./(Ploss-Pv12).*100);
set(H,'markersize',15);
xlabel('i3 (A)','fontsize',15,'VerticalAlignment','bottom');
ylabel('v12 (V)','fontsize',15,'VerticalAlignment','bottom');
zlabel('Efficiency (%)','fontsize',15);
title('Lr=8e-6H, Cr=800e-12F, QR Buck Converter','fontsize',15);
view(60,10);

```

```

%Define the object function in a separate file
function error=obj_v13b(fs)

%Define the global variables
global Lr Cr wr Zr vi3b_target
global R12 RLr RCr RSD RSMA RSMb Ri3b VFSD VFSMa VFSMb
global RCT RLT RALL a wo Aa Ab v12 i3b

global i j
global alpha beta T1 C1 K1 phase1 K2 phase2 K3 phase3 K4 phase4 KT2 phaseT2
T2
global C5a K5a Ta C5b K5b T3 K6a K6b

%Define the time scale interval
Ts=1/fs; Simulation_Time=Ts; resolution=10000;
Time_step=Simulation_Time/resolution;
Time_axis=Time_step:Time_step:Time_step*(resolution-1);
Time_length=length(Time_axis); %vCr=zeros(Time_length,1);
%viLr=zeros(Time_length,1); %vLr=zeros(Time_length,1);
vi3b_t=zeros(Time_length,1);

for k=1:Time_length,
    Time_now=rem(Time_axis(k),Ts);
    if (Time_now>0)&(Time_now<=T1)
        vi3b_t(k)=-i3b(j)*Ri3b-(v12(i)/alpha*wr*Time_now)-i3b(j)*RCr+v12(i)-
i3b(j)*R12;
    elseif (Time_now>T1)&(Time_now<=T2)
        vi3b_t(k)=-i3b(j)*Ri3b-(i3b(j)*(1-K3*exp(-a*(Time_now-
T1)))*sin(wo*(Time_now-T1)+...
phase3)))*RLT-VFSD-(K4*exp(-a*(Time_now-T1)))*sin(wo*(Time_now-
T1)+phase4));
    elseif (Time_now>T2)&(Time_now<=Ta)
        vi3b_t(k)=-i3b(j)*Ri3b-(C5a+K5a*exp(-Aa*(Time_now-T2)))*RLT-VFSD-...
K6a*exp(-Aa*(Time_now-T2));
    elseif (Time_now>Ta)&(Time_now<=T3)
        vi3b_t(k)=-i3b(j)*Ri3b-(C5b+K5b*exp(-Ab*(Time_now-Ta)))*RLT-VFSD-...
K6b*exp(-Ab*(Time_now-Ta));
    elseif (Time_now>T3)&(Time_now<=Ts)
        vi3b_t(k)=-i3b(j)*Ri3b-i3b(j)*RSMB-VFSMb+v12(i)-i3b(j)*R12;
    end
end

mean_v13b=mean(vi3b_t);
error=abs(mean_v13b-vi3b_target);

```

A.8 Regulated Lossy Boost QRC

These MATLAB scripts are used to simulate the regulated Lossy Boost QRC.

```
%Define the global variables
clear all
global Lr Cr wr Zr
global R12 R12a R12b
global RLr RCr RSD RSMA RSMb Ri3a VFSD VFSMa VFSMb
global RCT RLT RALL a wo Aa Ab v12 vi3a i12

global i j
global v12_target

%Define the components' parameters
syms x
Lr=8e-6;
Cr=800e-12;
wr=1/sqrt(Lr*Cr);
Zr=sqrt(Lr/Cr);
v12_target=30;

R12=0.1;
RLr=0.1;
RCr=0.1;
RSD=0.1;
RSMA=0.1;
RSMb=0.1;
Ri3a=0.1;
Ri3b=0.1;
Ri3c=0.1;
VFSD=0.7;
VFSMa=0.7;
VFSMb=0.7;

RCT=RCr+R12;
RLT=RLr+RSD;
RALL=RLT+RCT;
a=RALL/2/Lr;
wo=sqrt(wr^2-a^2);
Aa=(RLT+R12+RSMA)/Lr;
Ab=(RLT+R12+RSMb)/Lr;

%Define the analysis range
vi3a=-30:5:-5;
i12=5:5:30;
```

```

options1=optimset('fminsearch');
options1=optimset(options1,'Display','off');
options2=optimset('fzero');
options2=optimset(options2,'Display','off');

for i=1:length(vi3a),
    for j=1:length(i12),
        init(2)=[i12(j)*(-v12_target)/vi3a(i)];
        alpha=v12_target/Zr/init(2);
        init(1)=wr*(-vi3a(i)/v12_target)/(pi+asin(alpha)+alpha/2+(1+sqrt(1-
alpha^2))/alpha);
%       if (i==1)&(j==1)
%           init(1)=0.4e6;
%           init(2)=10;
%       elseif (i==1)
%           init(1)=fs(1,j-1);
%           init(2)=i3a(1,j-1);
%       elseif (j==1)
%           init(1)=fs(i-1,1);
%           init(2)=i3a(i-1,1);
%       else
%           init(1)=(fs(i-1,j-1)+fs(i-1,j)+fs(i,j-1))/3;
%           init(2)=(i3a(i-1,j-1)+i3a(i-1,j)+i3a(i,j-1))/3;
%       end
        if (init(1)>0)&(init(2)>0)
            out=fminsearch('obj_v13a_i12',init,options1);
            fs(i,j)=out(1);
            i3a(i,j)=out(2);
        else
            fs(i,j)=nan;
            i3a(i,j)=nan;
        end

        alpha=v12_target/Zr/i3a(i,j);
        beta=VFSD/Zr/i3a(i,j);
        if (alpha<=1)&(alpha>0),
            T1=Cr/i3a(i,j)*(v12_target-i3a(i,j)*RCr);
            C1=VFSD+v12_target+i3a(i,j)*RLT+i3a(i,j)*R12;
            K1=v12_target/alpha*sqrt(1+(wr^2/wo^2)*(RALL/2/Zr+beta)^2);
            phase1=2*pi-atan((RALL/Zr+beta)/(wr/wo-a/wo*(RALL/Zr+beta)));
            K2=K1/Zr;
            phase2=phase1+pi-atan(wo/a);
            K3=sqrt(1+(beta+a)^2/wo^2);
            phase3=atan(wo/(beta+a));
            K4=i3a(i,j)*K3*Zr;
            phase4=phase3+2*pi-atan(wo/a);
            KT2=K1*RCr*Cr*sqrt((1/RCr/Cr-a)^2+wo^2);
            phaseT2=phase1+atan(wo/(1/RCr/Cr-a));
            funf=char(eval('C1+KT2*exp(-a*x)*sin(wo*x+phaseT2)'));


```

```

T2=fzero(funf,[mod((pi-phaseT2),2*pi)/wo 3*2*pi/wo/4],options2)+T1;
% T2=fzero(funf,[2*pi/wo/4 2*pi*3/wo/4],options)+T1;
if ((T2-T1)<0),
    error('error: T2<T1');
end

C5a=(i3a(i,j)*RSMa-VFSD-VFSMa-v12_target)/(RLT+R12+RSMa);
K5a=i3a(i,j)*(1-K3*exp(-a*(T2-T1))*sin(wo*(T2-T1)+phase3))-C5a;
K6a=-Lr*K5a*Aa;
Ta=T2-1/Aa*log((i3a(i,j)-C5a)/K5a);

C5b=(i3a(i,j)*RSMb-VFSD+VFSMb-v12_target)/(RLT+R12+RSMb);
K5b=i3a(i,j)-C5b;
K6b=-Lr*K5b*Ab;
T3=Ta-1/Ab*log(-C5b/K5b);

if ((1/T3)<=fs(i,j))|(fs(i,j)<=0),
    fs(i,j)=nan;
    fs_org(i,j)=nan;
    Pv12(i,j)=nan;
    Pi3a(i,j)=nan;
    PR12(i,j)=nan;
    PRi3a(i,j)=nan;
    PRCr(i,j)=nan;
    PRLr(i,j)=nan;
    PRSD(i,j)=nan;
    PRSMA(i,j)=nan;
    PRSMB(i,j)=nan;
    PRSM(i,j)=nan;
    PVFSD(i,j)=nan;
    PVFSMA(i,j)=nan;
    PVFSMB(i,j)=nan;
    PVFSM(i,j)=nan;
    PCr(i,j)=nan;
    PLr(i,j)=nan;
    i12_final(i,j)=nan;
    vi3a_final(i,j)=nan;
else
    Ts=1/fs(i,j);
    Simulation_Time=Ts;
    resolution=100;
    Time_step=Simulation_Time/resolution;
    Time_axis=Time_step:Time_step:Time_step*(resolution-1);
    Time_length=length(Time_axis);
    vCr=zeros(Time_length,1);
    iCr=zeros(Time_length,1);
    iLr=zeros(Time_length,1);
    vLr=zeros(Time_length,1);
    iSMA=zeros(Time_length,1);

```

```

iSMb=zeros(Time_length,1);
i12_t=zeros(Time_length,1);
vi3a_t=zeros(Time_length,1);

for k=1:Time_length,
    Time_now=rem(Time_axis(k),Ts);
    if (Time_now>0)&(Time_now<=T1)
        vCr(k)=v12_target/alpha*wr*Time_now;
        iCr(k)=i3a(i,j);
        vi3a_t(k)=-i3a(i,j)*Ri3a-vCr(k)-i3a(i,j)*RCr;
    elseif (Time_now>T1)&(Time_now<=T2)
        vCr(k)=C1+K1*exp(-a*(Time_now-T1))*sin(wo*(Time_now-
T1)+phase1);
        iCr(k)=K2*exp(-a*(Time_now-T1))*sin(wo*(Time_now-
T1)+phase2);
        iLr(k)=i3a(i,j)*(1-K3*exp(-a*(Time_now-T1)))*sin(wo*(Time_now-
T1)+phase3));
        vLr(k)=K4*exp(-a*(Time_now-T1))*sin(wo*(Time_now-
T1)+phase4);
        i12_t(k)=iLr(k);
        vi3a_t(k)=-i3a(i,j)*Ri3a-vCr(k)-iCr(k)*RCr;
    elseif (Time_now>T2)&(Time_now<=Ta)
        iLr(k)=C5a+K5a*exp(-Aa*(Time_now-T2));
        vLr(k)=K6a*exp(-Aa*(Time_now-T2));
        iSMA(k)=i3a(i,j)-iLr(k);
        i12_t(k)=iLr(k);
        vi3a_t(k)=VFSMa-iSMA(k)*RSMA-i3a(i,j)*Ri3a;
    elseif (Time_now>Ta)&(Time_now<=T3)
        iLr(k)=C5b+K5b*exp(-Ab*(Time_now-Ta));
        vLr(k)=K6b*exp(-Ab*(Time_now-Ta));
        iSMb(k)=i3a(i,j)-iLr(k);
        i12_t(k)=iLr(k);
        vi3a_t(k)=-VFSMb-iSMb(k)*RSMb-i3a(i,j)*Ri3a;
    elseif (Time_now>T3)&(Time_now<=Ts)
        iSMb(k)=i3a(i,j);
        i12_t(k)=0;
        vi3a_t(k)=-VFSMb-iSMb(k)*RSMb-i3a(i,j)*Ri3a;
    end
end
mean_vCr=mean(vCr);
mean_iCr=mean(iCr);
rms_iCr=sqrt(mean(iCr.^2));
mean_iLr=mean(iLr);
rms_iLr=sqrt(mean(iLr.^2));
mean_vLr=mean(vLr);
mean_iSMA=mean(iSMA);
rms_iSMA=sqrt(mean(iSMA.^2));
mean_iSMb=mean(iSMb);
rms_iSMb=sqrt(mean(iSMb.^2));

```

```

mean_i12=mean(i12_t);
rms_i12=sqrt(mean(i12_t.^2));
mean_v13a=mean(v13a_t);

Pv12(i,j)=v12_target*mean_i12;
Pi3a(i,j)=i3a(i,j)*mean_v13a;
PR12(i,j)=R12*rms_i12^2;
PRi3a(i,j)=Ri3a*i3a(i,j)^2;
PRCr(i,j)=RCr*rms_iCr^2;
PRLr(i,j)=RLr*rms_iLr^2;
PRSD(i,j)=RSD*rms_iLr^2;
PRSMa(i,j)=RSMA*rms_iSMA^2;
PRSMb(i,j)=RSMb*rms_iSMB^2;
PRSM(i,j)=PRSMa(i,j)+PRSMb(i,j);
PVFSD(i,j)=VFSD*mean_iLr;
PVFSMa(i,j)=-VFSMa*mean_iSMA;
PVFSMb(i,j)=VFSMb*mean_iSMB;
PVFSM(i,j)=PVFSMa(i,j)+PVFSMb(i,j);
PCr(i,j)=mean_iCr*mean_vCr;
PLr(i,j)=mean_iLr*mean_vLr;
i12_final(i,j)=mean_i12;
vi3a_final(i,j)=mean_v13a;
v12(i,j)=v12_target;
end
else
fs(i,j)=nan;
fs_org(i,j)=nan;
Pv12(i,j)=nan;
Pi3a(i,j)=nan;
PR12(i,j)=nan;
PRi3a(i,j)=nan;
PRCr(i,j)=nan;
PRLr(i,j)=nan;
PRSD(i,j)=nan;
PRSMa(i,j)=nan;
PRSMb(i,j)=nan;
PRSM(i,j)=nan;
PVFSD(i,j)=nan;
PVFSMa(i,j)=nan;
PVFSMb(i,j)=nan;
PVFSM(i,j)=nan;
PCr(i,j)=nan;
PLr(i,j)=nan;
i12_final(i,j)=nan;
vi3a_final(i,j)=nan;
end
end
%Draw the figures

```

```
figure(1);
colormap([0 0 0]);
subplot(2,2,1);
H=mesh(i12,vi3a,fs./1e6);
set(H,'markersize',15);
view(20,30);
xlabel('i12 (A)','fontsize',15);
ylabel('vi3a (V)','fontsize',15);
zlabel('fs (MHz)','fontsize',15);
title('Lr=8e-6H, Cr=800e-12F, QR Boost Converter','fontsize',15);

%Draw the figures
subplot(2,2,2);
mesh(i12,vi3a,v12);
view(20,30);
xlabel('i12 (A)','fontsize',15);
ylabel('vi3a (V)','fontsize',15);
zlabel('v12 (V)','fontsize',15);
title('Lr=8e-6H, Cr=800e-12F, QR Boost Converter','fontsize',15);

%Draw the figures
subplot(2,2,3);
mesh(i12,vi3a,i3a);
view(20,30);
xlabel('i12 (A)','fontsize',15);
ylabel('vi3a (V)','fontsize',15);
zlabel('i3a (A)','fontsize',15);
title('Lr=8e-6H, Cr=800e-12F, QR Boost Converter','fontsize',15);

%Draw the figures
subplot(2,2,4);
mesh(i12,vi3a,Pi3a);
hold on;
mesh(i12,vi3a,Pv12);
hold off;
view(20,30);
xlabel('i12 (A)','fontsize',15);
ylabel('vi3a (V)','fontsize',15);
zlabel('Pi3a(-ve) Pv12(+ve) (W)','fontsize',15);
title('Lr=8e-6H, Cr=800e-12F, QR Boost Converter','fontsize',15);

%Draw the figures
figure(2)
colormap([0 0 0]);
subplot(3,3,1);
mesh(i12,vi3a,PR12./max(max(PRLr)));
xlabel('i12 (A)');
ylabel('vi3a (V)');
zlabel('Normalized PR12');
```

```

subplot(3,3,2);
mesh(i12,vi3a,PRLr./max(max(PRLr)));
xlabel('i12 (A)');
ylabel('vi3a (V)');
zlabel('Normalized PRLr');
subplot(3,3,3);
mesh(i12,vi3a,PRCr./max(max(PRLr)));
xlabel('i12 (A)');
ylabel('vi3a (V)');
zlabel('Normalized PRCr');
subplot(3,3,4);
mesh(i12,vi3a,PRSD./max(max(PRLr)));
xlabel('i12 (A)');
ylabel('vi3a (V)');
zlabel('Normalized PRSD');
subplot(3,3,5);
mesh(i12,vi3a,PRSMA./max(max(PRLr)));
xlabel('i12 (A)');
ylabel('vi3a (V)');
zlabel('Normalized PRSMA');
subplot(3,3,6);
mesh(i12,vi3a,PRSMb./max(max(PRLr)));
xlabel('i12 (A)');
ylabel('vi3a (V)');
zlabel('Normalized PRSMb');
subplot(3,3,7);
mesh(i12,vi3a,PRi3a./max(max(PRLr)));
xlabel('i12 (A)');
ylabel('vi3a (V)');
zlabel('Normalized PRi3a');
subplot(3,3,8);
mesh(i12,vi3a,PVFSD./max(max(PRLr)));
xlabel('i12 (A)');
ylabel('vi3a (V)');
zlabel('Normalized PVFSD');
subplot(3,3,9);
mesh(i12,vi3a,PVFSMA./max(max(PRLr)));
hold on;
mesh(i12,vi3a,PVFSMB./max(max(PRLr)));
hold off;
xlabel('i12 (A)');
ylabel('vi3a (V)');
zlabel('Normalized PVFSMA & PVFSMB','VerticalAlignment','bottom');

%Draw the figures
figure(3)
colormap([0 0 0]);
Ploss=PR12+PRLr+PRCr+PRSD+PRSMA+PRSMb+PRi3a+PVFSD+PVFSMA+PVFSMB;

```

```

H=mesh(i12,vi3a,Pv12./(Ploss-Pi3a).*100);
set(H,'markersize',15);
xlabel('i12 (A)', 'fontsize', 15, 'VerticalAlignment', 'bottom');
ylabel('vi3a (V)', 'fontsize', 15, 'VerticalAlignment', 'bottom');
zlabel('Efficiency (%)', 'fontsize', 15);
title('Lr=8e-6H, Cr=800e-12F, QR Boost Converter', 'fontsize', 15);
view(60,10);

%Define the object function in a separate file
function [error]=obj_vi3a_i12(input)

%Define global variables
global Lr Cr wr Zr
global R12 RLr RCr RSD RSMA RSMb Ri3a VFSD VFSMa VFSMb
global RCT RLT RALL a wo Aa Ab v12_target i12 vi3a

global i j

syms x

fs=input(1);
i3a=input(2);

options=optimset('display','off','Diagnostics','off');

alpha=v12_target/Zr/i3a;
beta=VFSD/Zr/i3a;
if (alpha<=1)&(alpha>0),
    T1=Cr/i3a*(v12_target-i3a*RCr);
    C1=VFSD+v12_target+i3a*RLT+i3a*R12;
    K1=v12_target/alpha*sqrt(1+(wr^2/wo^2)*(RALL/2/Zr+beta)^2);
    phase1=2*pi-atan((RALL/Zr+beta)/(wr/wo-a/wo*(RALL/Zr+beta)));
    K2=K1/Zr;
    phase2=phase1+pi-atan(wo/a);
    K3=sqrt(1+(beta+a)^2/wo^2);
    phase3=atan(wo/(beta+a));
    K4=i3a*K3*Zr;
    phase4=phase3+2*pi-atan(wo/a);
    KT2=K1*RCr*Cr*sqrt((1/RCr/Cr-a)^2+wo^2);
    phaseT2=phase1+atan(wo/(1/RCr/Cr-a));
    funf=char(eval(C1+KT2*exp(-a*x)*sin(wo*x+phaseT2)));
%
% Check the zero crossing
%       x_temp=1*2*pi/wo/64:2*pi/wo/6400:63*2*pi/wo/64;
%
%   plot(1*2*pi/wo/64:2*pi/wo/6400:63*2*pi/wo/64,C1+KT2.*exp(-
a.*x_temp).*sin(wo.*x_temp+phaseT2))

```

```

% hold on
%pause
% [T2,fval,exitflag,output]=fzero(funf,[1*2*pi/wo/4 3*2*pi/wo/4],options);
% [T2,fval,exitflag,output]=fzero(funf,[mod((pi-phaseT2),2*pi)/wo
3*2*pi/wo/4],options);
% output
%pause
if exitflag<0,
    error=NaN;
    break;
else
    T2=T2+T1;
end
% T2=fzero(funf,[2*pi/wo/4 2*pi*3/wo/4],options)+T1;
% if ((T2-T1)<0),
%     error('error: T2<T1');
% end

C5a=(i3a*RSMA-VFSD-VFSMa-v12_target)/(RLT+R12+RSMa);
K5a=i3a*(1-K3*exp(-a*(T2-T1)))*sin(wo*(T2-T1)+phase3))-C5a;
K6a=-Lr*K5a*Aa;
Ta=T2-1/Aa*log((i3a-C5a)/K5a);

C5b=(i3a*RSMb-VFSD+VFSMb-v12_target)/(RLT+R12+RSMb);
K5b=i3a-C5b;
K6b=-Lr*K5b*Ab;
T3=Ta-1/Ab*log(-C5b/K5b);
else
    error('error: alpha is out of range.');
end

Ts=1/fs; Simulation_Time=Ts; resolution=500;
Time_step=Simulation_Time/resolution;
Time_axis=Time_step:Time_step:Time_step*(resolution-1);
Time_length=length(Time_axis);
vCr=zeros(Time_length,1);
iCr=zeros(Time_length,1);
vi3a_t=zeros(Time_length,1);
iI2_t=zeros(Time_length,1);

for k=1:Time_length,
    Time_now=rem(Time_axis(k),Ts);
    if (Time_now>0)&(Time_now<=T1)
        vCr(k)=v12_target/alpha*wr*Time_now;
        iCr(k)=i3a;
        vi3a_t(k)=-i3a*Ri3a-vCr(k)-i3a*RCr;
    elseif (Time_now>T1)&(Time_now<=T2)
        vCr(k)=C1+K1*exp(-a*(Time_now-T1))*sin(wo*(Time_now-T1)+phase1);
    end
end

```

```

iCr(k)=K2*exp(-a*(Time_now-T1))*sin(wo*(Time_now-T1)+phase2);
iLr(k)=i3a*(1-K3*exp(-a*(Time_now-T1)))*sin(wo*(Time_now-T1)+phase3));
vLr(k)=K4*exp(-a*(Time_now-T1))*sin(wo*(Time_now-T1)+phase4);
i12_t(k)=iLr(k);
vi3a_t(k)=-i3a*Ri3a-vCr(k)-iCr(k)*RCr;
elseif (Time_now>T2)&(Time_now<=Ta)
    iLr(k)=C5a+K5a*exp(-Aa*(Time_now-T2));
    vLr(k)=K6a*exp(-Aa*(Time_now-T2));
    i12_t(k)=iLr(k);
    vi3a_t(k)=VFSMa-(i3a-iLr(k))*RSMA-i3a*Ri3a;
elseif (Time_now>Ta)&(Time_now<=T3)
    iLr(k)=C5b+K5b*exp(-Ab*(Time_now-Ta));
    i12_t(k)=iLr(k);
    vi3a_t(k)=-VFSMb-(i3a-iLr(k))*RSMb-i3a*Ri3a;
elseif (Time_now>T3)&(Time_now<=Ts)
    vi3a_t(k)=-VFSMb-i3a*RSMb-i3a*Ri3a;
end
end

mean_vi3a=mean(vi3a_t);
error(1)=(mean_vi3a-vi3a(i))^2;

mean_i12=mean(i12_t);
error(2)=(mean_i12-i12(j))^2;
error=(1+(mean_vi3a-vi3a(i))^2+(mean_i12-i12(j))^2)^2;

```

A.9 Regulated Lossy Buck-Boost QRC

These MATLAB scripts are used to simulate the regulated Lossy Buck-Boost QRC.

```
%Define the global variables
clear all
global Lr Cr wr Zr
global R12 R12a R12b
global RLr RCr RSD RSMA RSMb Ri3c VFSD VFSMa VFSMb
global RCT RLT RALL a wo Aa Ab v12 v12a v12b vi3c i12a i12b

global i j
global v12b_target

syms x

%Define the components' parameters
Lr=8e-6;
Cr=800e-12;
wr=1/sqrt(Lr*Cr);
Zr=sqrt(Lr/Cr);
v12b_target=30;
vi3c_target=0;

R12=0.1;
R12a=R12/2;
R12b=R12-R12a;
RLr=0.1;
RCr=0.1;
RSD=0.1;
RSMA=0.1;
RSMb=0.1;
Ri3a=0.1;
Ri3b=0.1;
Ri3c=0.1;
VFSD=0.7;
VFSMa=0.7;
VFSMb=0.7;

RCT=RCr+R12;
RLT=RLr+RSD;
RALL=RLT+RCT;
a=RALL/2/Lr;
wo=sqrt(wr^2-a^2);
Aa=(RLT+R12+RSMA)/Lr;
Ab=(RLT+R12+RSMb)/Lr;

v12=40:15:240;
```

```

v12a=v12-v12b_target;
i12b=5:5:30;
options1=optimset('fsolve');
%options1=optimset(options1,'Display','off');
options2=optimset('fzero');
options2=optimset(options2,'Display','off');

for i=1:length(v12a),
    for j=1:length(i12b),
        init(2)=i12b(j)*v12(i)/v12a(i); % Set initial value i3c
        alpha=v12(i)./Zr/init(2);
        if (alpha>1)|(alpha<=0)
            warning('The variable "alpha" is not valid.')
        end
        init(1)=wr*v12a(i)/v12(i)/(pi+asin(alpha)+alpha/2+(1+sqrt(1-alpha^2))/alpha);
    % Set initial value fs
    if (init(1)>0)&(init(2)>0)
        out=fsolve('obj_v13c_i12b',init,options1);
    % Find the conditions so that v13c=0 and expected i12b.
        fs(i,j)=out(1); % The switching frequency fs is found.
        i3c(i,j)=out(2); % The current condition is found.
    %
        fs(i,j)=init(1);
    %
        i3c(i,j)=init(2);
    else
        fs(i,j)=nan; % The switching frequency fs is not found.
        i3c(i,j)=nan; % The current condition is not found.
    end

    alpha=v12(i)/Zr/i3c(i,j);
    beta=VFSD/Zr/i3c(i,j);
    if (alpha<=1)&(alpha>0),
        T1=Cr/i3c(i,j)*(v12(i)-i3c(i,j)*R12a-i3c(i,j)*RCr);
        C1=VFSD+v12(i)+i3c(i,j)*RLT+i3c(i,j)*R12b;
        K1=v12(i)/alpha*sqrt(1+(wr^2/wo^2)*(RALL/2/Zr+beta)^2);
        phase1=2*pi-atan((RALL/Zr+beta)/(wr/wo-a/wo*(RALL/Zr+beta)));
        K2=K1/Zr;
        phase2=phase1+pi-atan(wo/a);
        K3=sqrt(1+(beta+a)^2/wo^2);
        phase3=atan(wo/(beta+a));
        K4=i3c(i,j)*K3*Zr;
        phase4=phase3+2*pi-atan(wo/a);
        KT2=K1*RCr*Cr*sqrt((1/RCr/Cr-a)^2+wo^2);
        phaseT2=phase1+atan(wo/(1/RCr/Cr-a));
        funf=char(eval('C1+KT2*exp(-a*x)*sin(wo*x+phaseT2)'));

    %
        figure(4)
    %
        temp_x=0:3*2*pi/wo/40:3*2*pi/wo/4;
    %
        plot(temp_x,C1+KT2*exp(-a.*temp_x).*sin(wo.*temp_x+phaseT2));
    %
        hold on;
    T2=fzero(funf,[mod((pi-phaseT2),2*pi)/wo 3*2*pi/wo/4],options2)+T1;

```

```

%      T2=fzero(funf,[2*pi/wo/4 2*pi*3/wo/4],options)+T1;
if ((T2-T1)<0),
    error('error: T2<T1');
end

C5a=(i3c(i,j)*R12a+i3c(i,j)*RSMa-VFSD-VFSMa-
v12(i))/(RLT+R12+RSMa);
K5a=i3c(i,j)*(1-K3*exp(-a*(T2-T1))*sin(wo*(T2-T1)+phase3))-C5a;
K6a=-Lr*K5a*Aa;
Ta=T2-1/Aa*log((i3c(i,j)-C5a)/K5a);

C5b=(i3c(i,j)*R12a+i3c(i,j)*RSMb-VFSD+VFSMb-
v12(i))/(RLT+R12+RSMb);
K5b=i3c(i,j)-C5b;
K6b=-Lr*K5b*Ab;
T3=Ta-1/Ab*log(-C5b/K5b);

if ((1/T3)<=fs(i,j))|(fs(i,j)<=0),
    fs(i,j)=nan;
    fs_org(i,j)=nan;
    Pv12a(i,j)=nan;
    Pv12b(i,j)=nan;
    Pi3c(i,j)=nan;
    PR12a(i,j)=nan;
    PR12b(i,j)=nan;
    PRi3c(i,j)=nan;
    PRCr(i,j)=nan;
    PRLr(i,j)=nan;
    PRSD(i,j)=nan;
    PRSMa(i,j)=nan;
    PRSMb(i,j)=nan;
    PRSM(i,j)=nan;
    PVFSD(i,j)=nan;
    PVFSMa(i,j)=nan;
    PVFSMb(i,j)=nan;
    PVFSM(i,j)=nan;
    PCr(i,j)=nan;
    PLr(i,j)=nan;
    i12a_final(i,j)=nan;
    i12b_final(i,j)=nan;
    vi3c_final(i,j)=nan;
else
    Ts=1/fs(i,j);
    Simulation_Time=Ts;
    resolution=10000;
    Time_step=Simulation_Time/resolution;
    Time_axis=Time_step:Time_step:Time_step*(resolution-1);
    Time_length=length(Time_axis);
    vCr=zeros(Time_length,1);

```

```

iCr=zeros(Time_length,1);
iLr=zeros(Time_length,1);
vLr=zeros(Time_length,1);
iSMa=zeros(Time_length,1);
iSMb=zeros(Time_length,1);
i12a_t=zeros(Time_length,1);
i12b_t=zeros(Time_length,1);
vi3c_t=zeros(Time_length,1);

for k=1:Time_length,
    Time_now=rem(Time_axis(k),Ts);
    if (Time_now>0)&(Time_now<=T1)
        vCr(k)=v12(i)/alpha*wr*Time_now;
        iCr(k)=i3c(i,j);
        i12a_t(k)=-i3c(i,j);
        i12b_t(k)=0;
        vi3c_t(k)=-i3c(i,j)*Ri3c-vCr(k)-iCr(k)*RCr-i3c(i,j)*R12a+v12a(i);
    elseif (Time_now>T1)&(Time_now<=T2)
        vCr(k)=C1+K1*exp(-a*(Time_now-T1))*sin(wo*(Time_now-
T1)+phase1);
        iCr(k)=K2*exp(-a*(Time_now-T1))*sin(wo*(Time_now-
T1)+phase2);
        iLr(k)=i3c(i,j)*(1-K3*exp(-a*(Time_now-T1)))*sin(wo*(Time_now-
T1)+phase3));
        vLr(k)=K4*exp(-a*(Time_now-T1))*sin(wo*(Time_now-
T1)+phase4);
        i12a_t(k)=iLr(k)-i3c(i,j);
        i12b_t(k)=iLr(k);
        vi3c_t(k)=-i3c(i,j)*Ri3c-vCr(k)-iCr(k)*RCr+(iLr(k)-
i3c(i,j))*R12a+v12a(i);
    elseif (Time_now>T2)&(Time_now<=Ta)
        iLr(k)=C5a+K5a*exp(-Aa*(Time_now-T2));
        vLr(k)=K6a*exp(-Aa*(Time_now-T2));
        iSMa(k)=i3c(i,j)-iLr(k);
        i12a_t(k)=iLr(k)-i3c(i,j);
        i12b_t(k)=iLr(k);
        vi3c_t(k)=-i3c(i,j)*Ri3c-(i3c(i,j)-iLr(k))*RSMa+VFSMa+(iLr(k)-
i3c(i,j))*R12a+v12a(i);
    elseif (Time_now>Ta)&(Time_now<=T3)
        iLr(k)=C5b+K5b*exp(-Ab*(Time_now-Ta));
        vLr(k)=K6b*exp(-Ab*(Time_now-Ta));
        iSMb(k)=i3c(i,j)-iLr(k);
        i12a_t(k)=iLr(k)-i3c(i,j);
        i12b_t(k)=iLr(k);
        vi3c_t(k)=-i3c(i,j)*Ri3c-(i3c(i,j)-iLr(k))*RSMb+VFSMb+(iLr(k)-
i3c(i,j))*R12a+v12a(i);
    elseif (Time_now>T3)&(Time_now<=Ts)
        iSMb(k)=i3c(i,j);
        i12a_t(k)=-i3c(i,j);

```

```

    i12b_t(k)=0;
    vi3c_t(k)=-i3c(i,j)*Ri3c-i3c(i,j)*RSMb-VFSMb-
i3c(i,j)*R12a+v12a(i);
    end
    end
    mean_vCr=mean(vCr);
    mean_iCr=mean(iCr);
    rms_iCr=sqrt(mean(iCr.^2));
    mean_iLr=mean(iLr);
    rms_iLr=sqrt(mean(iLr.^2));
    mean_vLr=mean(vLr);
    mean_iSMa=mean(iSMa);
    rms_iSMa=sqrt(mean(iSMa.^2));
    mean_iSMb=mean(iSMb);
    rms_iSMb=sqrt(mean(iSMb.^2));
    mean_i12a=mean(i12a_t);
    rms_i12a=sqrt(mean(i12a_t.^2));
    mean_i12b=mean(i12b_t);
    rms_i12b=sqrt(mean(i12b_t.^2));
    mean_vi3c=mean(vi3c_t);

    Pv12a(i,j)=v12a(i)*mean_i12a;
    Pv12b(i,j)=v12b_target*mean_i12b;
    Pi3c(i,j)=i3c(i,j)*mean_vi3c;
    PR12a(i,j)=R12a*rms_i12a^2;
    PR12b(i,j)=R12b*rms_i12b^2;
    PRi3c(i,j)=Ri3c*i3c(i,j)^2;
    PRCr(i,j)=RCr*rms_iCr^2;
    PRLr(i,j)=RLr*rms_iLr^2;
    PRSD(i,j)=RSD*rms_iLr^2;
    PRSMa(i,j)=RSMa*rms_iSMa^2;
    PRSMb(i,j)=RSMb*rms_iSMb^2;
    PRSM(i,j)=PRSMa(i,j)+PRSMb(i,j);
    PVFSD(i,j)=VFSD*mean_iLr;
    PVFSMa(i,j)=-VFSMa*mean_iSMa;
    PVFSMb(i,j)=VFSMb*mean_iSMb;
    PVFSM(i,j)=PVFSMa(i,j)+PVFSMb(i,j);
    PCr(i,j)=mean_iCr*mean_vCr;
    PLr(i,j)=mean_iLr*mean_vLr;
    i12a_final(i,j)=mean_i12a;
    i12b_final(i,j)=mean_i12b;
    vi3c_final(i,j)=mean_vi3c;
    v12b(i,j)=v12b_target;
    end
else
    fs(i,j)=nan;
    fs_org(i,j)=nan;
    Pv12a(i,j)=nan;
    Pv12b(i,j)=nan;

```

```

Pi3c(i,j)=nan;
PR12a(i,j)=nan;
PR12b(i,j)=nan;
PRI3c(i,j)=nan;
PRCr(i,j)=nan;
PRLr(i,j)=nan;
PRSD(i,j)=nan;
PRSMA(i,j)=nan;
PRSMb(i,j)=nan;
PRSM(i,j)=nan;
PVFSD(i,j)=nan;
PVFSMA(i,j)=nan;
PVFSMb(i,j)=nan;
PVFSM(i,j)=nan;
PCr(i,j)=nan;
PLr(i,j)=nan;
i12a_final(i,j)=nan;
i12b_final(i,j)=nan;
vi3c_final(i,j)=nan;
end
end
end

%Draw the figures
figure(1);
colormap([0 0 0]);
subplot(2,2,1);
H=mesh(i12b,v12a,fs./1e6);
set(H,'markersize',15);
view(20,30);
xlabel('i12b (A)','fontsize',15);
ylabel('v12a (V)','fontsize',15);
zlabel('fs (MHz)','fontsize',15);
title('Lr=8e-6H, Cr=800e-12F, QR Buck-Boost Converter','fontsize',15);

%Draw the figures
subplot(2,2,2);
mesh(i12b,v12a,vi3c_final);
hold on
mesh(i12b,v12a,v12b);
hold off
view(20,30);
xlabel('i12b (A)','fontsize',15);
ylabel('v12a (V)','fontsize',15);
zlabel('vi3c\_\_final v12b (V)','fontsize',15);
title('Lr=8e-6H, Cr=800e-12F, QR Buck-Boost Converter','fontsize',15);

%Draw the figures
subplot(2,2,3);

```

```
mesh(i12b,v12a,i12a_final);
hold on
mesh(i12b,v12a,i12b_final);
mesh(i12b,v12a,i3c);
hold off
view(20,30);
xlabel('i12b (A)', 'fontsize', 15);
ylabel('v12a (V)', 'fontsize', 15);
zlabel('i12a i12b i3c (A)', 'fontsize', 15);
title('Lr=8e-6H, Cr=800e-12F, QR Buck-Boost Converter', 'fontsize', 15);

%Draw the figures
subplot(2,2,4);
mesh(i12b,v12a,Pv12a);
hold on;
mesh(i12b,v12a,Pv12b);
hold off;
view(20,30);
xlabel('i12b (A)', 'fontsize', 15);
ylabel('v12a (V)', 'fontsize', 15);
zlabel('Pv12a(-ve) Pv12b(+ve) (W)', 'fontsize', 15);
title('Lr=8e-6H, Cr=800e-12F, QR Buck-Boost Converter', 'fontsize', 15);

%Draw the figures
figure(2)
colormap([0 0 0]);
subplot(3,3,1);
mesh(i12b,v12a,PR12a./max(max(PRLr)));
hold on;
mesh(i12b,v12a,PR12b./max(max(PRLr)));
hold off;
xlabel('i12b (A)');
ylabel('v12a (V)');
zlabel('Normalized PR12a PR12b');
subplot(3,3,2);
mesh(i12b,v12a,PRLr./max(max(PRLr)));
xlabel('i12b (A)');
ylabel('v12a (V)');
zlabel('Normalized PRLr');
subplot(3,3,3);
mesh(i12b,v12a,PRCr./max(max(PRLr)));
xlabel('i12b (A)');
ylabel('v12a (V)');
zlabel('Normalized PRCr');
subplot(3,3,4);
mesh(i12b,v12a,PRSD./max(max(PRLr)));
xlabel('i12b (A)');
ylabel('v12a (V)');
zlabel('Normalized PRSD');
```

```

subplot(3,3,5);
mesh(i12b,v12a,PRSMa./max(max(PRLr)));
xlabel('i12b (A)');
ylabel('v12a (V)');
zlabel('Normalized PRSMa');
subplot(3,3,6);
mesh(i12b,v12a,PRSMb./max(max(PRLr)));
xlabel('i12b (A)');
ylabel('v12a (V)');
zlabel('Normalized PRSMb');
subplot(3,3,7);
mesh(i12b,v12a,PRi3c./max(max(PRLr)));
xlabel('i12b (A)');
ylabel('v12a (V)');
zlabel('Normalized PRi3c');
subplot(3,3,8);
mesh(i12b,v12a,PVFSD./max(max(PRLr)));
xlabel('i12b (A)');
ylabel('v12a (V)');
zlabel('Normalized PVFSD');
subplot(3,3,9);
mesh(i12b,v12a,PVFSMa./max(max(PRLr)));
hold on;
mesh(i12b,v12a,PVFSMb./max(max(PRLr)));
hold off;
xlabel('i12b (A)');
ylabel('v12a (V)');
zlabel('Normalized PVFSMa & PVFSMb','VerticalAlignment','bottom');

%Draw the figures
figure(3)
colormap([0 0 0]);
Ploss=PR12a+PR12b+PRLr+PRCr+PRSD+PRSMa+PRSMb+PRi3c+PVFSD+PVFS
Ma+PVFSMb;
H=mesh(i12b,v12a,Pv12b./(Ploss-Pv12a).*100);
set(H,'markersize',15);
%mesh(i12b,v12a,Ploss+Pi3a+Pv12);
xlabel('i12b (A)','fontsize',15,'VerticalAlignment','bottom');
ylabel('v12a (V)','fontsize',15,'VerticalAlignment','bottom');
zlabel('Efficiency (%)','fontsize',15);
title('Lr=8e-6H, Cr=800e-12F, QR Buck-Boost Converter','fontsize',15);
view(60,10);

```

```
%Define the object function in a separate file
function [error]=obj_v13c_i12b(input)

%Define the global variables
global Lr Cr wr Zr
global R12 R12a R12b
global RLr RCr RSD RSMA RSMb Ri3c VFSD VFSMa VFSMb
global RCT RLT RALL a wo Aa Ab v12 v12a v12b vi3c i12a i12b

global i j
global v12b_target

syms x

options2=optimset('fzero');
options2=optimset(options2,'Display','off');

fs_find=input(1);
i3c_find=input(2);

alpha=v12(i)/Zr/i3c_find;
beta=VFSD/Zr/i3c_find;
if (alpha<=1)&(alpha>0),
    T1=Cr/i3c_find*(v12(i)-i3c_find*R12a-i3c_find*RCr);
    C1=VFSD+v12(i)+i3c_find*RLT+i3c_find*R12b;
    K1=v12(i)/alpha*sqrt(1+(wr^2/wo^2)*(RALL/2/Zr+beta)^2);
    phase1=2*pi-atan((RALL/Zr+beta)/(wr/wo-a/wo*(RALL/Zr+beta)));
    K2=K1/Zr;
    phase2=phase1+pi-atan(wo/a);
    K3=sqrt(1+(beta+a)^2/wo^2);
    phase3=atan(wo/(beta+a));
    K4=i3c_find*K3*Zr;
    phase4=phase3+2*pi-atan(wo/a);
    KT2=K1*RCr*Cr*sqrt((1/RCr/Cr-a)^2+wo^2);
    phaseT2=phase1+atan(wo/(1/RCr/Cr-a));
    funf=char(eval('C1+KT2*exp(-a*x)*sin(wo*x+phaseT2)'));

    T2=fzero(funf,[mod((pi-phaseT2),2*pi)/wo 3*2*pi/wo/4],options2)+T1;
    if ((T2-T1)<0),
        error('error: T2<T1');
    end

    C5a=(i3c_find*R12a+i3c_find*RSMA-VFSD-VFSMa-
v12(i))/(RLT+R12+RSMA);
    K5a=i3c_find*(1-K3*exp(-a*(T2-T1))*sin(wo*(T2-T1)+phase3))-C5a;
    K6a=-Lr*K5a*Aa;
    Ta=T2-1/Aa*log((i3c_find-C5a)/K5a);

    C5b=(i3c_find*R12a+i3c_find*RSMb-VFSD+VFSMb-
v12(i))/(RLT+R12+RSMb);

```

```

K5b=i3c_find-C5b;
K6b=-Lr*K5b*Ab;
T3=Ta-l/Ab*log(-C5b/K5b);

if ((1/T3)<=fs_find)|(fs_find<=0),
    error('fs_find is not valid');
else
    Ts=1/fs_find;
    Simulation_Time=Ts;
    resolution=10000;
    Time_step=Simulation_Time/resolution;
    Time_axis=Time_step:Time_step:Time_step*(resolution-1);
    Time_length=length(Time_axis);
    vCr=zeros(Time_length,1);
    iCr=zeros(Time_length,1);
    iLr=zeros(Time_length,1);
    vLr=zeros(Time_length,1);
    iSMA=zeros(Time_length,1);
    iSMb=zeros(Time_length,1);
    i12a_t=zeros(Time_length,1);
    i12b_t=zeros(Time_length,1);
    vi3c_t=zeros(Time_length,1);

for k=1:Time_length,
    Time_now=rem(Time_axis(k),Ts);
    if (Time_now>0)&(Time_now<=T1)
        vCr(k)=v12(i)/alpha*wr*Time_now;
        iCr(k)=i3c_find;
        i12a_t(k)=i3c_find;
        i12b_t(k)=0;
        vi3c_t(k)=-i3c_find*Ri3c-vCr(k)-iCr(k)*RCr-i3c_find*R12a+v12a(i);
    elseif (Time_now>T1)&(Time_now<=T2)
        vCr(k)=C1+K1*exp(-a*(Time_now-T1))*sin(wo*(Time_now-
T1)+phase1);
        iCr(k)=K2*exp(-a*(Time_now-T1))*sin(wo*(Time_now-
T1)+phase2);
        iLr(k)=i3c_find*(1-K3*exp(-a*(Time_now-T1))*sin(wo*(Time_now-
T1)+phase3));
        vLr(k)=K4*exp(-a*(Time_now-T1))*sin(wo*(Time_now-
T1)+phase4);
        i12a_t(k)=iLr(k)-i3c_find;
        i12b_t(k)=iLr(k);
        vi3c_t(k)=-i3c_find*Ri3c-vCr(k)-iCr(k)*RCr+(iLr(k)-
i3c_find)*R12a+v12a(i);
    elseif (Time_now>T2)&(Time_now<=Ta)
        iLr(k)=C5a+K5a*exp(-Aa*(Time_now-T2));
        vLr(k)=K6a*exp(-Aa*(Time_now-T2));
        iSMA(k)=i3c_find-iLr(k);
        i12a_t(k)=iLr(k)-i3c_find;

```

```

i12b_t(k)=iLr(k);
vi3c_t(k)=-i3c_find*Ri3c-(i3c_find-iLr(k))*RSMa+VFSMa+(iLr(k)-
i3c_find)*R12a+vi12a(i);
elseif (Time_now>Ta)&(Time_now<=T3)
    iLr(k)=C5b+K5b*exp(-Ab*(Time_now-Ta));
    vLr(k)=K6b*exp(-Ab*(Time_now-Ta));
    iSMb(k)=i3c_find-iLr(k);
    i12a_t(k)=iLr(k)-i3c_find;
    i12b_t(k)=iLr(k);
    vi3c_t(k)=-i3c_find*Ri3c-(i3c_find-iLr(k))*RSMb-VFSMb+(iLr(k)-
i3c_find)*R12a+vi12a(i);
elseif (Time_now>T3)&(Time_now<=Ts)
    iSMb(k)=i3c_find;
    i12a_t(k)=-i3c_find;
    i12b_t(k)=0;
    vi3c_t(k)=-i3c_find*Ri3c-i3c_find*RSMb-VFSMb-
i3c_find*R12a+vi12a(i);
end
end

mean_i12b=mean(i12b_t);
mean_vii3c=mean(vi3c_t);

error(1)=100*mean_vii3c;
error(2)=100*abs(mean_i12b-i12b(j));
end
else
    error('alpha is not valid.');
end

```

A.10 Regulated Lossy Cuk QRC

These MATLAB scripts are used to simulate the regulated Lossy Cuk QRC.

```
%Define the global variables
clear global
clear all
global Lr Cr wr Zr
global R12
global RLr RCr RSD RSMA RSMb Ri3a Ri3b VFSD VFSMa VFSMb
global RCT RLT RALL a wo Aa Ab v12 vi3a i3b

global i j
global vi3b_target

syms x

%Define the components' parameters
Lr=8e-6;
Cr=800e-12;
wr=1/sqrt(Lr*Cr);
Zr=sqrt(Lr/Cr);
vi3b_target=30;

R12=0.1;
RLr=0.1;
RCr=0.1;
RSD=0.1;
RSMA=0.1;
RSMb=0.1;
Ri3a=0.1;
Ri3b=0.1;
Ri3c=0.1;
VFSD=0.7;
VFSMa=0.7;
VFSMb=0.7;

RCT=RCr+R12;
RLT=RLr+RSD;
RALL=RLT+RCT;
a=RALL/2/Lr;
wo=sqrt(wr^2-a^2);
Aa=(RLT+R12+RSMA)/Lr;
Ab=(RLT+R12+RSMb)/Lr;

%Define the analysis range
vi3a=-40:-25:-240;
i3b=5:5:30;
```

```

options1=optimset('fsolve');
options1=optimset(options1,'Display','off');
options2=optimset('fzero');
options2=optimset(options2,'Display','off');

for i=1:length(vi3a),
    for j=1:length(i3b),
        v12(i,j)=vi3b_target-vi3a(i);
        init(2)=-v12(i,j)*i3b(j)/vi3a(i); % Set initial value i3
        alpha=v12(i,j)/Zr/init(2);
        if (alpha>1)|(alpha<=0)
            warning('The variable "alpha" is not valid.')
        end
        init(1)=wr*i3b(j)/init(2)/(pi+asin(alpha)+alpha/2+(1+sqrt(1-alpha^2))/alpha);
    % Set initial value fs
        fs_org(i,j)=init(1);
        if (init(1)>0)&(init(2)>0)
            [out,error_out,exitflag]=fsolve('obj_v13a_v13b_i12',init,options1);
    % Find the conditions so that i12=0 and expected vi3a vi3b.
        if exitflag>0
            fs(i,j)=out(1); % The switching frequency fs is found.
            i3(i,j)=out(2); % The current condition is found.
            error_v13a(i,j)=error_out(1);
            error_v13b(i,j)=error_out(2);
            error_i12(i,j)=error_out(3);
        else
            fs(i,j)=nan;
            i3(i,j)=nan;
            error_v13a(i,j)=nan;
            error_v13b(i,j)=nan;
            error_i12(i,j)=nan;
        end
    else
        fs(i,j)=nan; % The switching frequency fs is not found.
        i3(i,j)=nan; % The current condition is not found.
        error_v13a(i,j)=nan;
        error_v13b(i,j)=nan;
        error_i12(i,j)=nan;
    end
    i3a(i,j)=i3(i,j)-i3b(j);
    alpha=v12(i,j)/Zr/i3(i,j);
    beta=VFSD/Zr/i3(i,j);
    if (alpha<=1)&(alpha>0),
        T1=Cr/i3(i,j)*(-i3b(j)*R12+v12(i,j)-i3(i,j)*RCr);
        C1=VFSD+v12(i,j)+i3(i,j)*RLT+i3a(i,j)*R12;
        K1=v12(i,j)/alpha*sqrt(1+(wr^2/wo^2)*(RALL/2/Zr+beta)^2);
        phase1=2*pi-atan((RALL/Zr+beta)/(wt/wo-a/wo*(RALL/Zr+beta)));
    end
end

```

```

K2=K1/Zr;
phase2=phase1+pi-atan(wo/a);
K3=sqrt(1+(beta+a)^2/wo^2);
phase3=atan(wo/(beta+a));
K4=i3(i,j)*K3*Zr;
phase4=phase3+2*pi-atan(wo/a);
KT2=K1*RCr*Cr*sqrt((1/RCr/Cr-a)^2+wo^2);
phaseT2=phase1+atan(wo/(1/RCr/Cr-a));
funf=char(eval('C1+KT2*exp(-a*x)*sin(wo*x+phaseT2)'));

% figure(4)
% temp_x=0:3*2*pi/wo/40:3*2*pi/wo/4;
% plot(temp_x,C1+KT2*exp(-a.*temp_x).*sin(wo.*temp_x+phaseT2));
% hold on;
T2=fzero(funf,[mod((pi-phaseT2),2*pi)/wo 3*2*pi/wo/4],options2)+T1;
% T2=fzero(funf,[2*pi/wo/4 2*pi*3/wo/4],options)+T1;
if ((T2-T1)<0),
    error('error: T2<T1');
end

C5a=(i3b(j)*R12+i3(i,j)*RSMa-VFSD-VFSMa-v12(i,j))/(RLT+R12+RSMa);
K5a=i3(i,j)*(1-K3*exp(-a*(T2-T1)))*sin(wo*(T2-T1)+phase3))-C5a;
K6a=-Lr*K5a*Aa;
Ta=T2-1/Aa*log((i3(i,j)-C5a)/K5a);

C5b=(i3b(j)*R12+i3(i,j)*RSMb-VFSD+VFSMb-
v12(i,j))/(RLT+R12+RSMb);
K5b=i3(i,j)-C5b;
K6b=-Lr*K5b*Ab;
T3=Ta-1/Ab*log(-C5b/K5b);

if ((1/T3)<=fs(i,j))|(fs(i,j)<=0)|(fs(i,j)==nan),
    fs(i,j)=nan;
    fs_org(i,j)=nan;
    Pv12(i,j)=nan;
    Pi3a(i,j)=nan;
    Pi3b(i,j)=nan;
    PR12(i,j)=nan;
    PRi3a(i,j)=nan;
    PRi3b(i,j)=nan;
    PRCr(i,j)=nan;
    PRLr(i,j)=nan;
    PRSD(i,j)=nan;
    PRSMa(i,j)=nan;
    PRSMb(i,j)=nan;
    PRSM(i,j)=nan;
    PVFSD(i,j)=nan;
    PVFSMa(i,j)=nan;
    PVFSMb(i,j)=nan;
    PVFSM(i,j)=nan;

```

```

PCr(i,j)=nan;
PLr(i,j)=nan;
i12_final(i,j)=nan;
vi3a_final(i,j)=nan;
vi3b_final(i,j)=nan;
else
    Ts=1/fs(i,j);
    Simulation_Time=Ts;
    resolution=1000;
    Time_step=Simulation_Time/resolution;
    Time_axis=Time_step:Time_step:Time_step*(resolution-1);
    Time_length=length(Time_axis);
    vCr=zeros(Time_length,1);
    iCr=zeros(Time_length,1);
    iLr=zeros(Time_length,1);
    vLr=zeros(Time_length,1);
    iSMA=zeros(Time_length,1);
    iSMb=zeros(Time_length,1);
    i12_t=zeros(Time_length,1);
    vi3a_t=zeros(Time_length,1);
    vi3b_t=zeros(Time_length,1);

% Define the time scale interval
for k=1:Time_length,
    Time_now=rem(Time_axis(k),Ts);
    if (Time_now>0)&(Time_now<=T1)
        vCr(k)=v12(i,j)/alpha*wr*Time_now;
        iCr(k)=i3(i,j);
        i12_t(k)=-i3b(j);
        vi3a_t(k)=-i3a(i,j)*Ri3a-vCr(k)-iCr(k)*RCr;
        vi3b_t(k)=-i3b(j)*Ri3b-vCr(k)-iCr(k)*RCr+v12(i,j)-i3b(j)*R12;
    elseif (Time_now>T1)&(Time_now<=T2)
        vCr(k)=C1+K1*exp(-a*(Time_now-T1))*sin(wo*(Time_now-
T1)+phase1);
        iCr(k)=K2*exp(-a*(Time_now-T1))*sin(wo*(Time_now-
T1)+phase2);
        iLr(k)=i3(i,j)*(1-K3*exp(-a*(Time_now-T1)))*sin(wo*(Time_now-
T1)+phase3));
        vLr(k)=K4*exp(-a*(Time_now-T1))*sin(wo*(Time_now-
T1)+phase4);
        i12_t(k)=iLr(k)-i3b(j);
        vi3a_t(k)=-i3a(i,j)*Ri3a-vCr(k)-iCr(k)*RCr;
        vi3b_t(k)=-i3b(j)*Ri3b-iLr(k)*RLT-VFSD-vLr(k);
    elseif (Time_now>T2)&(Time_now<=Ta)
        iLr(k)=C5a+K5a*exp(-Aa*(Time_now-T2));
        vLr(k)=K6a*exp(-Aa*(Time_now-T2));
        iSMA(k)=i3(i,j)-iLr(k);
        i12_t(k)=iLr(k)-i3b(j);
        vi3a_t(k)=VFMSA-iSMA(k)*RSMA-i3a(i,j)*Ri3a;
    end
end

```

```

vi3b_t(k)=-i3b(j)*Ri3b-iLr(k)*RLT-VFSD-vLr(k);
elseif (Time_now>Ta)&(Time_now<=T3)
    iLr(k)=C5b+K5b*exp(-Ab*(Time_now-Ta));
    vLr(k)=K6b*exp(-Ab*(Time_now-Ta));
    iSMb(k)=i3(i,j)-iLr(k);
    i12_t(k)=iLr(k)-i3b(j);
    vi3a_t(k)=-VFSMb-iSMb(k)*RSMb-i3a(i,j)*Ri3a;
    vi3b_t(k)=-i3b(j)*Ri3b-iLr(k)*RLT-VFSD-vLr(k);
elseif (Time_now>T3)&(Time_now<=Ts)
    iSMb(k)=i3(i,j);
    i12_t(k)=-i3b(j);
    vi3a_t(k)=-VFSMb-iSMb(k)*RSMb-i3a(i,j)*Ri3a;
    vi3b_t(k)=-i3b(j)*Ri3b-iSMb(k)*RSMb-VFSMb+v12(i,j)-i3b(j)*R12;
end
end
mean_vCr=mean(vCr);
mean_iCr=mean(iCr);
rms_iCr=sqrt(mean(iCr.^2));
mean_iLr=mean(iLr);
rms_iLr=sqrt(mean(iLr.^2));
mean_vLr=mean(vLr);
mean_iSMA=mean(iSMA);
rms_iSMA=sqrt(mean(iSMA.^2));
mean_iSMb=mean(iSMb);
rms_iSMb=sqrt(mean(iSMb.^2));
mean_i12=mean(i12_t);
rms_i12=sqrt(mean(i12_t.^2));
mean_vi3a=mean(vi3a_t);
mean_vi3b=mean(vi3b_t);

Pv12(i,j)=v12(i,j)*mean_i12;
Pi3a(i,j)=i3a(i,j)*mean_vi3a;
Pi3b(i,j)=i3b(j)*mean_vi3b;
PR12(i,j)=R12*rms_i12^2;
PRI3a(i,j)=Ri3a*i3a(i,j)^2;
PRI3b(i,j)=Ri3b*i3b(j)^2;
PRCr(i,j)=RCr*rms_iCr^2;
PRLr(i,j)=RLr*rms_iLr^2;
PRSD(i,j)=RSD*rms_iLr^2;
PRSMa(i,j)=RSMA*rms_iSMA^2;
PRSMb(i,j)=RSMb*rms_iSMb^2;
PRSM(i,j)=PRSMa(i,j)+PRSMb(i,j);
PVFSD(i,j)=VFSD*mean_iLr;
PVFSMa(i,j)=-VFSMa*mean_iSMA;
PVFSMb(i,j)=VFSMb*mean_iSMb;
PVFSM(i,j)=PVFSMa(i,j)+PVFSMb(i,j);
PCr(i,j)=mean_iCr*mean_vCr;
PLr(i,j)=mean_iLr*mean_vLr;
i12_final(i,j)=mean_i12;

```

```

    vi3a_final(i,j)=mean_v13a;
    vi3b_final(i,j)=mean_v13b;
end
else
    fs(i,j)=nan;
    fs_org(i,j)=nan;
    Pv12(i,j)=nan;
    Pi3a(i,j)=nan;
    Pi3b(i,j)=nan;
    PR12(i,j)=nan;
    PRi3a(i,j)=nan;
    PRi3b(i,j)=nan;
    PRCr(i,j)=nan;
    PRLr(i,j)=nan;
    PRSD(i,j)=nan;
    PRSMa(i,j)=nan;
    PRSMb(i,j)=nan;
    PRSM(i,j)=nan;
    PVFSD(i,j)=nan;
    PVFSMa(i,j)=nan;
    PVFSMb(i,j)=nan;
    PVFSM(i,j)=nan;
    PCr(i,j)=nan;
    PLr(i,j)=nan;
    i12_final(i,j)=nan;
    vi3a_final(i,j)=nan;
    vi3b_final(i,j)=nan;
end
end
end

%Draw the figures
figure(1);
colormap([0 0 0]);
subplot(2,2,1);
H=mesh(i3b,vi3a,fs./1e6);
set(H,'markersize',15);
view(20,30);
xlabel('i3b (A)', 'fontsize', 15);
ylabel('vi3a (V)', 'fontsize', 15);
zlabel('fs (MHz)', 'fontsize', 15);
title('Lr=8e-6H, Cr=800e-12F, QR Cuk Converter', 'fontsize', 15);

%Draw the figures
subplot(2,2,2);
mesh(i3b,vi3a,vi3a_final);
hold on
mesh(i3b,vi3a,vi3b_final);
mesh(i3b,vi3a,v12);

```

```

hold off
view(20,30);
xlabel('i3b (A)','fontsize',15);
ylabel('vi3a (V)','fontsize',15);
zlabel('vi3a\_final vi3b\_final v12 (V)','fontsize',15);
title('Lr=8e-6H, Cr=800e-12F, QR Cuk Converter','fontsize',15);

%Draw the figures
subplot(2,2,3);
mesh(i3b,vi3a,i12_final);
hold on
mesh(i3b,vi3a,i3a);
hold off
view(20,30);
xlabel('i3b (A)','fontsize',15);
ylabel('vi3a (V)','fontsize',15);
zlabel('i12\_final i3a (A)','fontsize',15);
title('Lr=8e-6H, Cr=800e-12F, QR Cuk Converter','fontsize',15);

%Draw the figures
subplot(2,2,4);
mesh(i3b,vi3a,Pi3a);
hold on;
mesh(i3b,vi3a,Pi3b);
hold off;
view(20,30);
xlabel('i3b (A)','fontsize',15);
ylabel('vi3a (V)','fontsize',15);
zlabel('Pi3a(-ve) Pi3b(+ve) (W)','fontsize',15);
title('Lr=8e-6H, Cr=800e-12F, QR Cuk Converter','fontsize',15);

%Draw the figures
figure(2)
colormap([0 0 0]);
subplot(3,3,1);
mesh(i3b,vi3a,PR12./max(max(PRLr)));
xlabel('i12b (A)');
ylabel('v12a (V)');
zlabel('Normalized PR12','VerticalAlignment','bottom');
subplot(3,3,2);
mesh(i3b,vi3a,PRLr./max(max(PRLr)));
xlabel('i12b (A)');
ylabel('v12a (V)');
zlabel('Normalized PRLr','VerticalAlignment','bottom');
subplot(3,3,3);
mesh(i3b,vi3a,PRCr./max(max(PRLr)));
xlabel('i12b (A)');
ylabel('v12a (V)');
zlabel('Normalized PRCr','VerticalAlignment','bottom');

```

```

subplot(3,3,4);
mesh(i3b,vi3a,PRSD./max(max(PRLr)));
xlabel('i12b (A)');
ylabel('v12a (V)');
zlabel('Normalized PRSD','VerticalAlignment','bottom');
subplot(3,3,5);
mesh(i3b,vi3a,PRSMA./max(max(PRLr)));
xlabel('i12b (A)');
ylabel('v12a (V)');
zlabel('Normalized PRSMA','VerticalAlignment','bottom');
subplot(3,3,6);
mesh(i3b,vi3a,PRSMb./max(max(PRLr)));
xlabel('i12b (A)');
ylabel('v12a (V)');
zlabel('Normalized PRSMb','VerticalAlignment','bottom');
subplot(3,3,7);
mesh(i3b,vi3a,PRi3a./max(max(PRLr)));
hold on;
mesh(i3b,vi3a,PRi3b./max(max(PRLr)));
hold off;
xlabel('i12b (A)');
ylabel('v12a (V)');
zlabel('Normalized PRi3a PRi3b','VerticalAlignment','bottom');
subplot(3,3,8);
mesh(i3b,vi3a,PVFSD./max(max(PRLr)));
xlabel('i12b (A)');
ylabel('v12a (V)');
zlabel('Normalized PVFSD','VerticalAlignment','bottom');
subplot(3,3,9);
mesh(i3b,vi3a,PVFSMA./max(max(PRLr)));
hold on;
mesh(i3b,vi3a,PVFSMB./max(max(PRLr)));
hold off;
xlabel('i12b (A)');
ylabel('v12a (V)');
zlabel('Normalized PVFSMA & PVFSMB','VerticalAlignment','bottom');

%Draw the figures
figure(3)
colormap([0 0 0]);
Ploss=PR12+PRLr+PRCr+PRSD+PRSMA+PRSMb+PRi3a+PRi3b+PVFSD+PVFS
Ma+PVFSMB;
H=mesh(i3b,vi3a,Pi3b./(Ploss-Pi3a).*100);
set(H,'markersize',15);
%mesh(i3b,vi3a,Ploss+Pi3a+Pv12);
xlabel('i3b (A)','fontsize',15,'VerticalAlignment','bottom');
ylabel('vi3a (V)','fontsize',15,'VerticalAlignment','bottom');
zlabel('Efficiency (%)','fontsize',15);
title('Lr=8e-6H, Cr=800e-12F, QR Cuk Converter','fontsize',15);

```

```
view(60,10);

%Draw the figures
figure(4)
colormap([0 0 0]);
subplot(2,2,1);
mesh(i3b,vi3a,error_vi3a);
xlabel('i3b (A)', 'fontsize', 15, 'VerticalAlignment', 'bottom');
ylabel('vi3a (V)', 'fontsize', 15, 'VerticalAlignment', 'bottom');
zlabel('error\ vi3a', 'VerticalAlignment', 'bottom');
subplot(2,2,2);
mesh(i3b,vi3a,error_vi3b);
xlabel('i3b (A)', 'fontsize', 15, 'VerticalAlignment', 'bottom');
ylabel('vi3a (V)', 'fontsize', 15, 'VerticalAlignment', 'bottom');
zlabel('error\ vi3b', 'VerticalAlignment', 'bottom');
subplot(2,2,3);
mesh(i3b,vi3a,error_i12);
xlabel('i3b (A)', 'fontsize', 15, 'VerticalAlignment', 'bottom');
ylabel('vi3a (V)', 'fontsize', 15, 'VerticalAlignment', 'bottom');
zlabel('error\ i12', 'VerticalAlignment', 'bottom');
```

```
%Define the object function in a separate file
function [error]=obj_v13a_v13b_i12(input)

%Define the global variables
global Lr Cr wr Zr
global R12
global RLr RCr RSD RSMA RSMb Ri3a Ri3b VFSD VFSMa VFSMb
global RCT RLT RALL a wo Aa Ab v12 vi3a i3b

global i j
global vi3b_target

syms x

options2=optimset('fzero');
options2=optimset(options2,'Display','off');

fs_find=input(1);
i3_find=input(2);

i3a_find=i3_find-i3b(j);
alpha=v12(i,j)/Zr/i3_find;
beta=VFSD/Zr/i3_find;
if (alpha<=1)&&(alpha>0),
    T1=Cr/i3_find*(-i3b(j)*R12+v12(i,j)-i3_find*RCr);
    C1=VFSD+v12(i,j)+i3_find*RLT+i3a_find*R12;
    K1=v12(i,j)/alpha*sqrt(1+(wr^2/wo^2)*(RALL/2/Zr+beta)^2);
    phase1=2*pi-atan((RALL/Zr+beta)/(wr/wo-a/wo*(RALL/Zr+beta)));
    K2=K1/Zr;
    phase2=phase1+pi-atan(wo/a);
    K3=sqrt(1+(beta+a)^2/wo^2);
    phase3=atan(wo/(beta+a));
    K4=i3_find*K3*Zr;
    phase4=phase3+2*pi-atan(wo/a);
    KT2=K1*RCr*Cr*sqrt((1/RCr/Cr-a)^2+wo^2);
    phaseT2=phase1+atan(wo/(1/RCr/Cr-a));
    funf=char(eval('C1+KT2*exp(-a*x)*sin(wo*x+phaseT2)'));

    T2=fzero(funf,[mod((pi-phaseT2),2*pi)/wo 3*2*pi/wo/4],options2)+T1;

    if ((T2-T1)<0),
        error('error: T2<T1');
    end
    ↓
    C5a=(i3b(j)*R12+i3_find*RSMA-VFSD-VFSMa-
v12(i,j))/(RLT+R12+RSMA);
    K5a=i3_find*(1-K3*exp(-a*(T2-T1))*sin(wo*(T2-T1)+phase3))-C5a;
    K6a=-Lr*K5a*Aa;
    Ta=T2-1/Aa*log((i3_find-C5a)/K5a);
```

```

C5b=(i3b(j)*R12+i3_find*RSMb-VFSD+VFSMb-
v12(i,j))/(RLT+R12+RSMb);
K5b=i3_find-C5b;
K6b=-Lr*K5b*Ab;
T3=Ta-1/Ab*log(-C5b/K5b);

if ((1/T3)<=fs_find)|(fs_find<=0)|(fs_find==nan),
%warning('fs_find is not valid');
error(1)=nan;
error(2)=nan;
error(3)=nan;
else
Ts=1/fs_find;
Simulation_Time=Ts;
resolution=500;
Time_step=Simulation_Time/resolution;
Time_axis=Time_step:Time_step:Time_step*(resolution-1);
Time_length=length(Time_axis);
vCr=zeros(Time_length,1);
iCr=zeros(Time_length,1);
iLr=zeros(Time_length,1);
vLr=zeros(Time_length,1);
iSMA=zeros(Time_length,1);
iSMB=zeros(Time_length,1);
i12_t=zeros(Time_length,1);
vi3a_t=zeros(Time_length,1);
vi3b_t=zeros(Time_length,1);

for k=1:Time_length,
Time_now=rem(Time_axis(k),Ts);
if (Time_now>0)&(Time_now<=T1)
    vCr(k)=v12(i,j)/alpha*wr*Time_now;
    iCr(k)=i3_find;
    i12_t(k)=-i3b(j);
    vi3a_t(k)=-i3a_find*Ri3a-vCr(k)-iCr(k)*RCr;
    vi3b_t(k)=-i3b(j)*Ri3b-vCr(k)-iCr(k)*RCr+v12(i,j)-i3b(j)*R12;
elseif (Time_now>T1)&(Time_now<=T2)
    vCr(k)=C1+K1*exp(-a*(Time_now-T1))*sin(wo*(Time_now-
T1)+phase1);
    iCr(k)=K2*exp(-a*(Time_now-T1))*sin(wo*(Time_now-
T1)+phase2);
    iLr(k)=i3_find*(1-K3*exp(-a*(Time_now-
T1))*sin(wo*(Time_now-T1)+phase3));
    vLr(k)=K4*exp(-a*(Time_now-T1))*sin(wo*(Time_now-
T1)+phase4);
    i12_t(k)=iLr(k)-i3b(j);
    vi3a_t(k)=-i3a_find*Ri3a-vCr(k)-iCr(k)*RCr;
    vi3b_t(k)=-i3b(j)*Ri3b-iLr(k)*RLT-VFSD-vLr(k);
end;
end;

```

```

elseif (Time_now>T2)&(Time_now<=Ta)
    iLr(k)=C5a+K5a*exp(-Aa*(Time_now-T2));
    vLr(k)=K6a*exp(-Aa*(Time_now-T2));
    iSMa(k)=i3_find-iLr(k);
    i12_t(k)=iLr(k)-i3b(j);
    vi3a_t(k)=VFSMa-iSMa(k)*RSMa-i3a_find*Ri3a;
    vi3b_t(k)=i3b(j)*Ri3b-iLr(k)*RLT-VFSD-vLr(k);
elseif (Time_now>Ta)&(Time_now<=T3)
    iLr(k)=C5b+K5b*exp(-Ab*(Time_now-Ta));
    vLr(k)=K6b*exp(-Ab*(Time_now-Ta));
    iSMb(k)=i3_find-iLr(k);
    i12_t(k)=iLr(k)-i3b(j);
    vi3a_t(k)=-VFSMb-iSMb(k)*RSMb-i3a_find*Ri3a;
    vi3b_t(k)=-i3b(j)*Ri3b-iLr(k)*RLT-VFSD-vLr(k);
elseif (Time_now>T3)&(Time_now<=Ts)
    iSMb(k)=i3_find;
    i12_t(k)=-i3b(j);
    vi3a_t(k)=-VFSMb-iSMb(k)*RSMb-i3a_find*Ri3a;
    vi3b_t(k)=-i3b(j)*Ri3b-iSMb(k)*RSMb-VFSMb+v12(i,j)-i3b(j)*R12;
end
end

mean_i12=mean(i12_t);
mean_v13a=mean(vi3a_t);
mean_v13b=mean(vi3b_t);

error(1)=1*(mean_v13a-v13a(i));
error(2)=1*(mean_v13b-v13b_target);
error(3)=1*mean_i12;
end
else
%warning('alpha is not valid.');
    error(1)=nan;
    error(2)=nan;
    error(3)=nan;
end

```

References

- [1] F. C. Lee, "High-frequency quasi-resonant converter technologies," Proceedings of the IEEE, vol. 76, no. 4, April 1988, pp. 377 –390.
- [2] K. H. Liu and F. C. Lee, "Zero-voltage switching technique in DC/DC converters," IEEE Trans. Power Electronics, vol. 5, no. 3, July 1990, pp. 293–304.
- [3] W. C. Ho and M. H. Pong, "Power loss and efficiency analysis of quasi-resonant converters," in Proc. IEEE IECON 1993, vol. 2, pp. 842 –847.
- [4] B. T. Lin and Y. S. Lee, "A unified approach to modeling, synthesizing, and analyzing quasi-resonant converters," IEEE Trans. Power Electronics, vol. 12, no. 6, Nov 1997, pp. 983-992.
- [5] Igor Goryanskey, "Zero-Voltage Switching Quasi Square Wave Converters", http://www.powerdesigners.com/InfoWeb/design_center/articles/ZVS%20Converters/zero_vol.shtm, Jan 1998.
- [6] D. Hanselman and B. Littlefield, Mastering Matlab 5: a comprehensive tutorial and reference, Prentice Hall, 1998.

- [7] D. Czarkowski and M. K. Kazimierczuk, "Linear circuit models of PWM flyback and buck / boost converters," IEEE Trans. Circuits Syst.-I: Fundamental Theory and Applications, vol. 39, no. 8, August 1992, pp. 688-693.
- [8] R. B. Ridley, "A new, continuous-time model for current-mode control," IEEE Trans. Power Electronics, vol. 6, no. 2, April 1991, pp. 271-280.
- [9] D. Maksimovic and S. Cuk, "A general approach to synthesis and analysis of quasi-resonant converters," IEEE Trans. Power Electronics, vol. 6, no. 1, January 1991, pp. 127-140.
- [10] Y. S. Lee, "A systematic and unified approach to modeling switches in switch-mode power supplies," IEEE Trans. Industrial Electronics, vol. IE-32, no. 4, November 1985, pp. 445-448.
- [11] A. Szabo, M. Kansara and E. S. Ward, "The averaging technique applied to the modeling of multi-resonant and quasi-resonant converters," in Proc.IEE Power Electronics and Variable Speed Drives, 21-23 September 1998, pp. 69-73.
- [12] T. F. Wu and T. H. Yu, "Off-line applications with single-stage converters," IEEE Trans. Industrial Electronics, vol. 44, no. 5, October 1997, pp. 638-647.
- [13] Z. Puklus, "Resonant flyback converter," in Proc. IEEE IECON '98 24th Annual Conference, vol. 2, 1998, pp. 1066 -1071.
- [14] V. Vorperian, "Simplified analysis of PWM converters using model of PWM switch. Part II: discontinuous conduction mode," IEEE Trans. Aerospace and Electronic Systems, vol. 26, no. 3, May 1990, pp. 497-505.
- [15] V. Vorperian, "Simplified analysis of PWM converters using model of PWM switch. Part I: continuous conduction mode," IEEE Trans. Aerospace and Electronic Systems, vol. 26, no. 3, May 1990, pp. 490-496.

- [16] M. K. Kazimierczuk, S. T. Nguyen, "Small-signal analysis of open-loop PWM flyback dc-dc converter for CCM," in Proc. IEEE National Aerospace and Electronics Conference, NAECON 1995, vol. 1, pp. 69-76.
- [17] J. M. F. Dores Costa and M. Medeiros Silva, "Small-signal models of quasi-resonant converters," ISIE'97, pp. 258-262.
- [18] V. Vorperian, "Quasi-square-wave converters: topologies and analysis," IEEE Trans. Power Electronics, vol. 3, no. 2, April 1988, pp. 183-191.
- [19] T. F. Wu and Y. K. Chen, "A systematic and unified approach to modeling PWM DC/DC converters based on the graft scheme," IEEE Trans. Industrial Electronics, vol. 45, no. 1, February 1998, pp. 88-98.
- [20] B. T. Lin, K. W. Siu and Y. S. Lee, "Actively clamped zero-current-switching quasi-resonant converters using IGBT's," IEEE Trans. Industrial Electronics, vol. 46, no. 1, February 1999, pp. 75-81.
- [21] P. R. K. Chetty, "Current injected equivalent circuit approach to modeling of switching DC-DC converters in discontinuous inductor conduction mode," IEEE Trans. Industrial Electronics, vol. IE-29, no. 3, August 1982, pp. 230-234.
- [22] A. E. Emanuel, "Powers in nonsinusoidal situations a review of definitions and physical meaning," IEEE Trans. Power Delivery, vol. 5, no. 3, July 1990, pp. 1377-1389.
- [23] K. Liu, R. Oruganti and F. C. Y. Lee, "Quasi-resonant converters – topologies and characteristics," IEEE Trans. Power Electronics, vol. PE-2, no. 1, January 1987, pp. 62-72.
- [24] V. Vorperian, R. Tymerski and F. C. Y. Lee, "Equivalent circuit models for resonant and PWM switches," IEEE Trans. Power Electronics, vol. 4, no. 2, April 1989, pp. 205-214.

- [25] M. F. Schlecht and L. F. Casey, "Comparison of the square-wave and quasi-resonant topologies," *IEEE Trans. Power Electronics*, vol. 3, no. 1, January 1988, pp. 83-92.
- [26] W. A. Tabisz, P. M. Gradzki and F. C. Y. Lee, "Zero-voltage-switched quasi-resonant buck and flyback converters – experimental results at 10MHz," *IEEE Trans. Power Electronics*, vol. 4, no. 2, April 1989, pp. 194-204.
- [27] P. C. Theron and J. A. Ferreira, "The zero voltage switching partial series resonant converter," *IEEE Trans. Industry Applications*, vol. 31, no. 4, July 1995, pp. 879-886.
- [28] G. Hua, E. X. Yang, Y. Jiang and F. C. Y. Lee, "Novel zero-current-transition PWM converters," *IEEE Trans. Power Electronics*, vol. 9, no. 2, March 1994, pp. 213-219.
- [29] G. Hua, E. X. Yang, Y. Jiang and F. C. Y. Lee, "Novel zero-current-transition PWM converters," *IEEE Trans. Power Electronics*, vol. 9, no. 6, November 1994, pp. 601-606.
- [30] D. M. Divan and G. Skibinski, "Zero-switching-loss inverters for high-power applications," *IEEE Trans. Industry Applications*, vol. 25, no. 4, July 1989, pp. 634-643.

Contributions and Conference presentations:

- [31] C. T. Choi and C. K. Li, "Large signal modeling of quasi-resonant Buck converter using regulated unified model," *Proceedings of the 39th IEEE Conference on Decision and Control*, vol. 5, December 2000, pp. 4647-4648.
- [32] C. T Choi, C. K. Li and S. K. Kok, "Modeling of an active clamp discontinuous conduction mode flyback converter under variation of operating conditions,"

- Proceedings of the IEEE 1999 International Conference on Power Electronics and Drive Systems PEDS'99, vol. 2, July 1999, pp.730-733.
- [33] C. T Choi, C. K. Li and S. K. Kok, "Control of an active clamp discontinuous conduction mode flyback converter," Proceedings of the IEEE 1999 International Conference on Power Electronics and Drive Systems PEDS'99, vol. 2, July 1999, pp.1120-1123.
- [34] C. T. Choi and C. K. Li, "Large signal modeling of quasi-resonant converters using regulated unified model," IEEE 7th Workshop on Computers in Power Electronics 2000, COMPEL2000, USA, 2000.
- [35] C. T. Choi and C. K. Li, "Power distribution and efficiency analysis of quasi-resonant converters," China Fifteenth Conference on Circuits and Systems Proceedings, pp. 218-221.
- [36] C. T. Choi, C. P. Chan, Y. C. Chen, C. K. Li and Q. S. Cao, "Animation of electromagnetic wave propagation using an improved MRTD method," China Fifteenth Conference on Circuits and Systems Proceedings, pp. 528-531.
- [37] C. T. Choi and C. K. Li, " Large signal modeling of quasi-resonant converters using regulated unified model," in 19th Chinese Control Conference, December 2000.